

PREDICTION OF ROCK PROPERTIES AND SPECIFIC ENERGY USING SOUND LEVELS PRODUCED DURING DIAMOND DRILLING

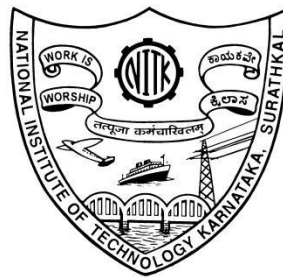
Thesis

Submitted in partial fulfilment of the requirements for the degree of

DOCTOR OF PHILOSOPHY

by

CH. VIJAYA KUMAR



**DEPARTMENT OF MINING ENGINEERING
NATIONAL INSTITUTE OF TECHNOLOGY KARNATAKA,
SURATHKAL, MANGALORE - 575025**

February, 2021

DECLARATION

by the Ph.D Research Scholar

I hereby *declare* that the Research Thesis entitled “**Prediction of Rock Properties and Specific Energy using Sound Levels Produced during Diamond Drilling**” which is being submitted to the **National Institute of Technology Karnataka, Surathkal** in partial fulfillment of the requirements for the award of the Degree of **Doctor of Philosophy** in Department of **Mining Engineering** is a *bonafide report of the research work carried out by me*. The material contained in this Research Thesis has not been submitted to any University or Institution for the award of any degree.



Ch. Vijaya Kumar

(Reg. No.:158040MN15F11)

Department of Mining Engineering

Place: NITK, Surathkal

Date: 21.02.2021

CERTIFICATE

This is to *certify* that the Research Thesis entitled “**Prediction of Rock Properties and Specific Energy using Sound Levels Produced during Diamond Drilling**” submitted by **Ch.Vijaya Kumar** (Register Number: **158040MN15F11**) as the record of the research work carried out by him, is *accepted as the Research Thesis submission* in partial fulfillment of the requirements for the award of the degree of **Doctor of Philosophy**.

Research Guides

Dr. Ch. S. N. Murthy

Professor

Dr. Harsha Vardhan

Professor

Dr. K. Ram Chandar

Chairman-DRPC

ACKNOWLEDGEMENT

I would like to extend my thanks to many people, who so generously helped in completing my Ph.D. thesis. First of all, I would like to express my sincere gratitude to my research guides Prof. Ch. S. N. Murthy and Prof. Harsha Vardhan, Department of Mining Engineering, National Institute of Technology Karnataka (NITK), Surathkal, for their valuable guidance and consistent encouragement throughout the research work. Both the research guides made themselves always available to clarify my doubts and are approachable. I am highly grateful to them. I would like to thank the Research Progress Assessment Committee (RPAC) and Doctoral Research Programme Committee (DRPC) members. I sincerely thank Prof. A. O. Surendranathan, Department of Metallurgical and Materials Engineering and Dr. M Aruna, Department of Mining Engineering, RPAC Members, for their insightful comments and encouragement. I extend my gratitude to the authorities of NITK, Surathkal and staff of Department of Mining Engineering for their help during my research work. My special thanks to Dr. K. Ram Chandar, Head of the Department and Chairman, DRPC also faculty members of Mining Engineering, NITK. I would like to thank my fellow research scholars/ students in Mining Engineering Department and my friend Dr. M. P. Arun kumar, Post Doc Fellow from Xi'an Jiaotong University and from Xi'an, Shaanxi, China.

I owe this work to my beloved parents: Sri. Ch. ChakradharaRao (Late) and Ch. SiluvaKumari. I also thank my family members: Wife: Ch. Hima Bindu, Son: Ch. Roopesh, Daughter: Ch. Rishika, and to my uncle Sri. N. Rama Rao and auntie N. Rani. I am greatly indebted to my love of life, Ch. Hima Bindu, whose support cannot be expressed in words. Thank you for your support, unconditional devotion, enlivening spirit and encouragement to meet challenges with determination and to strive for success.



(Ch. Vijaya Kumar)

Place: NITK, Surathkal

Date: 21.02.2021

ABSTRACT

Drilling is widely used in many engineering applications such as mining, geotechnical and petroleum industries. Drilling operations produce sound that can be used to estimate rock properties and specific energy. The conventional method of determining of rock properties and specific energy is expensive and time-consuming. In this study, a new technique was developed to estimate rock properties and specific energy (SE) using dominant frequencies and A-weighted equivalent sound pressure levels generated during diamond drilling operations. First, sound pressure level was recorded while performing rock drilling experiments on seven different types of rock samples using computer numerical control (CNC) drilling machine BMV 45 T20 and sound signals of these sound frequencies were analyzed using Fast Fourier transform (FFT). Using simple linear, multiple regression analysis and artificial neural networks, mathematical equations were developed for various rock properties, i.e. uniaxial compressive strength, Brazilian tensile strength, density, abrasivity, impact strength index using dominant frequencies of sound pressure levels. This study also reports the methods for prediction of SE, effect of physico-mechanical rock properties on SE and effect of operational variables on SE using A - weighted equivalent sound levels produced during diamond drilling operations. Initially SE was determined for all selected rock types and a correlation was developed between SE and physico-mechanical rock properties (PMRP) and operating variables. The developed prediction models were validated using determination coefficients (R^2), t-test, F-test and performance predictions i.e. values account for (VAF), root mean square error (RMSE) and mean absolute percentage error (MAPE). For SE, the R^2 values obtained a range from 75.58 % to 78.76 %, RMSE values obtained a range from 0.074411 to 0.578601, VAF values obtained a range from 72.826808 to 84.155813 and MAPE values obtained a range from 0.061218 to 2.321007 for selected rock samples and t and F values also obtained below the tabulated values (2.44). Concerning SE's relation to PMRP, it was observed that SE increased with increasing uniaxial compressive strength, Brazilian tensile strength and dry density and decreased with increasing abrasivity. For PMRP, the R^2 values obtained from 92.25 %, 90.99 %, 47.15 %, 93.39 %, corresponded to uniaxial compressive strength, Brazilian tensile strength, density and abrasivity. Similarly, regarding SE's relation with operational variables, it was found that SE decreased with

increasing drill bit diameter, penetration rate and drill bit speed. The developed models can be used to predict rock properties and specific energy at early stage of planning and design.

Keywords: rock properties, sound pressure level, Fast Fourier transform (FFT), sound signal, diamond drilling, dominant frequencies, excitation frequencies, and specific energy.

CONTENTS

	Page No.	
Declaration	i	
Certificate	ii	
Acknowledgement	iii	
Abstract	iv	
Contents	vi	
List of Figures	x	
List of Tables	xiv	
Nomenclature	xviii	
Notations	xix	
CHAPTER-1	INTRODUCTION	1
1.1	Background	2
1.2	Origin of the Research Work	2
1.3	Definition of the Problem	2
1.4	Objectives of the Study	2
1.5	Justification	3
1.6	Structure of the Thesis	3
CHAPTER-2	LITERATURE REVIEW	5
2.1	Application of Acoustic Emission in Geotechnical Engineering and Rock Drilling	5
2.2	Prediction of Specific Energy	8
2.3	Regression Techniques for Prediction of Rock Properties	13
2.4	Artificial Neural Network Techniques for Prediction of Rock Properties	15
CHAPTER-3	METHODOLOGY	19
3.1	Equipment Used	19
	3.1.1 CNC drilling machine	19
	3.1.2 Data - acquisition system	19
	3.1.3 Noise dosimeter	20
	3.1.4 Sound level calibrator	21

3.1.5	Compression testing machine	22
3.1.6	Brazilian tensile strength testing machine	22
3.1.7	Los Angeles abrasion testing machine	23
3.1.8	Dynamometer	23
3.1.9	Impact strength index testing machine	24
3.2	Experimental Procedure	25
3.2.1	Rock samples used in the investigation	25
3.3	Determination of Physico - Mechanical Properties of Rocks	26
3.3.1	Determination of uniaxial compressive strength	26
3.3.2	Determination of Brazilian tensile strength	26
3.3.3	Determination of density	27
3.3.4	Determination of abrasivity	27
3.3.5	Determination of impact strength index	28
3.4	Experimental Set-Up	29
3.5	Sound Pressure Level Measurement	30
3.6	Determination of the Dominant Frequencies of Audio Signals from Rock Drilling Operations	30
3.7	Determination of A-Weighted Equivalent Sound Pressure Levels	32
3.8	Determination of Specific Energy	32
3.8.1	Details of parametric variation for determination of specific energy	33
3.9	Analytical Techniques	33
3.9.1	Modeling of physico - mechanical properties of rocks	34
3.9.2	Development of simple linear regression models	34
3.9.3	Development of multiple linear regression models	35
3.9.4	Development of multiple regression models	35
3.9.5	Development of artificial neural network models	36
CHAPTER-4	RESULTS AND DISCUSSION	37
4.1	Effect of the Operating Variables on A-weighted Sound Pressure Level	37
4.2	Effect of the Operating Variables on Specific Energy	38

4.3	Effect of Thrust on A - weighted Sound Pressure Level	40
4.4	Effect of Torque on A – weighted Sound Pressure Level	42
4.5	Effect of Rock Properties on A-weighted Sound Pressure Level	44
4.6	Development of Regression Models	47
	4.6.1 Development of rock properties predictive models at constant drill bit diameter, drill bit speed, and penetration rate	47
	4.6.2 Modeling of rock properties	50
	4.6.3 Excitation frequency (Hz) versus sound pressure level (SPL) for rock blocks	54
4.7	Development of Rock Properties Predictive Models for varying Combinations of Drill bit Diameters, Drill bit Speed, and Penetration rate	56
	4.7.1 Sound pressure level measurement	56
	4.7.2 Modeling of rock properties	57
4.8	Development of Rock Properties Predictive Models for Combinations of the Drill bit Diameters, Drill bit Speed, and Penetration rate	62
	4.8.1 Modelling of rock properties using multiple regression analysis	62
	4.8.2 Analysis of variance (ANOVA)	63
	4.8.3 Validation of the derived models	65
	4.8.4 Performance prediction of derived models	66
4.9	Development of Artificial Neural Network Models	66
4.10	Prediction of Specific Energy	69
	4.10.1 Modeling of specific energy using multiple linear regression analysis	69
	4.10.2 Analysis of variance (ANOVA)	70
	4.10.3 Performance prediction of derived models	71
	4.10.4 Validation of the specific energy models	72
	4.10.5 Effect of physico - mechanical rock properties on specific energy	74

CHAPTER-5	CONCLUSIONS AND RECOMMENDATIONS	79
5.1	Conclusions	79
5.2	Recommendations for Further Research	81
	References	83
	Appendix-A	101
	Appendix-B	119
	Publications	161
	Curriculum vitae	163

LIST OF FIGURES

Figure No.	Caption	Page No.
3.1	BMV 45 T20 CNC drilling machine	19
3.2	Data acquisition system	19
3.3	Noise dosimeter (Spark 705+)	20
3.4	Sound calibrator CAL 150	21
3.5	HEICO, Compression testing machine	22
3.6	Brazilian tensile strength testing machine	22
3.7	Los Angeles abrasion test machine	23
3.8	Drill tool dynamometer, Model-601C	23
3.9	Impact strength index testing equipment	24
3.10	Experimental Set-up of BMVK 45 T20 CNC drilling machine	29
3.11a	Labview block diagram code utilised for acquiring the sound signal data from microphone	31
3.11b	Labview block diagram code for sound signal analysis	31
4.1a	Effect of drill bit diameter on A – weighted sound pressure level on various rock samples at 30 mm depth	37
4.1b	Effect of penetration rate on A – weighted sound pressure level on various rock samples at 30 mm depth	38
4.1c	Effect of drill bit speed on A – weighted sound pressure level on various rock samples at 30 mm depth	38
4.2a	Effect of drill bit diameter on specific energy on various rock samples at 30 mm depth	39

4.2b	Effect of penetration rate on specific energy on various rock sample at 30 mm depth	40
4.2c	Effect of drill bit speeds on specific energy on various rock samples at 30 mm depth	40
4.3a	Effect of thrust on A-weighted sound pressure level at varying drill bit diameter on various rock samples at 30 mm depth	41
4.3b	Effect of thrust on A-weighted sound pressure level at varying penetration rate on various rock samples at 30 mm depth	41
4.3c	Effect of thrust on A-weighted sound pressure level at varying drill bit speed on various rock samples at 30 mm depth	43
4.4a	Effect of torque on A-weighted sound pressure level at varying drill bit diameter on various rock samples at 30 mm depth	43
4.4b	Effect of torque on A-weighted sound pressure level at varying penetration rate on various rock samples at 30 mm depth	44
4.4c	Effect of torque on A-weighted sound pressure level at varying drill bit speed on various rock samples at 30 mm depth	44
4.5a	Uniaxial compressive strength on A-weighted sound pressure level on various rock samples at 30 mm depth	45
4.5b	Brazilian tensile strength on A-weighted sound pressure level on various rock samples at 30 mm depth	45
4.5c	Density on A-weighted sound pressure level on various rock samples at 30 mm depth	46
4.5d	Abrasivity on A-weighted sound pressure level on various rock samples at 30 mm depth	46
4.5e	Impact strength index on A-weighted sound pressure level on various rock samples at 30 mm depth	47

4.6	Time domain plots for various rock types i.e. (a) ochre, (b) bituminous coal, (c) laterite, (d) pink limestone and (e) hematite	49
4.7	Selected five dominant frequencies between 5000 Hz to 8000 Hz from the FFT results i.e., (a) ochre, (b) bituminous coal, (c) laterite, (d) pink limestone and (e) hematite	50
4.8	Simple linear regression prediction model, and distribution of validation points corresponding to UCS, BTS, and Density	53
4.9a	Sound pressure level vs. excitation frequency for ochre rock	54
4.9b	Sound pressure level vs. excitation frequency for bituminous coal	54
4.9c	Sound pressure level vs. excitation frequency for laterite	55
4.9d	Sound pressure level vs. excitation frequency for pink limestone	55
4.9e	Sound pressure level vs. excitation frequency for hematite	56
4.10	Simple linear regression prediction model, and distribution of validation points corresponding UCS, BTS, and density.	61
4.11	Measured UCS, BTS, density, and abrasivit vs. predicted UCS. BTS, density, and abrasivity	65
4.12	Illustration of an artificial neural network model	67
4.13	Specific energy error graph for ochre	72
4.14	Specific energy error graph for coal	72
4.15	Specific energy error graph for laterite	73
4.16	Specific energy error graph for pink limestone	73
4.17	Specific energy error graph for black limestone	73
4.18	Specific energy error graph for hematite	74
4.19	Specific energy error graph for dolomite	74

4.20a	Relations between uniaxial compressive strength and specific energy	75
4.20b	Relations between Brazilian tensile strength and specific energy	76
4.20c	Relations between density and specific energy	76
4.20d	Relations between abrasivity to specific energy	77
4.20e	Relations between impact strength index and specific energy	77

LIST OF TABLES

Table No.	Caption	Page No.
3.1	Calibrations chart of cutting tool dynamometer	24
3.2	Location and types of collected rock block	25
3.3	Rock properties	26
3.4	Details of parametric variation for determination of specific energy	33
4.A1	A-weighted sound pressure level of ochre, bituminous coal, laterite, pink limestone, black limestone, hematite, and dolomite for different drill bit diameter	101
4.A2	A-weighted sound pressure level of ochre, bituminous coal, laterite, pink limestone, black limestone, hematite, and dolomite for different penetration rate	101
4.A3	A-weighted sound pressure level of ochre, bituminous coal, laterite, pink limestone, black limestone, hematite, and dolomite for different drill bit speed	101
4.A4	Specific energy of ochre, bituminous coal, laterite, pink limestone, black limestone, hematite, and dolomite for different drill bit diameter	102
4.A5	Specific energy of ochre, bituminous coal, laterite, pink limestone, black limestone, hematite, and dolomite for different penetration rate	102
4.A6	Specific energy of ochre, bituminous coal, laterite, pink limestone, black limestone, hematite, and dolomite for different drill bit speed	102
4.A7	Thrust for different drill bit diameter while drilling ochre, bituminous coal, laterite, pink limestone, black limestone, hematite, and dolomite samples	103
4.A8	Thrust for different penetration rate while drilling ochre, bituminous coal, laterite, pink limestone, black limestone, hematite, and dolomite samples	103

4.A9	Thrust for different drill bit speed while drilling ochre, bituminous coal, laterite, pink limestone, black limestone, hematite, and dolomite samples	103
4.A10	Torque for different drill bit diameters of ochre, bituminous coal, laterite, pink limestone, black limestone, hematite, and dolomite samples	104
4.A11	Torque for different penetration rates while drilling ochre, bituminous coal, laterite, pink limestone, black limestone, hematite, and dolomite samples	104
4.A12	Torque for different drill bit speeds while drilling of ochre, bituminous coal, laterite, pink limestone, black limestone, hematite, and dolomite samples	104
4.13	Dominant frequencies for various rock types	50
4.14	The prediction model coefficients for predicting uniaxial compressive strength	51
4.15	The prediction model coefficients for predicting Brazilian tensile strength	51
4.16	The prediction model coefficients for predicting density	52
4.A17	Predicted values, measured values, and model error from the prediction model for uniaxial compressive strength (ten rock samples for validation)	105
4.A18	Predicted values, measured values, and model error from the prediction model for Brazilian tensile strength (ten rock samples for validation)	105
4.A19	Predicted values, measured values, and model error from the prediction model for density (ten rock samples for validation)	106
4.20	Five dominant frequencies for selected rock samples	57
4.21	Model summary for the dependent variable	58
4.22	Analysis of variance (ANOVA) for the dependent variable	58
4.23	Coefficients of a presented model for predicting UCS	58
4.24	Coefficients of a presented model for predicting BTS	59

4.25	Coefficients of a presented model for predicting density	59
4.26	Predicted values, measured values from prediction model and model error for uniaxial compressive strength (Three validation rock samples)	60
4.27	Predicted values, measured values from prediction model and model error for Brazilian tensile strength (Three validation rock samples)	60
4.28	Predicted values, measured values from prediction model and model error for density (Three validation rock samples)	60
4.A29	Experimental results of 125 dominant frequencies (Hz) for each rock sample	107
4.A30	Statistical analysis of significant regression models for various rocks	115
4.31	Results of ANOVA for various rocks	64
4.32	Performance indices of the developed regression model	66
4.33	Schematic representation of network architecture	68
4.A34	Performance indices of the developed regression modal	117
4.B1	Statistical analysis of significant regression models for various rocks	119
4.B2	Results of ANOVA for various rocks	122
4.3	Performance indices of the developed regression models	71
4.4	Correlations between specific energy and physico-mechanical properties	75
4.B5	Table 4.B5: Experimental 125 test conditions results of thrust, torque and A-SPL, for ochre rock sample	126
4.B6	Experimental 125 test conditions results of thrust, torque and A-SPL, for bituminous coal	131
4.B7	Experimental 125 test conditions results of thrust, torque and A-SPL, for laterite rock type	136

4.B8	Experimental 125 test conditions results of thrust, torque and A-SPL, for pink limestone	141
4.B9	Experimental 125 test conditions results of thrust, torque and A-SPL, for black limestone	146
4.B10	Experimental 125 test conditions results of thrust, torque and A-SPL, for hematite	151
4.B11	Table 4.B11: Experimental 125 test conditions results of thrust, torque and A-SPL, for dolomite	156

NOMENCLATURE

AE	Acoustic Emission
A-SPL	A-weighted equivalent Sound Pressure Level (dB)
ANN	Artificial Neural Networks
ANOVA	Analysis of Variance
ASTM	American Society for Testing and Materials
BP	Back Propagation
CNC	Computer Numerically Controlled
DF	Degree of Freedom
DD	Drill bit diameter (mm)
ISRM	International Society for Rock Mechanics
MAPE	Mean Absolute Percentage Error
MLP	Multi-Layer Perception
MS	Mean Square
MSE	Mean Square Error
PR	Penetration rate (mm/min)
RBF	Radial Basis Function
RBFNN	Radial Basis Function Neural Network
RMSE	Root Mean Square Error
RPM	Revolutions per minute
SE	Specific energy (Nm/m ³)
SS	Spindle speed (rpm)
BTS	Brazilian Tensile Strength (MPa)
UCS	Uniaxial Compressive Strength (MPa)
VAF	Values Account For

NOTATIONS

ρ	Density
σ_t	Brazilian Tensile Strength
M	Mass of the sample (Kg/m ³)
V	Volume of the specimen (m ³)
dB	Decibel
L_{eq}	Equivalent sound level
F	Frequencies
x(t)	Time domain signal
X(f)	Fast Fourier transform
ft	The frequency to analyze
DFT	Discrete Fourier transform
ADC	Analog to digital converter
x	Input sequence
X	Discrete Fourier Transform (DFT)
n	No. of samples in both the discrete – time and the discrete – frequency domain
J2	Imaginary number
π	Constant
ft	Frequency to be analyzed
k	Constant
$P_{r.m.s}$	Sound pressure root mean square
P_{ref}	Reference sound pressure ($2 \times 10^{-5} \text{ N m}^{-2}$)
a	Quadratic model
x_i , and a_i	Quadratic effect
n	Independent variables of $X_i, X_j, X_n, \dots, X_n$
Y	Dependent variables of $X_i, X_j, X_n, \dots, X_n$
ϵ	Fitting error in regression model
R^2	Regression coefficient or regression coefficient
DF	Dominant Frequency (Hz)

SS	Sum of Squares
MS	Mean Squares

CHAPTER - 1

INTRODUCTION

1.1 Background

Drilling is an integral operation in mining, quarrying, construction and petroleum industry. It is also an essential activity in mineral exploration and blast hole design in opencast mines. In underground mines, drilling is widely used for a variety of tasks such as rock blasting, tunneling, and excavation. Drilling is invariably associated with noise production. Noise/acoustic has been widely used in other domains of engineering. However, its application in mining/geotechnical domain is limited. According to Vardhan et al. (2009), rock properties are crucial for an effective blast hole design and other construction projects. The lack of knowledge of rock properties has an adverse effect on the environment, when the energy is released during blasting. Usually, rock properties are not readily available at mining and construction sites. As a result, it is needed to send rock samples to a national laboratory, which is a time-consuming process. An alternative way of determining rock properties is highly desirable. One of the possible approaches is to record noise signals while drilling and analyse these signals for the purpose of rock characterization. The objective of this study is to explore the possibility of using noise/sound generated during drilling to determine physico-mechanical properties of rocks, which will be of interest and useful to geotechnical and mining engineers.

Minerals and their related products are the principal raw materials for the basic industry around the world. Diamond drilling plays a major role in mining and allied industries. Exploration is very essential to recognise the mineral presence in the bedrock and success of any mining company largely depends on the accuracy in exploration. In most of the exploration work, diamond drilling plays a major role and hence, every effort should be made so that the diamond drilling is efficient and cost-effective. The specific energy (SE) is an important parameter to assess the efficiency in rock drilling. For practical purpose, SE is a useful parameter for estimating the energy requirement for a particular drilling operation, planning and design of

excavation projects. SE can be used to indicate drill bit condition, rock strength and rock hardness during drilling operation. SE in rock drilling depends on operational parameters, such as penetration rate, drill bit speed, drill bit diameter, torque, thrust and rock properties. A very good indication as to how well drill bit performs in a particular bit-rock combination has been given by specific energy. Any rock drilling operation creates sound/noise as a by-product. This noise/sound could be used to predict SE during drilling.

1.2 Origin of the Research Work

The concept of the determination of the rock properties and specific energy using frequency analysis, A-weighted sound level during diamond drilling operations and also developing prediction models using simple linear, multiple regression, and artificial neural network have not been reported. Considering this research gap, the research work was formulated.

1.3 Definition of the Problem

The rock properties and specific energy i.e., the energy required to excavate a unit volume of rock are not available at mining and construction sites. As a result, it is needed to send rock blocks or drill cores to a laboratory, which is time consuming. As an alternative method to determine rock properties could be the application of sound pressure level produced during core drilling. The thesis mainly focuses on the prediction of physico-mechanical rock properties using sound pressure levels generated at dominant frequencies, and the prediction of specific energy using A-weighted sound level during drilling operations.

1.4 Objectives of the Study

The following are the objectives of the study

1. Determination of rock properties such as uniaxial compressive strength, Brazilian tensile strength, density, abrasivity and Impact Strength Index (I.S.I). Influence of these properties on noise levels produced during diamond drilling.
2. Determination of specific energy in diamond drilling and its influence on noise levels produced during drilling.

3. Prediction of rock properties using frequency analysis in diamond drilling and development of correlations between rock properties and dominant frequencies produced during drilling using simple and multiple regression models.
4. Prediction of rock properties using frequency analysis in diamond drilling and development of correlations between rock properties and dominant frequencies produced during drilling using Artificial Neural Networks (ANN).
5. Comparison of the models developed based on simple, multiple regression and ANN.

1.5 Justification

Using the developed prediction models, one can easily estimate the rock properties and specific energy by recording the sound pressure levels during diamond drilling, and substituting this value along with drill bit diameter, drill bit speed, and penetration rate. This technique, which is an indirect method to predict rock properties and specific energy can be used at early stage of design. Prediction of rock properties using frequency analysis and prediction of specific energy (required time to remove a unit volume of rock mass) using A- weighted equivalent sound level produced during the diamond drilling operations has not been reported anywhere by earlier investigators. Hence, the present research work can be taken in this direction.

1.6 Structure of the Thesis

This study focuses on the quantification of physico-mechanical rock properties and specific energy using sound pressure levels at dominant frequencies and A-weighted equivalent sound levels generated through diamond drilling operations. The focus is on the development of predictive models. The developed models can be utilized for quantification of rock properties and specific energy with an acceptable degree of accuracy in realistic applications.

In this thesis, five chapters are presented in a logical order. Chapter 1 provides a general introduction about rock properties and specific energy along with problem identification, justification. It also briefly describes various topics covered by the different chapters of this thesis. Chapter 2 presents the review of literature for quantification of the physico-mechanical rock properties and specific energy.

Chapter 3 describes the equipment used in the investigation, methodology of the present study, experimental set-up/procedure.

Chapter 4 describes the prediction of rock properties using sound levels at dominant frequencies. The prediction models were developed by simple linear, multiple regression analysis, and artificial neural networks. This chapter presents specific energy prediction equations developed using multiple linear regression analysis, then correlations of this specific energy with rock properties and operating variables. Hence, the conclusions and the recommendations of further research work are discussed in Chapter 5.

CHAPTER - 2

LITERATURE REVIEW

2.1 Applications of Acoustic Emission in Geotechnical Engineering and Rock Drilling

Initially, the acoustic applications were implemented by Obert (1941). Obert (1941), Obert and Duvall (1942) utilised acoustic frequencies for estimating rock burst in metal mines. It was found that different stress states in rock produces various acoustic noises. The authors used sub-audible noises for predicting the rock burst in underground metal mines.

Hardy (1972) conducted an inclusive review of acoustic emissions in the area of rock mechanics. The authors conducted acoustic emission experiments related to mine design and the alleviation of rock burst in North America in the 1930s. It was concluded that the acoustic emission technique provides the behaviour of geologic rock materials' deformation and failure.

Rafavich et al. (1984) conducted a detailed laboratory investigation on the characteristics of carbonate rock and acoustic properties with a vast range of lithology. The rock composition indicates that porosity is the most influencing factor for P-wave and S-wave velocity. The results are based on the property of rocks used for evaluation of lithology and porosity changes for seismic section from Williston basin (the USA and Canada).

McNally (1990) studied the quantification of coal strength and elastic moduli in Queensland using sonic log techniques. The author developed mathematical relationships between geotechnical parameters and sonic log interval transit times.

Zborovjan (2001), Zborovjan (2002), Zborovjan et al. (2003) investigated the identification of rock types based on the hidden Markov model for rock drilling operations. This model recognized the particular acoustic signature of every rock type being drilled. It was said that the maximum information contained appropriate signal

transfer, and the rock drilling acoustic signature could be found between 5000 hertz to 8000 hertz.

Miklusova et al. (2006) and Krepelka et al. (2007) investigated the rock strength characteristics and the feasibility of utilisation of optimum control parameters, such as thrust and speed, during drilling operations. It was discovered that the change in the audio signal depends on the drilling regime and the audio signal can be used for the control of rock disintegration process.

Gradl et al. (2007) carried out the drill bit diagnosis using noise of a bit during drilling operations based on the acoustic data. It was revealed that the bit physical characteristics and bit diagnosis (broken teeth and bit balling) can be performed using the noise of a bit in real time projects based on the acoustic data.

Later, Vardhan and Murthy (2007) and Vardhan et al. (2009) introduced a novel concept of quantification of physico-mechanical rock properties by utilising sound levels generated through drilling operations. Various types of rock samples were used to find the rock properties using a fabricated jackhammer drilling machine. It was concluded that this technique is effective for the quantification of rock properties.

Kumar et al. (2011a, 2011b, 2011c, 2013a, 2013b) investigated in detail the quantification of rock properties (sedimentary, metamorphic and igneous) using sound levels produced in rock drilling operations. A set of mathematical equations were formulated for predicting the various rock properties with an admissible degree of accuracy.

Shreedharan et al. (2014) probed on the identification of rock type based on acoustic fingerprinting.

Karakus and Perez (2014) conducted laboratory experiments using impregnated diamond core drilling operations. The authors developed linear relationships between the acoustic emission signals and diamond drill bit wear. It was concluded that the developed linear relationships could predict the depth of the cut, weight on the drill bit, wear of the drill bit, and torque on the drill bit, using the time domain of the acoustical signal.

Kivade et al. (2015) used radial basis function & multilayer perception, two neural network methods, for predicting the geo-mechanical properties of various rocks using noise levels produced in percussive drilling operations.

Delibalta et al. (2015) quantified the physico-mechanical rock properties using noise level. Laboratory experiments were conducted using an automatic rock cutting machine with 54 types of rock samples. It was concluded that increasing the density increases the sound level and increasing porosity decreases the sound level.

Rostami et al. (2015), Qin et al. (2018), Xiao et al. (2018), and Flegner et al. (2019) investigated lithological rock recognition, based on the vibro-acoustic signal approach during rock drilling operations. The authors captured vibro-acoustic signals using vibration sensors and spectral wideband acoustic sensors. These captured signals were analysed in terms of time domain and time-frequency domain for analysing the rock characteristics. It was concluded that the spectral wideband acoustic sensors were providing better signals to the noise ratio than vibration sensors.

Zhang et al. (2018a) introduced a new index for evaluating coal brittleness from fracture networks, using the hydraulic fracturing process. The acoustical signals were captured during uniaxial compression and triaxial compression tests; these captured signals were correlated with coal brittleness. It was concluded that acoustical signals showed sudden changes when reaching the yield stress and peak strength, representing high brittleness.

Zhang et al. (2018b) reported that the acoustic emission technique was employed to detect the initiation and evolution of micro cracks of rocks during the laboratory investigations.

Li et al. (2018), Jai et al. (2018), and Feng et al. (2019) conducted a laboratory investigation on hydraulic fracturing, using layered shale rock samples using the acoustic emission technique. The result concluded that the characteristics of the injection pressure curve and acoustic emission response detected the hydraulic behaviour growth in layered shale.

Hu et al. (2019) conducted a laboratory experiment on the rock burst process of bore holes using the acoustic emission technique. It was concluded that sharp and high amplitude acoustical signals could be used for the quantification of the rock burst, while micro cracks and splitting dominated the failure process.

He et al. (2019) investigated rock burst disasters in thick coal seams and steeply inclined coal seams. The authors used micro seismic and acoustic emission techniques as an early warning before the rock burst occurred during mining.

Sheng et al. (2019) carried out a detailed study on water jet rock drilling efficiency in relation to acoustic emission. The authors correlated rock drilling efficiency to acoustical signals during drilling operations. It was concluded that the high frequency band reported a good correlation with the rate of penetration.

2.2 Prediction of Specific Energy

The concept of SE in rotary drilling for the first time was introduced by Teale (1965). He suggested that the work done per unit volume of broken rock relates the process to the physico-mechanical properties of rock, such as compressive strength of rock and density. Any rock drilling operation creates sound/noise as a by-product. This noise/sound could be used to predict SE during drilling. It may also be useful for determining the physico-mechanical properties of rocks during drilling, which will be of interest to geotechnical and mining engineers.

Some studies are reported on the determination of SE from rock cutting/drilling operation. SE has been successfully used in the diamond tool industry for optimising drilling and cutting parameters (Ersoy 2003, Ersoy and Atici 2004, 2007, 2009, Miller and Ball 1990, Seimer-Oisen and Blindheim 1970, Becker et al. 1984). Several researchers have indicated how well drill bit performs in a particular bit-rock combination on SE in rock drilling. A very good indication as to has been given by studies done by (Chiang and Stamm 1998; Luis et al. 2004; Balci et al. 2004; Curry et al. 2005; Dupriest and Koederitz, 2005; Tiryaki and Dikmen 2006; Banks 2013; Luo et al. 2014).

Evans (1962, 1984) established a theoretical connection between conical bit-type cutters and the cutting force for wedge picks, which were directly associated to SE.

Fowell and McFeat-Smith (1976) conducted laboratory investigational studies to correlate SE obtained by small-scale cutting tests to a few mechanical and index properties of rocks, such as compressive strength, Schmidt hammer rebound value, cone indenter index, cementation coefficient.

Goktan (1991) developed the relationship between SE obtained from micro-scale laboratory rock-cutting tests. It was concluded that a reasonable relationship cannot be found between the brittleness index and SE.

Pessier and Fear (1992) developed a new mathematical equation for the penetration rate based on the SE equation derived by Teale. They altered Teale's SE model by replacing an equation they derived; the new equation conveyed torque as a function of weight on the bit, bit diameter and bit-specific coefficient of sliding friction. The authors showed that under atmospheric drilling conditions, mean SE is nearly equal to the uniaxial compressive strength (UCS) of the rock being drilled.

Reddish and Yasar (1996) investigated the rock strength index test based on SE of drilling. It was concluded that the rock strength index was more reliable than other index tests and the test results can be applied practically in the field.

Chiang and Stamm (1998) developed a method to estimate the instantaneous specific rock energy using corrected down-the-hole (DTH) drill monitoring data. Accordingly, the authors were able to generate a specific rock energy profile for every hole drilled and thus map an entire drilling site for this index.

Copur et al. (2001) conducted laboratory experiments on rock cutting operations with a conical cutter. In this study, eleven rock types and ores were selected for the determination of optimum SE during rock cutting operations. It was concluded that the developed prediction equations can be used to estimate the cut ability, optimum SE and production rate.

Waughman et al. (2002) established a real-time monitoring of SE data in combination with sonic data and drilling data, which benefits in taking a decision, when to pull the

bit out of the hole. They outlined a guide on the application of SE monitoring technique to the field. The concept was proved to work in water based mud treated with anti-balling chemicals and synthetic based mud systems.

Altindag (2003) correlated SE with rock brittleness in rock cutting. The relationship between the brittleness of rock and rock cutting efficiency was established using regression analysis. The high brittleness value (the ratio between compressive strength and tensile strength) indicates that the high SE is required for efficient rock cutting.

Luis et al. (2004) investigated specific rock energy (SRE) using DTH drill monitoring data. They characterised the rock at a given drilling site and helpful in identifying the different rock formations. It was said that there were two important correlations between DTH hammer operational variables. The first correlation was observed between the frequency and penetration rate; with increasing penetration rate, the frequency dropped. The second correlation was observed between penetration and torque; as the torque increased, the penetration increased. It was concluded that the rock drilling impact hammer performance improved then by reducing the operational costs.

Balci et al. (2004) established statistical relations between optimum SE and rock properties. The statistical analysis indicated that the optimum SE achieved in the laboratory from the full-scale rock cutting tests can be predicted reliably from UCS, Brazilian tensile strength (BTS), static and dynamic elastic moduli and Schmidt rebound values of the rocks. Finally, the strongest relations were established by using UCS and BTS.

Curry et al. (2005) introduced a technique to characterise the difficulty of drilling a specific formation in its down-hole pressure environment, using the concept of SE. The authors developed an algorithm to evaluate the technical limit of SE from wire-line sonic, lithology and pressure data. It was concluded that the technical limit of SE denotes the lowest SE that can be reasonably expected for a particular combination of rock properties and air pressures.

Dupriest and Koederitz (2005) conducted laboratory experiments to estimate the drilling efficiency of drill bits using mechanical specific energy (MSE). It was concluded that MSE can identify the efficiency of the drilling system, optimum operating parameters, cost justify changes and bit selection during real-time projects.

Tiryaki and Dikmen (2006) examined the effects of textural and mineralogical properties of sand stones on SE, along with physico–mechanical properties. The relationship between SE and compositional, textural and engineering properties of sandstones were evaluated through bivariate correlation and linear regression analysis using SPSS 11 Software package. Finally, Poisson’s ratio revealed the best correlation to SE and more reliable SE prediction tool in sandstone.

Erosoy and Atici (2007) reported a study on ultrasonic technology technique in volcanic and carbonate rock cutting to measure P-S wave velocities. Cutting SE was defined as the energy required for excavating a unit volume of rock. It was a useful parameter in crushing, drilling, cutting, excavation and breaking. The effect of cutting SE and rock properties on P and S wave velocities were evaluated with simple linear regression analysis. It was concluded that this seismic technology can be widely used in the field and laboratory.

Acaroglu et al. (2008) established a fuzzy logic model to estimate SE from tunnel boring machine (TBM). A model was proven to predict the SE requirement of constant cross-section disc cutters in rock cutting operations. It was found that the model predicts SE value as output parameter for given disc cutter, rock and cutting parameters. The model values exhibited that the fuzzy logic values are close to the experimental values.

Atici and Ersoy (2009) developed a statistical relation among brittleness, destruction SE and both cuttability and drillability using the optimum data obtained from the experimental work. The optimum data for the bits and saw blades were extracted for each series of drilling and cutting results and were analysed based on maximum penetration and cutting rates. The results based on regression analysis indicated a strong exponential, linear and logarithmic relations between cutting SE of circular diamond saw blades and brittleness.

Aydin and Aydiner (2012) conducted laboratory investigations on the sawing of granites by circular diamond saw blades, depending on operational variables. The authors developed mathematical models for estimation of SE in the sawing process. The developed models were validated through statistical tests, such as t and F tests.

Neves et al. (2012) investigated the geomechanical behaviour in rock cutting with diamond saw blades. The energy of elastic and plastic deformation was determined by uniaxial compression tests and the energy consumed per unit volume in the cutting process. Finally, the correlation between overall cutting SE and deformation specific energy was analysed.

Engine et al. (2013) studied the efficiency of abrasive water jet cutting (AWJC) and circular sawing (CS). The relationship between SE values and rock properties was as discussed. It was concluded that shore hardness and abrasive resistance were found to be strongly related to SE.

Yurdakul and Akdas (2012) conducted laboratory experiments for quantification of the cutting SE using operational parameters. The authors used seven types of cutters for six varied carbonate rocks. The developed prediction models was recommended to predict SE in the petroleum and mining industry.

Banks (2013) investigated minimising mechanical SE while drilling, using extreme seeking control; minimising mechanical SE requires continual monitoring as the drill bit wears. Extreme control was used by putting in a perturbation in the penetration per revolution to estimate the total local gradient of the mechanical SE. It was concluded that this control method is stable and hence can be used in bench marking different drill bits.

Luo et al. (2014) investigated the reduction of drilling noise from roof bolting operations through proper control of drilling operation. Lower SE and higher SE were achieved at proper selection of high bit depth according to drill bit and strength of the rock. It was concluded that by reducing wasted energy and improving the efficiency, the heat, noise, fire dust and bit wear were reduced.

Shewalla et al. (2015) conducted a detailed study on rock cutting operation to measure the required load to fail the rock under confining stress. Their results show a non-linear relation of SE with bore hole pressure.

Recent studies attempted to predict of rock properties using sound level produced during drilling operations (Vardhan and Murthy 2007; Vardhan et al. 2009; Kumar et al. 2011a, 2011b, 2011c, 2013a, 2013b, 2019a, 2019b; Kivade et al. 2012a, 2012b, 2013, 2015; Delibalta et al. 2014, 2015; Shreedharan et al. 2014; Forouharmajd et al. 2015; Brown 1981; Mellor and Hawkes 1971; Ulusay and Hudson 2007; Kahraman 2013; Kalyan 2016; Masood 2015; Macias 2017). These studies used sound pressure level and frequency of sound signals to develop empirical equations for prediction of rock properties.

Based on the findings of the above studies, SE is a very important parameter in planning and designing of excavation projects, mining and petroleum industry and depends on rock properties. However, most of the previous investigators determined SE using conventional methods, but the prediction of SE using A-weighted equivalent sound pressure level from diamond core drilling operations has not been studied in detail. Hence, the present investigation was taken up for prediction of SE using A-weighted equivalent sound pressure level during diamond core drilling operations.

2.3 Regression Techniques for Prediction of Rock Properties

Regression analysis is a powerful tool to derive relationship between the several dependent and independent variables.

Sachapazis (1990) conducted a laboratory experiment to quantify the deformation of the carbonate rock samples. The empirical equations were developed for the physico-mechanical properties of carbonate rocks such as UCS, tangent Young's modulus, Schmidt hammer rebound hardness using multiple regression analysis. It was concluded that the regression coefficient (R^2) value higher corresponding the rock properties.

Kim and Gao (1995) studied variations of rock mass mechanical properties and deformation module of rock mass using borehole jacking tests. The authors have

proposed “Monte Carlo” method to estimate the probability distributions of deformation modules, and compressive strength of rock mass. They concluded that the simulation results demonstrate a reasonable representation of the probability distribution of the rock mass characteristics.

Katz et al. (2000) developed empirical correlations between Schmidt hammer rebound hardness, density, UCS, and Young’s modulus. The developed estimation equations can be used in the field and laboratory with the following limitations such as (i) tested rock is well-cemented and apparently elastic (ii) rocks crack under the impacts not properly tested (iii) Hammer measurements should be accompanied on smooth surfaces (iv) loose blocks can be measured if the intact part of the block weighs a few tens of kilograms or more. Yasar and

Erdogan (2004) conducted laboratory experiments for quantification of rock properties using hardness methods. In this investigation found that rock properties can be quantified using shore hardness, Schmidt hammer compared with the calculated value from various statistical equations. It was concluded that this method can be used for estimation of UCS, and unit weight.

Faisal et al. (2007) performed a simple linear regression analysis between various types of hardness and intact rock properties. The obtained results show very strong correlations of regression coefficient value compared with similar investigations. It was concluded that Poisson’s ratio decreased with an increase in rock strength.

Kilic and Teymen (2008) determined physico-mechanical properties using non-destructive and indirect methods. For laboratory tests, nineteen different rock samples were collected from different locations. The mathematical equations were developed in the relation of UCS, point load index, sound velocity, Schmidt hardness, abrasion resistance, and indirect tensile strength. It was concluded that the UCS, wear resistance, and indirect tensile strength can be estimated by using nondestructive methods.

Mahdiabadi and Khanlari (2019) developed correlations between UCS and modulus of elasticity. For this study, eighty calcareous mudstone core samples were used to develop prediction equations using multiple regression analysis, ANN, and adaptive

neuro-fuzzy inference system. The developed models were validated using MPE, RMSE, and VAF. The results show that the fuzzy interface system was a powerful tool to estimate the modulus of elasticity and UCS compared with other statistical analysis tools.

Kahraman et al. (2019) determined mean particle size in the relations of rock properties and mineralogical percentage. In this study, six granite samples were tested in the laboratory. The prediction equations were developed in the relation of rock properties results and mineralogical percentage to mean particle size. The results show that the multiple regression equation was given the highest coefficient correlation value than simple linear regression analysis. The multiple regression techniques can be used for prediction of practical size at the preliminary estimation of the project cost.

2.4 Artificial Neural Network Techniques for Prediction of Rock Properties

Estimating the rock properties using an approximate calculation (soft computing) is an alternative tool for researchers. Artificial Neural Network Techniques (ANN) are better than statistical analysis because empirical relationships derived from regression analysis, estimates only the mean value; as a result, low experimental values are overvalued, high experimental values are miscalculated. The ANN does not force the predicted value to be a mean value, thus, accurately maintaining the existing difference between the measured data.

ANN also investigates the self-organised interactions between variables. Many researchers reported on the modelling of the rock properties and its behaviour using neural networks (Ghabousi et al. 1991; Haykin et al. 1998; Singh et al. 2001; Singh et al. 2003; Bhatnagar and Khandelwal 2012; Salimia et al. 2015; Momeni et al. 2015; Tripathy et al. 2015; Madhubabu et al. 2016; Abdi et al. 2018; Rastegarnia et al. 2018). ANN has the ability to significantly generate the suitable output from difficult or inexact information (data). It can detect the exact patterns from complex data which are neither predictable by the human brain nor by statistical analysis.

Rumelhart et al. (1986) proved that the ANN model was perfect for classifying complex information for the demands of a new situation (Simpson, 1990). Another

advantage of ANN includes self-organisation, adaptive learning based on real time operations, self-organises redundant information coding and fault tolerance. Various networks can be retained even when the main network is impaired (Yilmaz & Sendir 2002; Yilmaz & Yuksek 2008; Yilmaz 2010; Yilmaz & Kaynar 2011).

Meulenkamp et al. (1999) examined the possibility of estimating unconfined compressive strength using ANN for the toughness of rocks with Equotip hardness tester based on rock toughness, dry density, and sizes of the grains.

Singh et al. (2001) established the necessary models to predict the physico-mechanical behaviour of the rock mass. Statistical analysis (ANN) was performed to estimate the rock properties i.e., uniaxial compressive strength, point load strength index, and Brazilian tensile strength based on the texture and composition of the rock mass. Several researchers have also established ANN predictive models to evaluate the physico-mechanical properties of rock mass such as static modulus of elasticity (E), uniaxial compressive strength, density, shore scleroscope test hardness, shear strength, slack durability and point load strength index many other complex properties of rock mass (Sarkar et al. 2010; Dehghan 2010; Zorlu et al. 2008; Sonmez et al. 2006; Tiryaki 2008a; Tiryaki 2008b; Tiryaki et al. 2011; Ocak & Seker 2012).

Yilmaz & Kaynar (2011) developed prediction equations for rock mass from soft computing methods. The neuro-fuzzy and ANN techniques were used to predict the swell percentage of the soil. It was concluded that these soft computing techniques are useful for reducing the uncertainties in the geotechnical applications.

However, some of studies reported the utility of the perceptible noises to estimate of the rock bursts in the metal mines and derived relationships between the geomechanical rock materials and acoustic emission for prediction of rock the rock properties (Obert 1941; Obert and Duvall 1942; Rafavich et al. 1984; Hardy 1972; McNally 1990; Milkusova et al. 2006; Krepelka and Futo 2007; Gradl et al. 2007; Zborovjan 2001; Zborovjan 2002; Zborovjan et al. 2003; Flegner et al. 2014; Flegner et al. 2019; Liu et al. 2019).

Vardan and Murthy (2007) conducted a laboratory experiment to predict rock properties with equivalent noise levels generated by jackhammer percussive drilling.

After many researchers developed mathematical models for prediction of rock mass properties (Vardhan and Murthy 2007; Vardhan et al. 2007; Kumar et al. 2011a; Kumar et al. 2011b; Kumar et al. 2013a; Kumar et al. 2013b; Kumar et al. 2011c; Kivade et al. 2015; Shreedharan et al. 2014; Masood 2015; Delibalta et al. 2015; Kahraman et al. 2013; Alvarez et al. 1999; Finol et al. 2001; Gokceoglu 2002; Hu et al. 2019; Hassanpour et al. 2011; Teymen 2019; Krúpa et al. 2018; Omar et al. 2018; Aldeeky and Hattamleh 2018; Cao et al. 2010; Liao et al. 2018).

The literature suggests that the ANN modelling approach is more advanced than the conventional statistical techniques (ex: regression). The use of neural networks reduces the potential inconsistency of correlations. However, predictions of rock properties using ANN have not been used in the rock mechanics using dominant frequencies of acoustics.

Most of the previous investigators utilised an equivalent sound level for predicting physico-mechanical rock properties while some of them used frequency analysis for rock identification/rock type. The audio signal processing from rock drilling operations has not been investigated in detail, although it was suggested to carry out work in this direction, as Kumar et al. (2011b). Hence, the objective of this investigation was to predict the physico-mechanical rock properties using dominant frequencies from rock drilling operations using frequency analysis with the help of audio signals.

CHAPTER - 3

METHODOLOGY

3.1 Equipment Used

3.1.1 CNC drilling machine



Figure 3.1: BMV 45 T20 CNC drilling machine

A BMV 45 T20 CNC machine, which is highly automated (Fig.3.1) was used for all rock drilling experiments. The CNC machine had 450 mm x 900 mm table size, 6 bar optimum air pressure and was connected to a 415 V, 3 Phase and 50 Hertz power supply. The experiment chamber was covered completely with glass and fiber panels with dimensions of 6 m length, 5 m width and 9 m height.

3.1.2 Data acquisition system

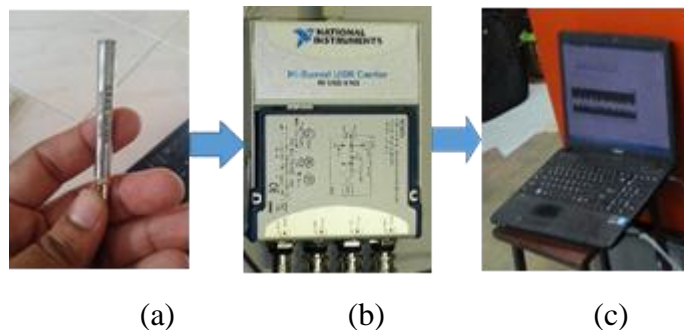


Figure 3.2: Data acquisition system

The data acquisition system measures the sound pressure using a computer interface. It consists of a computer, a microphone and a data acquisition card hardware along

with a Labview software. It is an effective measuring instrument compared to the traditional measurement systems (Forouharmajd et al. 2015). The Labview software is a flexible software for the analysis of any measurement system. The microphone G.R.A.S. Type 40 PH and the data acquisition cards NIUSB – 9234 (from national instruments) as shown in Fig. 3.2 were used for measuring the sound pressure level in the diamond drilling operations. The microphone was highly sensitive for recording accurate sound pressure levels (audio signals) from the diamond drilling operations. The specifications of G.R.A.S. type 40 PH microphone and data acquisition card hardware NIUSB-9234. Are as follows:

The microphone specifications:

Frequency range = 10 Hz to 20 KHz

Dynamic range = 32 dB (A)–135 dB

Sensitivity = 50 mv/pa

The data acquisition card NIUSB-9234 specifications:

No. of channel = 4 analogue input channels

ADC resolution = 24 bits

Type of ADC = delta-sigma (with analogue prefiltering)

3.1.3 Noise dosimeter



Figure 3.3: Noise dosimeter (Spark 705+)

The spark 705+ (Larson Davis, USA) RC personal noise dosimeter (Fig. 3.3) is one of the popular noise exposure measurement instruments. It has advanced features with an

ergonomic design. It consists of high visibility of graphical LCD display, which delivers back lighting, allowing high visibility in any environment. The instrument provides options in English for fast and easy setup and simple control during noise measurement. For multiple simultaneous dose calculations, ceiling and peak level displays and continuous data logging, the 705 RC computes compliance results for any standard – present or proposed – and with quick download using Blaze software. The instrument gives the noise dose brief reports and colour graphs for analysis. These reports can be downloaded directly from personal computer, using the Blaze software.

3.1.4 Sound level calibrator

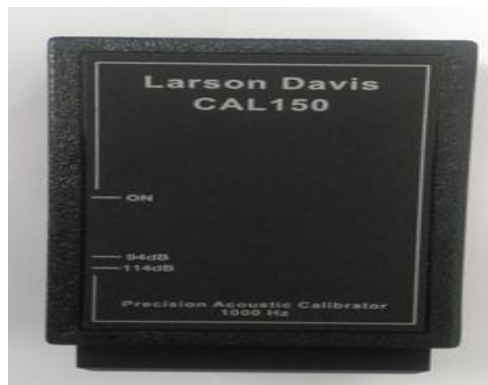


Figure 3.4: Sound calibrator (CAL-150)

The sound level calibrator (Larson Davis - CAL150) was used for microphone calibration purpose. It provides an output level range of 94.0 dB to 114.0 dB, with a switch selectable at a frequency range of 1 kHz. The sound level calibrator (Fig.3.4) is designed for laboratory and field use; its accuracy has been calibrated to a reference traceable to the National Institute of Standards and Technology.

Specifications of the calibrator CAL 150:

- Sound level calibrator CAL 150: Class 2 type
- User selectable dual output levels: 94.0 dB and 114.0 dB
- Output frequency range: 1 kHz
- Internal batteries for portable operation opening for use with 1/2 microphones

3.1.5 Compression testing machine



Figure 3.5: HEICO, Compression testing machine

Uniaxial compressive strength (UCS) is the mechanical property of rocks. The compression-testing machine (Fig.3.5) was used to measure UCS of the prepared cylindrical core rock specimens as per the ISRM's suggested methods (Brown 1981). The maximum loading capacity of the compression-testing machine was 2,000 kN.

3.1.6 Brazilian tensile strength testing machine



Figure 3.6: Brazilian Tensile Strength Testing Machine

The tensile strength of the prepared rock specimens was determined indirectly by the Brazilian tensile strength testing machine as per the ISRM's suggested methods (Brown 1981 and Mellor and Hawkes 1971). The Brazilian tensile testing machine, as shown in Fig.3.6, has upper and lower jaws along with a guide pin. A hydraulic jack (100 kN) is fixed in the middle of the jaws between the guide pin. This hydraulic jack consists of an oil reservoir, an integral pumping unit and an operating handle. On

the top of the machine, the pressure gauge (100 kN) is fixed to the jack for displaying the load on the specimen.

3.1.7 Los Angeles abrasive testing machine



Figure 3.7: Los Angeles abrasive machine

The abrasion of the rock samples was determined as per ISRM suggested methods using Los Angeles abrasion testing machine (Fig.3.7). It has a hollow cylinder with both ends closed. The inside length and diameter of the cylinder is $508\pm 5\text{mm}$ and $711\pm 5\text{mm}$. The cast iron spheres are used for abrasion charge weighing between 390 and 445 grams.

3.1.8 Dynamometer



Figure 3.8: Drill tool dynamometer, Model-601C

An IEICOS cutting tool dynamometer (model 601C-sensor type) was used to measure thrust and torque, during the drilling operation. The important specification of dynamometer is: Thrust is 5000 N, Torque is 200 Nm. The cutting tool dynamometer calibration chart as shown in Table 3.1. The dynamometer was fixed directly on the

drilling machine table using the slots provided. On the top of this dynamometer, the vice was fixed directly with the help of two long nuts and bolts as shown in Fig.3.8. The cutting tool dynamometer measured simultaneously two forces in mutually perpendicular directions: vertical thrust and rotating torque. The direction of force/thrust measurement was vertically downwards and torque was in a clockwise rotation direction.

Table 3.1: Calibrations chart of cutting tool dynamometer

Applied Load (kg)	Thrust (N)	Applied load (kg)	Torque (N-m)
0	0	0	0
50	494	0.5	5
100	1052	1	10
150	1534	1.5	15
200	2040	2	20
250	2515	2.5	25
300	2990	3	30
350	3480	3.5	35
400	3996	4	40
450	4426	4.5	45
500	4996	5	50

3.1.9 Impact strength index testing machine



Figure 3.9: Impact strength index testing equipment

The impact strength index equipment consists of vertical steel cylinder of 44.5 mm internal diameter closed at upper end by a screw cap and fixed permanently at the

bottom. A steel plunger of 1.8 kg in mass and 4.3 cm diameter at the bottom fits loosely inside the hollow cylinder. A steel cap is provided through which a plunger handle moves to prevent the dust escaping from the steel cylinder. The steel cap prevents hammer from coming out of the cylinder.

3.2 Experimental Procedure

3.2.1 Rock samples used in the investigation

The experiments were conducted using prepared cubical shaped rock blocks of 20 cm length x 20 cm width x 20 cm height (Kumar et al. 2011). A total of five different cubical-shaped rock blocks were used in these experiments. These blocks were collected from different construction sites in Andhra Pradesh and Karnataka. Table 3.2 gives the location and rock block types collected. The collected cubical-shaped rock blocks were inspected for any macroscopic (visible) defects, fractures and joints before conducting the experiment.

Table 3.2: Location and types of collected rock block

Sl.no	Location	Rock type
1	Veldurthy (Village) / Kurnool (District) Andhra Pradesh state, India	Ochre
2	Khammam (Village) /Kothagudem (District) Telangana State, India	Bituminous coal
3	Padubidri (Village) /Udupi (District) Karnataka state, India	Laterite
4	Bethamcherla (Village) / Kurnool (District) Andhra Pradesh state, India	Pink limestone
5	Bethamcherla (Village) / Kurnool (District) Andhra Pradesh state, India	Black limestone
6	Bethamcherla (Village) / Kurnool (District) Andhra Pradesh state, India	Hematite
7	Bethamcherla (Village) / Kurnool (District) Andhra Pradesh state, India	Dolomite

3.3 Determination of Physico-Mechanical Properties of Rocks

The rock properties were determined as per ISRM suggested methods, as listed in Table 3.3.

Table 3.3: Rock properties

S. No	Name of rock sample	Rock properties				
		UCS (MPa)	BTS (MPa)	Density (g/cm ³)	Abrasivity (%)	Impact Strength Index (%)
1	Ochre	14.77	1.02	2.38	70.84	50.00
2	Bituminous coal	16.37	1.09	1.75	57.25	59.90
3	Laterite	39.99	1.87	2.93	50.66	61.98
4	Pink limestone	51.49	2.32	2.49	23.52	70.00
5	Black limestone	53.01	2.66	2.62	18.29	68.00
6	Hematite	120.25	7.54	3.60	16.29	70.50
7	Dolomite	127.74	7.62	3.01	10.98	74.50

3.3.1 Determination of uniaxial compressive strength

The capacity of a rock to sustain the compressive load is known as the compressive strength of the rock. The uniaxial compressive strength (UCS) of rock specimen was determined as per the ISRM's suggested methods (Brown 1981). For this, NX size oven-dried cylindrical core specimens of 54 mm in diameter and a ratio of 2.5: 1 length to diameter were prepared in the laboratory. The load was continuously applied until the failure occurred on the prepared rock core specimens, and the corresponding total applied load (kN) on the specimen was recorded. The uniaxial compressive strength was calculated by the maximum load applied on the specimen, until failure divided the cross-sectional area of the specimen. Five tests were carried out on each type of rock core specimen and the mean value of the uniaxial compressive strength of different rocks was considered for the analysis.

3.3.2 Determination of Brazilian tensile strength

The capacity of a rock to withstand the load that pulls apart is known as its tensile strength. Rock core specimens of 54 mm diameter (NX-size) and thickness approximately equal to specimen radius were prepared as per the ISRM's suggested methods (Brown 1981 and Mellor and Hawkes 1971). The cylindrical surfaces were

prepared to avoid irregularities around the thickness of the specimen using a polishing machine in laboratory, and the end faces were made flat within 0.25 mm and parallel to within 0.25⁰. The specimen was loaded onto the Brazilian tensile strength testing machine across its diameter. The load was applied continuously until the specimen failed, and the maximum load at failure (kN) was recorded. Ten tests were carried on each type of rock core specimen and the mean value of tensile strength was determined. The Brazilian tensile strength data was obtained by the following equation:

$$\text{Brazilian tensile strength } (\sigma_t) = 0.636 P/D t \text{ (MPa)} \quad (3.1)$$

Where, P = the load at failure (N)

D = the diameter of the test specimen (mm)

t = the thickness of the test specimen measured at the centre (mm)

3.3.3 Determination of density

Density is a measure of mass per unit volume and is represented by ' ρ '. The SI unit of density is kg/m³, and it is frequently expressed in g/cm³. The density of rocks often varies due to their porosity. The density of every rock core specimen was determined after the removal of moisture from it (Ulusay and Hudson 2007). The dry density data were obtained by the following equation:

$$\text{Density of rock } (\rho) = \text{Mass of the specimen} / \text{Volume of the specimen (kg/m}^3) \quad (3.2)$$

Where, M = mass of the specimen (kg)

V = Volume of the specimen (m³)

3.3.4 Determination of abrasivity

Los Angeles abrasion defined as the resistance to wear abrasion of rock aggregates. Initially, various types of rock aggregates were prepared as per ISRM standards (i.e., sieve passing through 25.4 mm hole size, retained on 19.0 mm hole size). The rock aggregates with 1250±25 g were placed in the Los Angeles abrasion testing machine and tightly locked. The cylindrical drum was permitted to rotate at 500 revolutions at a constant speed of 30-33 rpm. After discharge, the material was sieved on 1.7 mm

sieve. The rock aggregates coarser than 1.7 mm was washed substantially weighted to nearest gram to determine of Los Angeles abrasion percentage wear.

$$\text{Wear (\%)} = \frac{\text{Original weight} - \text{Final weight}}{\text{Original weight}} * 100 \% \quad (3.3)$$

3.3.5 Determination of impact strength index

Impact strength index (ISI) is an important property of a rock mass and it is used widely in geotechnical engineering. Initially, the rock samples collected from mines and sieved through 2.54 cm. The oversized material was broken to obtain maximum yield of fragments under 2.54 cm. The 0.95-0.32 cm fractions were then removed from broken material by hand sieving. A sample of 100 g was carefully weighted using weighing machine. The 100 g sample was poured into hollow cylinder, which was placed a level of floor. Keeping the cylinder steady by feet, the plunger was raised to the fully extent and allowed to drop it freely 20 times. Finally the cap of plunger was removed and the sample was sieved through a 300 micron size sieve. The impact strength index was obtained by calculating the ratio of final weight to the initial weight.

$$\text{ISI (\%)} = \frac{\text{Weight of the sample retained through 300 } \mu\text{m sieve after experiment}}{\text{Weight of the sample taken, 100 g}} * 100 \% \quad (3.4)$$

3.4 Experimental Set-Up

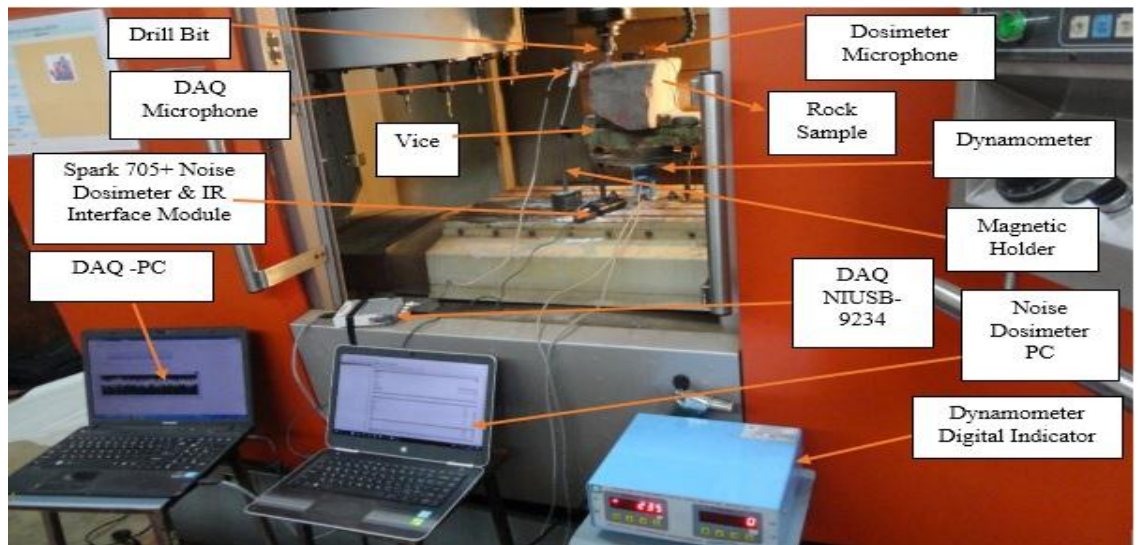


Figure 3.10: Experimental set-up of BMVK 45 T20 CNC drilling machine

Fig.3.10 shows the experimental set-up for carrying out drilling using the CNC machine on rock blocks and sound pressure level measurement. Fig.3.10 also shows a dynamometer and a dynamometer digital indicator, a noise dosimeter with a microphone and a dosimeter PC that were used for the purpose of determination of specific energy and A-Weighted sound levels. The rock blocks were held at a particular position firmly during drilling using a vice and two long nuts and bolts. In this investigation, drill bits of diameters 6, 10, 16, 18 and 20 mm (industrial diamond core drill bit) at speeds of 150, 200, 250, 300 and 350 rpm and penetration rates of 2, 3, 4, 5 and 6 mm/min were used for all the rock drilling operations. The CNC machine was set to drill 30 mm drill hole length throughout the experiments.

The microphone of the data acquisition system (DAQ-NIUSB-9234) was held at a distance of 1.5 cm from the drill bit with the help of a magnetic holder. The DAQ microphone was connected to DAQ-NIUSB-9234 with 1-channel cable, which was in turn connected to a personal computer with windows operating system (64-bit) using the USB cable. The data recorded using the data acquisition system can be visually seen on the data acquisition personal computer (DAQ-PC).

3.5 Sound Pressure Level Measurement

The sound pressure level was measured for all bit-rock combinations using the DAQ microphone by means of the Labview software. For all sound pressure level measurements, the microphone was set aside at a distance of 1.5 cm from the outer edge of the drill bit diameter, as shown in Fig.3.10. The audio signals during drilling was recorded by the microphone to the computer using the DAQ NIUSB-9234 (data acquisition module from national instrumentation) 24-bit ADC (Analog to digital converter), which allowed capturing 51,200 samples within one second. The resolution of the response was maintained at 1Hz by reading all the samples, which were obtained in one second. This module was connected to the system, and the data was obtained using serial communication. Fast Fourier transformation (FFT) was used to obtain the dominant frequencies with their amplitude of sound pressure level. Graphical programming language software (NI Labview) was used for signal analysis to capture accurate signals from the diamond core drilling operations. The audio signals during drilling were measured up to a drilling depth of 30 mm (required time to drill 30 mm depth hole is around 300 seconds). The sound pressure level data (dB) was obtained by the following equation:

$$\text{The sound pressure level (SPL)} = 20 \log_{10} (P_{r.m.s}/P_{ref}) \text{ (dB)} \quad (3.5)$$

Where, $P_{r.m.s}$ = the Sound pressure measured in root mean square (r.m.s)

$$P_{ref} = \text{reference sound pressure } (2 \times 10^{-5} \text{ N m}^{-2} \text{ or } 20 \text{ } \mu\text{Pa})$$

3.6 Determination of the Dominant Frequencies of audio signals from rock drilling operations

The drilling audio signals captured from rock drilling operations were analysed using fast Fourier transformations (FFT). The acquired data from the microphone (Fig.3.11a) was put onto a fast Fourier analyser to convert the time domain signals to frequency domain signals. Append signals toolkit (Fig.3.11b) was also used to understand the time domain response of the whole signal, and FFT was conducted based on the peak amplitude observed from the time domain plots. The FFTs were obtained after filtering the raw data obtained from the experimental measurement. A Butterworth band pass filter (Fig.3.11b) was used to ensure that the FFT was free

3.7 Determination of A-weighted Equivalent Sound Pressure Levels

Sound levels were measured for the rotation speeds of 150 rpm, 200 rpm, 250 rpm, 300 rpm and 350 rpm and penetration rates of 2, 3, 4, 5 and 6 mm/ min on each rock block. For each combination of drill bit diameter, drill bit speed and penetration rate, a total of 125 sets of test conditions were arrived at for drill bit diameters of 6 mm, 10 mm, 16 mm, 18 mm and 20 mm. A-weighted equivalent continuous sound level (L_{eq}) was recorded for all 125 different drill holes of 30 mm depth on each rock block. The data for seven rock types were used to develop the model for prediction of specific energy during diamond drilling operations. So in a total 875 (i.e. $125 \times 7 = 875$) L_{eq} (Equivalent sound level) values were used to develop the multiple linear regression models. For all measurements, the sound level meter was kept at a distance of 1.5 cm from the periphery of the drill bit (Fig. 3.10). For a particular condition and for the same rock block, the sound level was determined five times in relatively rapid successions. The recorded equivalent sound levels were almost consistent.

3.8 Determination of Specific Energy

Specific energy (SE) is defined as the energy required for removing a unit volume of rock. For determination of SE, a cutting tool dynamometer was used to measure thrust and torque force during diamond core drilling operations. The dynamometer was fixed on the work table above which the vice was fixed. The cubic rock sample (20cm X 20cm X 20cm) was fixed firmly between the vice jaws. The experimental set up is shown in Fig. 3.10. During drilling operation, thrust and torque are recorded for all 125 different drill holes of 30 mm depth on each rock block (combination of drill bit diameter, drill bit speed and penetration rate). SE was determined by the following equation:

$$\text{Specific energy (S.P.E)} = E / V \quad \text{Nm/m}^3 \quad (3.6)$$

Where, E = Energy consumed (Nm)

F = Force (N)

D = Depth of the cut (m)

V = Volume of the rock broken (m^3)

3.8.1 Details of parametric variation for determination of specific energy

Table 3.4: Details of parametric variation for determination of specific energy

Parameters	Variables
Laboratory investigations	
(A) Drilling experiments	
(a) Bit parameters	
1) Bit type	Diamond core drill bits
2) Bit geometry	Circular with industrial diamond
3) Bit diameter	5 different diameters (6 mm, 10 mm, 16 mm, 18 mm, and 20 mm)
(b) Operational Parameters	
1) Penetration rate	Five magnitudes (2 mm/min, 3 mm/min, 4 mm/min, 5 mm/min, and 6 mm/min)
2) Drilling speed(RPM)	Five magnitudes (150 rpm, 200 rpm, 250 rpm, 300 rpm, and 350 rpm)
3) Depth of the hole	30 mm
(c) Rock parameters	
1) Type	Ochre, bituminous coal, laterite, pink limestone, black limestone, hematite, dolomite
2) Rock properties considered	Uniaxial compressive strength, Brazilian tensile strength, density, abrasivity, impact strength index
(d) Measured parameters	Noise levels, thrust, torque, specific energy
(e) Drilling conditions	Dry condition

3.9 Analytical Techniques

Simple and multiple linear regressions, multiple regression analysis and ANN are powerful tools for deriving mathematical relationships between the several dependent and independent variables. It provides information about independent variables and their uses to make much more powerful and accurate predictions of the dependent variables. The mathematical modelling for dominant frequencies, A-weighted equivalent sound levels produced during rock drilling, was carried out using SPSS Statistics 20, ANN, and Minitab17.

3.9.1 Modeling of physico-mechanical properties of rocks

Rock properties prediction models were developed in three cases using DAQ microphone with the help of Labview software i.e.

- (i) At a constant drill bit diameter of 20 mm, a speed of 350 rpm, and a penetration rate 6 mm/min. The audio signals during drilling were measured up to a drilling depth of 30 mm (required time to drill 30 mm depth hole is 300 s corresponding to ochre, bituminous coal, laterite, pink limestone, and hematite respectively).
- (ii) At a few experimental combinations by varying drill bit diameters of (6, 10, 16, 18 and 20 mm), speeds of (150, 200, 250, 300, and 350 rpm), penetration rates of (2, 3, 4, 5 and 6 mm/min). In this investigation, the drilling times of 40 s, 30 s, 24 s, 20 s, and 17 s, correspond to ochre, bituminous coal, laterite, pink limestone, and hematite respectively.
- (iii) The audio signals produced during drilling were measured for 60 seconds for various drill bit diameters, penetration rates, and spindle speeds (i.e., combinations of the drill bit diameters of 6 mm, 10 mm, 16 mm, 18 mm, and 20 mm at penetration rates of 2 mm/min, 3 mm/min, 4 mm/min, 5 mm/min, and 6 mm/min and speeds of 150 rpm, 200 rpm, 250 rpm, 300 rpm, and 350 rpm) correspond to ochre, bituminous coal, laterite, pink limestone, black limestone hematite and dolomite. Hence, for each rock type, a total of 125 test conditions were arrived at: For each rock = 125 test conditions, Total: seven (7) different rock types \times 125 = 875 test conditions were used to predict rock properties.

3.9.2 Development of simple linear regression models

It is a statistical approach that permits to recapitulate and study relationships between two (dependent and independent) quantitative variables. The simple linear regression equation is generally expressed as:

$$Y = \beta_0 + \beta_1 x_1 + \text{error} \quad (3.7)$$

Where Y denotes dependent variables, x_1 indicate independent variables and β_0 , β_1 , indicate the regression coefficients in the model. Simple regression analysis was carried out to predict rock properties. The mathematical modeling for dominant

frequencies produced during rock drilling was carried out using SPSS Statistics 20. For development of prediction models, the independent variable considered as input parameters i.e., dominant frequencies (Hz). The dependent variable was UCS, BTS, and density.

3.9.3 Development of multiple linear regression models

Multiple linear regression analysis was carried out to predict specific energy (SE). A number of statistical parameters or terms are associated with the multiple linear regression analysis. Some of the most important ones include the coefficient of multiple determinations, confidence level, standard error, model error, significance level, t- distribution, F- distribution and errors (Field, 2009). Hence, a multiple linear regression model with k predictor variables X_1, X_2, \dots, X_k and a response Y can be written as:

$$Y = \beta_0 + \beta_1 x_1 + \beta_2 x_2 + \dots + \beta_k x_k + \text{error} \quad (3.8)$$

Where Y denotes dependent variables, x_1, x_2, \dots, x_k indicate independent variables and $\beta_0, \beta_1, \beta_2, \dots, \beta_k$ indicate the regression coefficients in the model.

The mathematical modeling for A-weighted equivalent sound pressure level produced during rock drilling was carried out using Minitab 2017. For development of prediction models, the independent variable considered as input parameters i.e., drill bit diameter (mm), spindle speed (rpm), penetration rate (mm/min) and A-weighted equivalent sound pressure level (dB), thrust (N), torque (Nm). The response (output) was SE.

3.9.4 Development of multiple regression models

Multiple regression analysis is one of the tools for estimating the relationship between the several dependent and independent variables. It provides information about the independent variables and their uses to make much more powerful and accurate predictions of the dependent variables. The mathematical modelling for dominant frequencies, produced during rock drilling, were carried out using Minitab17. Dominant frequencies produced during drilling depend on a number of parameters, such as drill bit diameter, spindle speed, and penetration rate. For the development of

the prediction models, four important operational parameters were used as the dependent variables (input parameters) – drill bit diameter (mm), spindle speed (rpm), penetration rate (mm/min), and dominant frequencies (Hz). The responses (output) were UCS, BTS, Los Angeles abrasion, and abrasivity. Hence, the detailed operational parameters represent a quadratic model. The quadratic model involves ‘n’ independent variables, namely $X_i, X_j \dots X_n$, and the multiple regression equation is generally expressed as:

$$Y = a_0 + \sum_{i=0}^n a_i X_i + \sum_{i=1}^n a_{ij} X_i^2 + \sum_{i < j}^n a_{ij} X_i X_j + error \quad (3.9)$$

Where, Y denotes dependent variables, $X_i, X_j \dots X_n$ indicate the independent variables, a_i is the linear parametric effect of x_i , and a_{ij} represents the quadratic effect, and the third and fourth terms represent the combination of both. The regression model includes linear, squared, and cross product terms.

3.9.5 Development of artificial neural network models

ANN is the biologically inspired computer programs designed to imitate the way in which the human brain processes information. ANN gathers its knowledge by detecting the patterns and relationships in data and learns or trained through experience. The artificial neurons were interconnected to input layer to output layer with the help of hidden layer and train the data efficiently. In this investigation multilayer perception neural network model was adopted. The network architecture panel details the particular network used to solve the problems with sigmoid activation function in the hidden and output layer. One hidden layer was used to predict the physico-mechanical properties of rocks in this investigation. The spindle speed, penetration rate, dominant frequencies and drill bit diameter were employed as input parameters while the output responses were UCS, BTS, density and abrasivity in this model. The hidden layer computes the weighted inputs and produces the net input which is then applied with sigmoid activation functions to produce the actual output. This can be written as:

$$a = f \left(\sum_{i=1}^{i=r} w_i p_i + b \right) \quad (3.10)$$

Whereas: a = neuron output, f = transfer function, w_i = weight value, p_i = input parameter, b = summed with bias.

CHAPTER-4

RESULTS AND DISCUSSION

4.1 Effect of the Operating Variables on A-weighted Sound Pressure Level

Figures 4.1a to 4.1c show the plots of A-weighted sound pressure levels against three different operational parameters, namely drill bit diameter, spindle speed and penetration rate. The plots show that the A-weighted sound pressure levels increase from 73 dB to 142 dB with an increase in the drill bit diameter, spindle speed, and penetration rate while drilling in rock samples of ochre, bituminous coal, laterite, pink limestone, black limestone, hematite and dolomite. This may be due to the significant increase in the uniaxial compressive strength of rocks and due to the increase in the drill bit diameter area which results in more friction at bit-rock interface. However, the trend of A-weight SPL with the compressive strength is inconsistent which might be due to influences of other rock properties such as abrasivity (Kivade et al. 2014), mineralogical compositions or petrographic features (grain size, grain bindings, and micro-cracking) in the rock samples (Macias, 2017). The average value of noise levels is shown in Table 4.A1 to 4.A3 in Appendix-A.

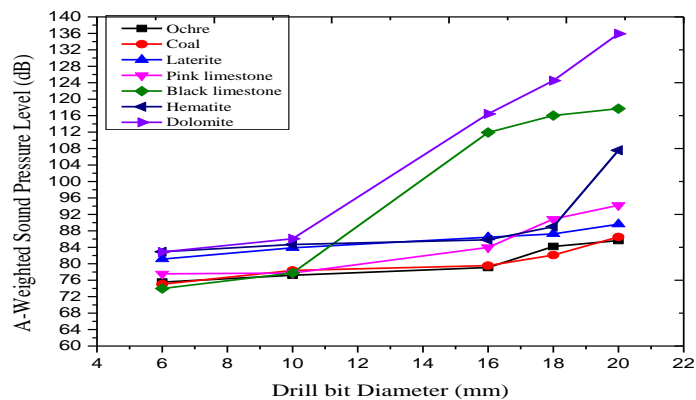


Figure 4.1a: Effect of drill bit diameter on A- weighted sound pressure level on various rock samples at 30 mm depth

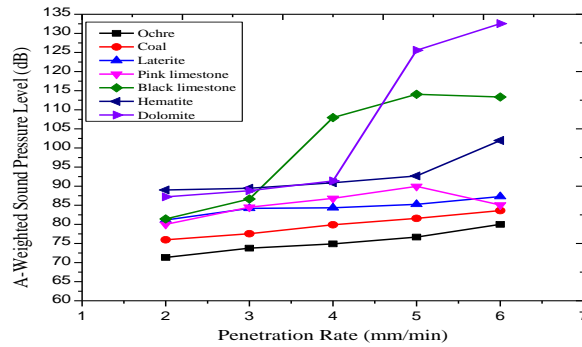


Figure 4.1b: Effect of penetration rate on A- weighted sound pressure level on various rock samples at 30 mm depth

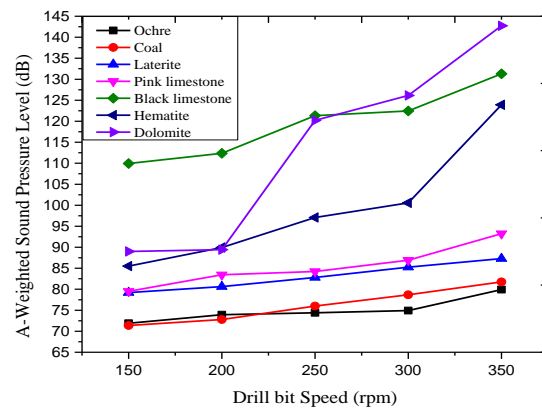


Figure 4.1c: Effect of drill bit speed on A- weighted sound pressure level on various rock samples at 30 mm depth

4.2 Effect of the Operating Variables on Specific Energy

The operating parameters have great interactions in combinations with the drill bit diameter, penetration rate, and drill bit speed. The effect of the drill bit diameter, penetration rate, and drill bit speed on specific energy in the diamond drilling operations is shown in Figures 4.2a to 4.2c. Specific energy was determined for various bit and rock combinations drill bit diameters of 6 mm to 20 mm and spindle speed of 150 rpm to 250 rpm, penetration rates of 2 mm/min to 6 mm/min.

- Figure 4.2a shows that SE decreased from 30.381 Nm/m³ to 1.672 Nm/m³ with an increase in the drill bit diameters from 6 mm, 10 mm, 16 mm, 18 mm, and 20 mm,

corresponding to ochre, bituminous coal, laterite, pink limestone, black limestone, hematite and dolomite. This is due to the increase in the drill bit diameter area, which contributes a higher volume removal rate, with consequently a decrease of SE during the drilling operation at 30 mm depth; this may be attributed to greater friction effects on the circumference of a smaller drill bit in relation to the area extracted by it (Reddish and Yasar 1996).

- Figure 4.2b shows that the SE decreased from 25.076 Nm/m³ to 1.502 Nm/m³ with an increase in the penetration rate from 2 mm/min to 6 mm/min corresponding to selected rock types. This is due to the increase in the specific removal rate, i.e. where the material drilled in unit time (Reddish and Yasar, 1996).
- Figure 4.2c shows that the SE decreased from 16.417 Nm/m³ to 1.024 Nm/m³ with an increase in the drill bit speed from 150 rpm to 350 rpm corresponding to the selected rock types. This is due to the increase in the specific removal rate, i.e. where the material is drilled in unit time (Reddish and Yasar, 1996). The average values of specific energy are shown in Table 4.A4 to 4.A6 in Appendix-A.

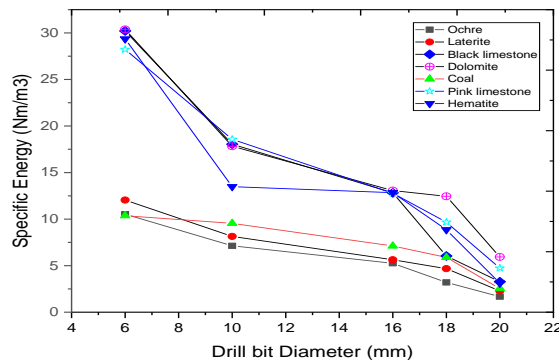


Figure 4.2a: Effect of drill bit diameter on specific energy on various rock samples at 30 mm depth

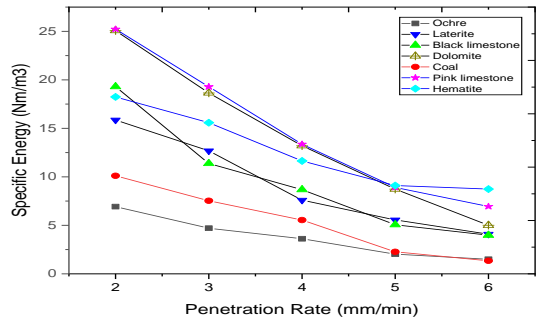


Figure 4.2b: Effect of penetration rate on specific energy on various rock samples at 30 mm depth

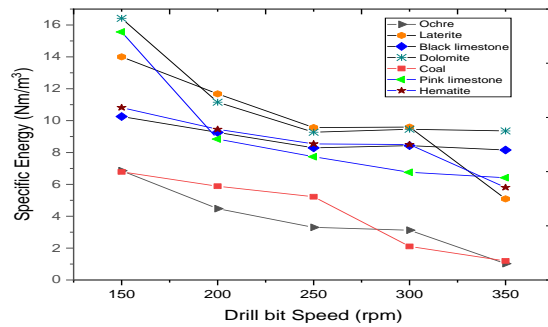


Figure 4.2c: Effect of drill bit speeds on specific energy on various rock samples at 30 mm depth

4.3 Effect of Thrust on A - weighted Sound Pressure Level

Figure 4.3a shows the plot of A-weighted sound pressure level against thrust which was varied by varying drill bit diameter. Figure 4.3b shows a similar plot of A-weighted sound pressure level versus thrust, which was obtained by the penetration rate. A similar plot of A-weighted sound pressure level is shown in Figure 4.3c, where thrust was increased by increasing the drill bit speed. These figures show that A-weighted sound pressure level increases from 71 dB to 142 dB when thrust was increases from 109.23 N to 1001.96 N while drilling in rock samples of ochre, bituminous coal, laterite, pink limestone, black limestone, hematite and dolomite. The average value of thrust which increases with the drill bit diameter, drill bit speed, and penetration rate is shown in Table 4.A7 to 4.A9 in Appendix-A. This may be due to the normal forces which maintain bit-rock contact frictional forces between diamond drill bit and rock sample. The relationships between the normal forces and tangential force are dependent on the contact friction at the bottom of the diamond drill bit (bit-

rock contact). The reason for high thrust force and the friction between the cutting side and crushed zone becomes a resistant force in the penetration process for transferring the normal force to the crushed zone (He et al. 2020). An increase in the drill bit diameter increases the thrust during drilling operations. For this reason the thrust increases corresponding drill bit diameter, drill bit speed and penetration rate.

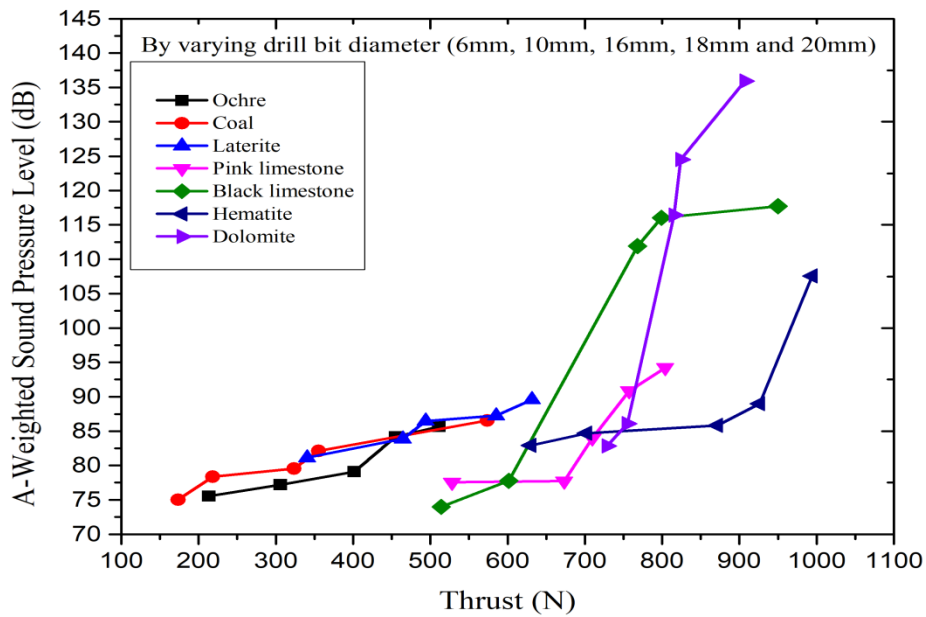


Figure 4.3a: Effect of thrust on A-weighted sound pressure level at varying drill bit diameter on various rock samples at 30 mm depth

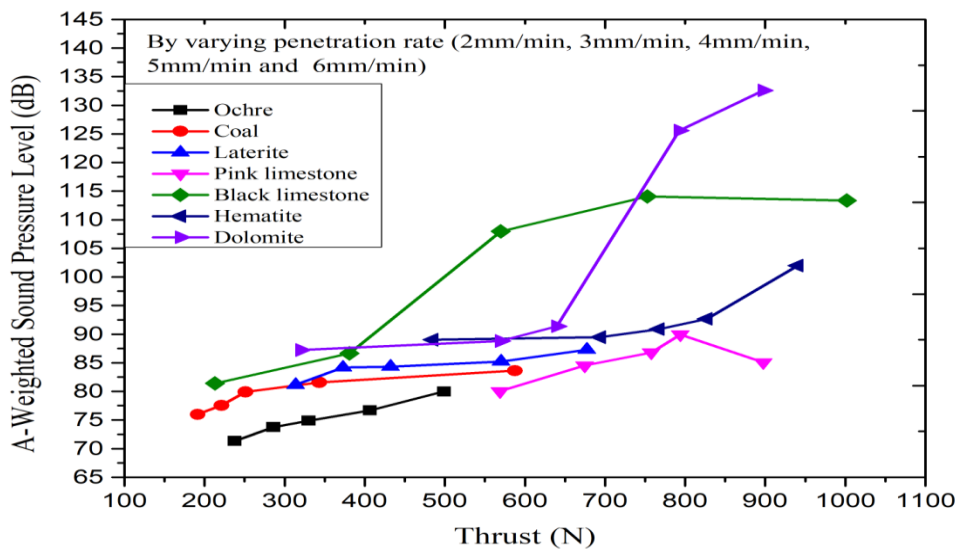


Figure 4.3b: Effect of thrust on A-weighted sound pressure level at varying penetration rate on various rock samples at 30 mm depth

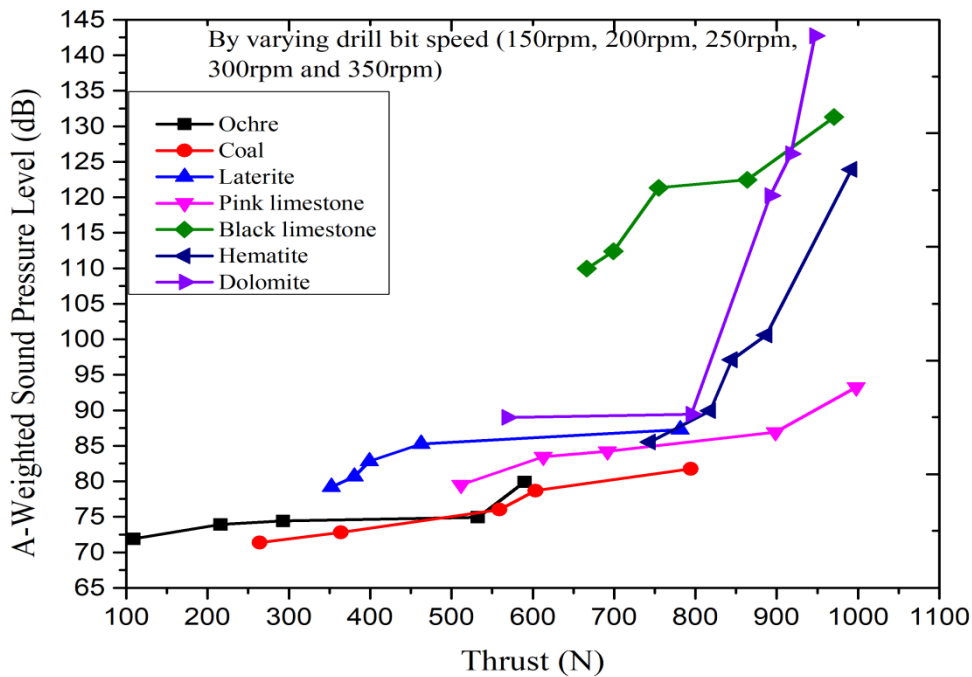


Figure 4.3c: Effect of thrust on A-weighted sound pressure level at varying drill bit speed on various rock samples at 30 mm depth

4.4 Effect of Torque on A – weighted Sound Pressure Level

Figures 4.3a to 4.3c show the plots of torque on A-weighted sound pressure levels with varying drill bit diameter, spindle speed and penetration rate. The plots show that torque and A-weighted sound pressure level increases from 2 Nm to 11.88 Nm, 71 dB to 142 dB with an increase in the drill bit diameter, spindle speed, and penetration rate while drilling in rock samples of ochre, bituminous coal, laterite, pink limestone, black limestone, hematite and dolomite. This may be due to the significant increase in the uniaxial compressive strength of rocks (hardness of the rock), The rock hardness is characterized by a high torque values for hard rock, and also observed that, low torque values for in the soft rocks (Sinkala 1990). Furthermore, the torque is applied mainly to move drill bit inserts to new surfaces (clark 1982; Lundberg 1971; Wijk 1982). Hence, apart from that mineralogical compositions or petrographic features like grain size, grain bindings, and micro-cracking also might contribute substantially for increasing the torque. The average value of torque is shown in Table 4.A10 to 4.A12 in Appendix-A.

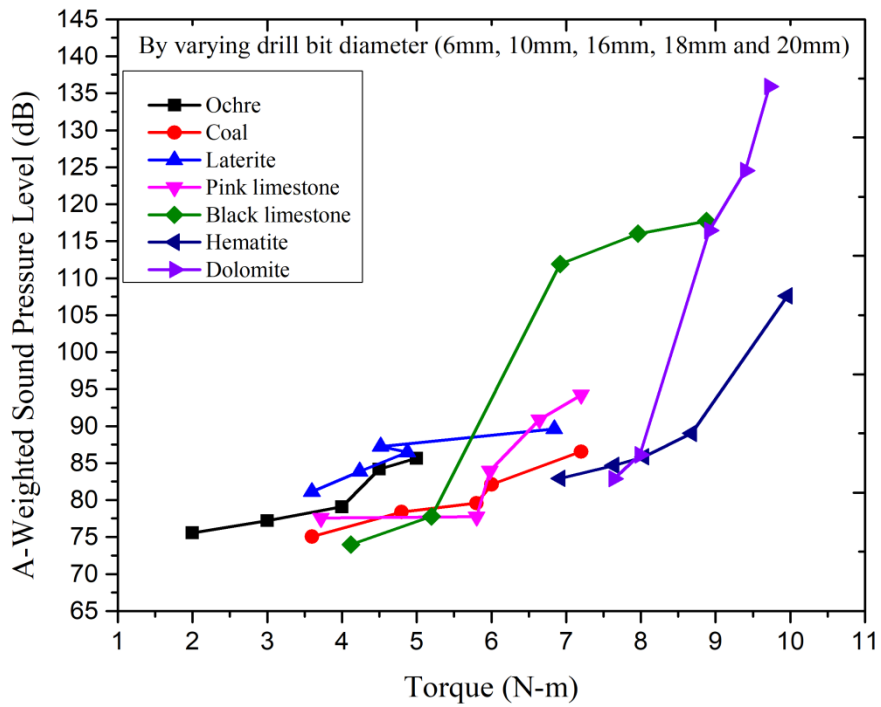


Figure 4.4a: Effect of torque on A-weighted sound pressure level at varying drill bit diameter on various rock samples at 30 mm depth

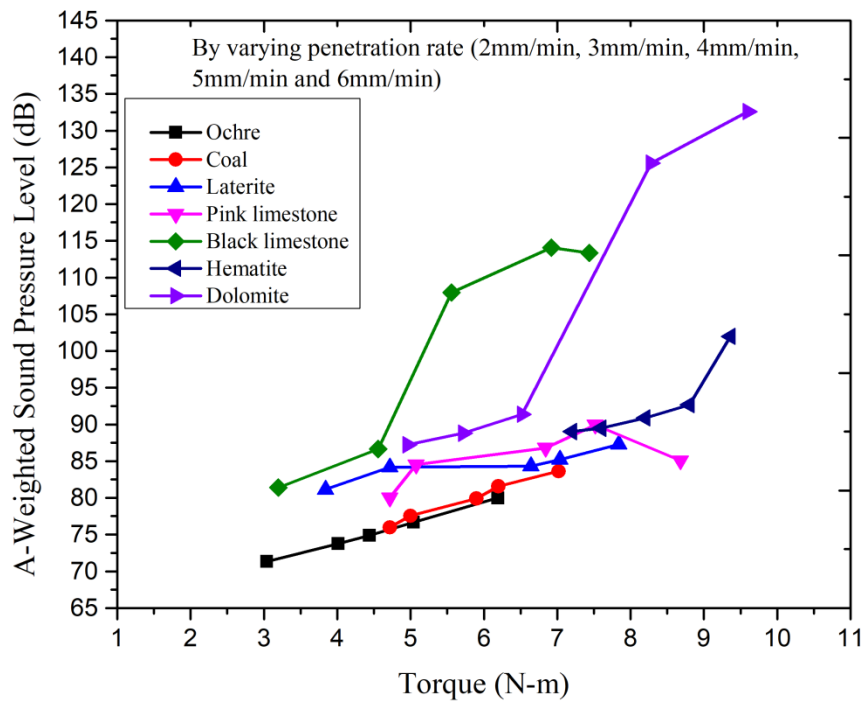


Figure 4.4b: Effect of torque on A-weighted sound pressure level at varying penetration rate on various rock samples at 30 mm depth

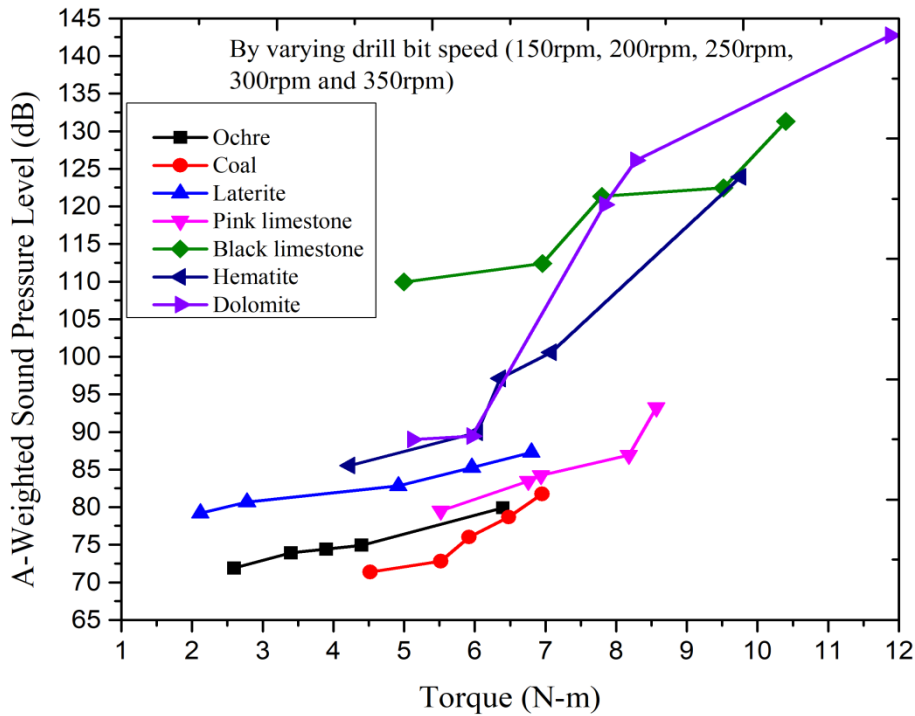


Figure 4.4c: Effect of torque on A-weighted sound pressure level at varying drill bit speed on various rock samples at 30 mm depth

4.5 Effect of Rock Properties on A-weighted Sound Pressure Level

Figures 4.5a to 4.5e show the plots of physico-mechanical rock properties on average values of A-weighted sound pressure level for various rock samples. From Figures 4.5a, 4.5b, 4.5c and 4.5e it can be observed that, the A-weighted sound pressure level increases with rock properties such as uniaxial compressive strength, Brazilian tensile strength, density, and impact strength index. Generally A-weighted sound pressure level is higher obtained when drilling in hard rocks having higher uniaxial compressive strength and density (Vardhan et al. 2009; Kivade et al. 2013; Masood 2015; Delibalta et al 2015) whereas from Fig. 4.5d it can be observed that A-weighted sound pressure level decreased with increasing the abrasivity. It may be the possible the percentage wear loss were observed in the rock samples.

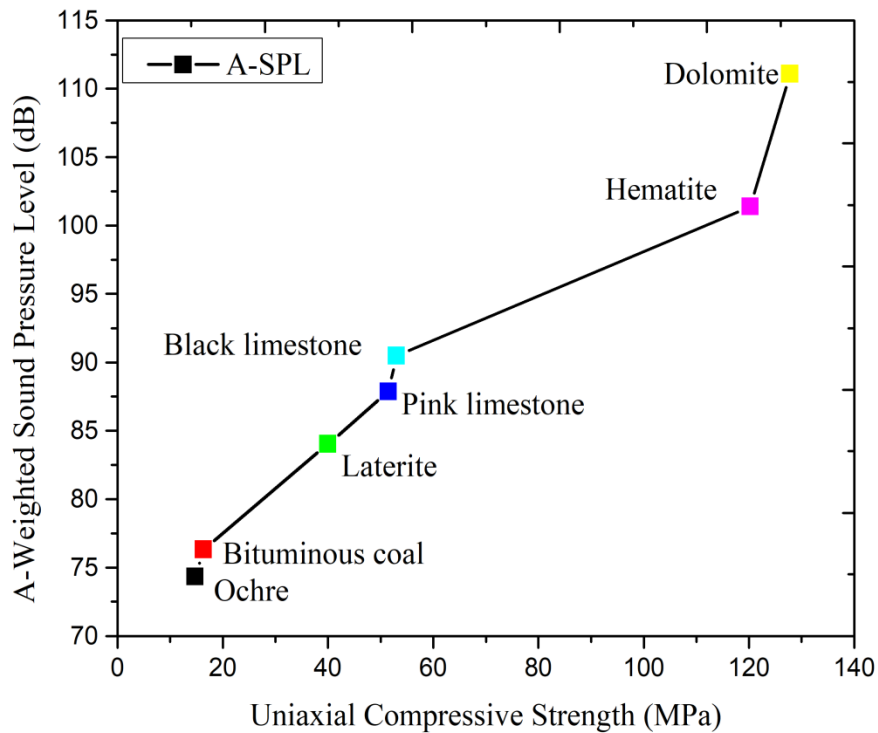


Figure 4.5a: Uniaxial compressive strength on A-weighted sound pressure level on various rock samples at 30 mm depth

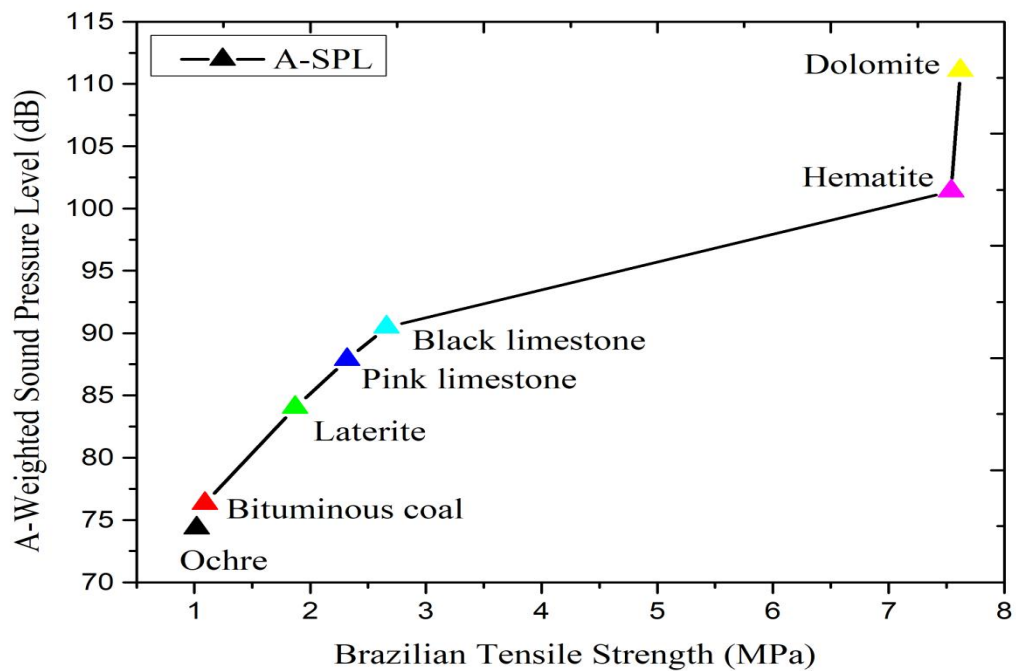


Figure 4.5b: Brazilian tensile strength on A-weighted sound pressure level on various rock samples at 30 mm depth

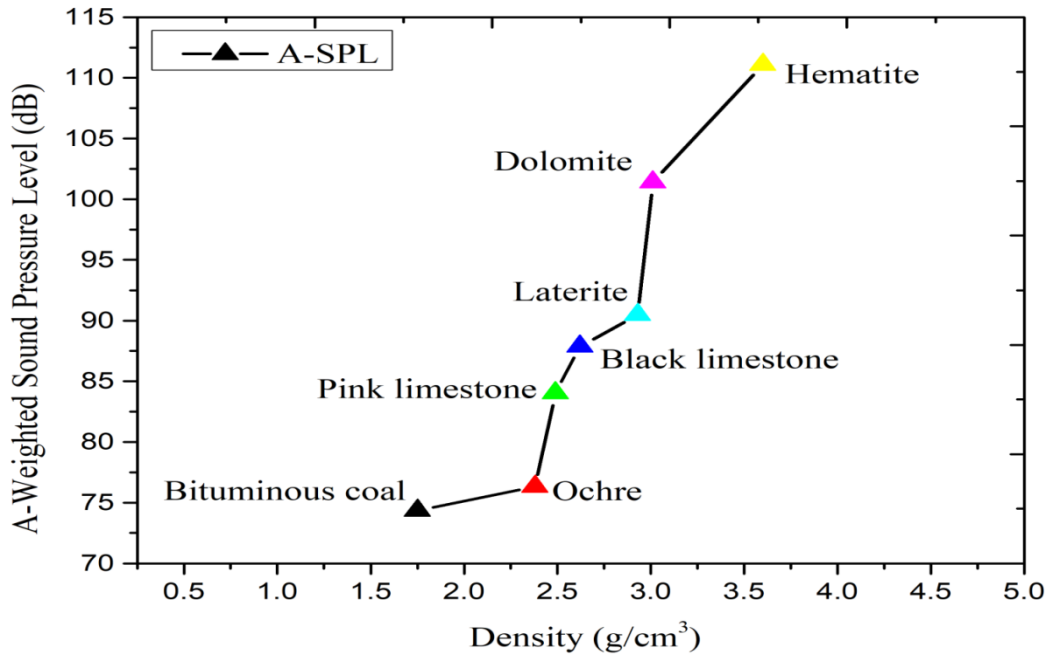


Figure 4.5c: Density on A-weighted sound pressure level on various rock samples at 30 mm depth

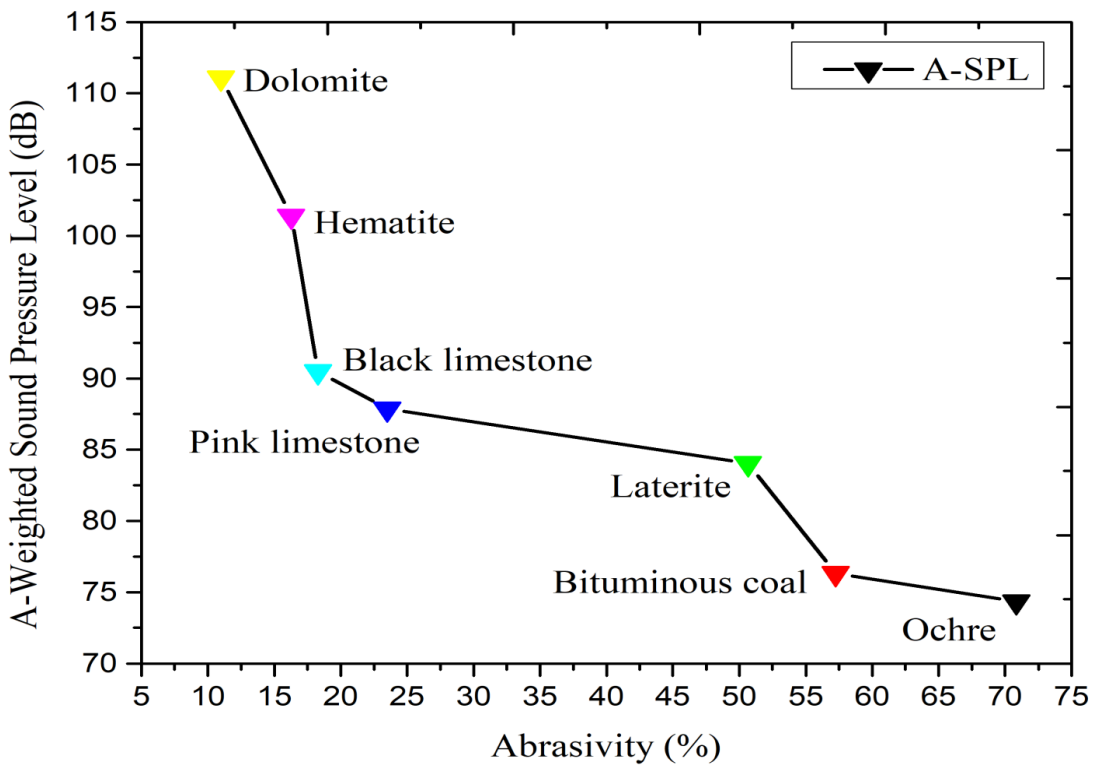


Figure 4.5d: Abrasivity on A-weighted sound pressure level on various rock samples at 30 mm depth

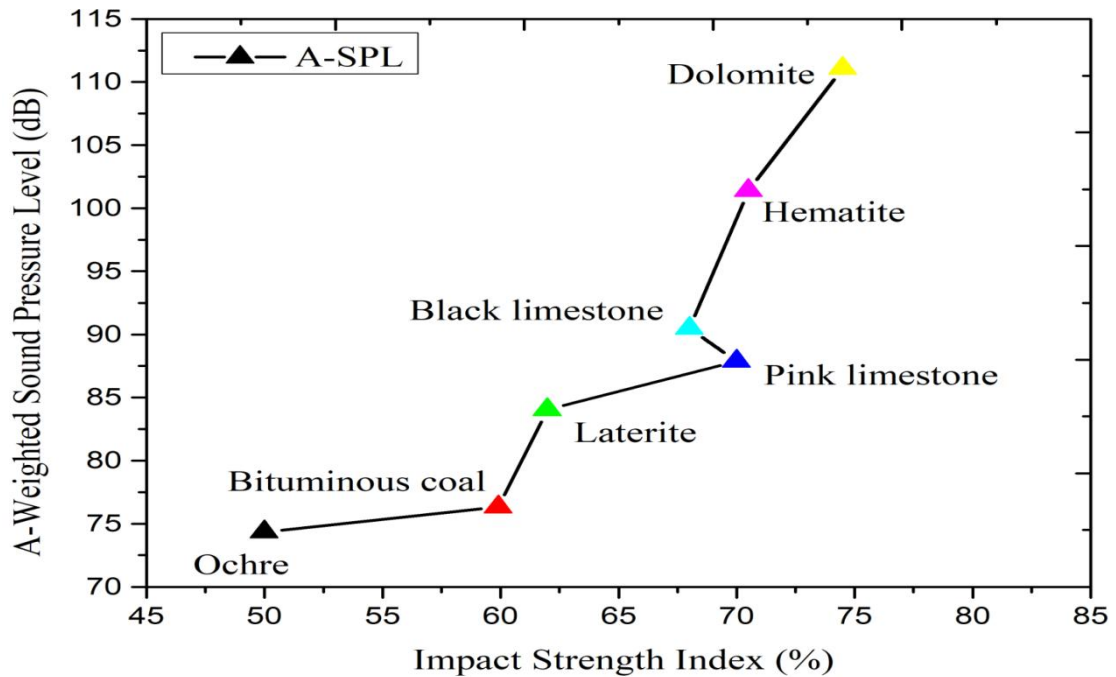


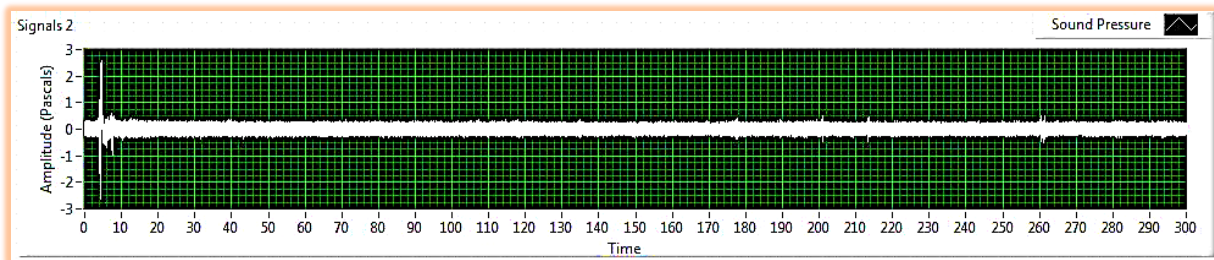
Figure 4.5e: Impact strength index on A-weighted sound pressure level on various rock samples at 30 mm depth

4.6 Development of Regression Models

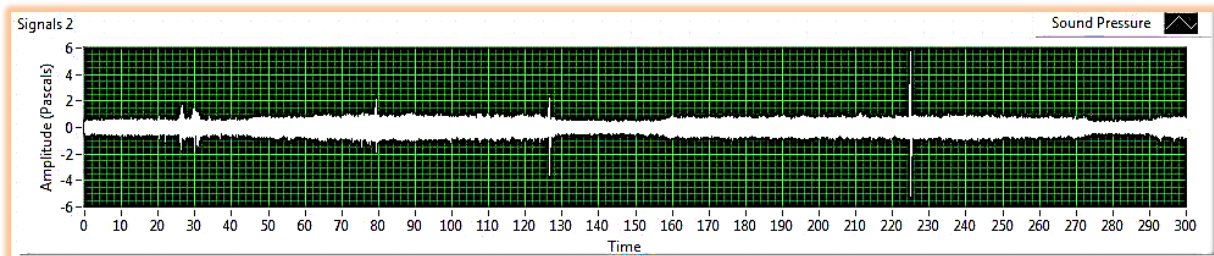
4.6.1 Development of rock properties predictive models at constant drill bit diameter, drill bit speed, and penetration rate

The drilling audio signals were analysed using fast Fourier transformations (FFT) after capturing the audio signals from rock drilling operations. The acquired data from the microphone (Figure 3.11a) was put onto a fast Fourier analyser to convert the time domain signals to frequency domain signals. Append signals toolkit (Figure 3.11b) was also used to understand the time domain response of the whole signal, and FFT was conducted based on the peak amplitude observed from the time domain plots. The FFT's were obtained after filtering the raw data obtained from the experimental measurement. A Butterworth band pass filter (Figure 3.11b) was used to ensure that the FFT is free from noisy signals with the help of the Labview software. Hence, the sound measurement is accurate, and noisy signals are avoided. The Labview block diagram code for sound signal measurement is shown in Figure 3.11a and Figure 3.11b.

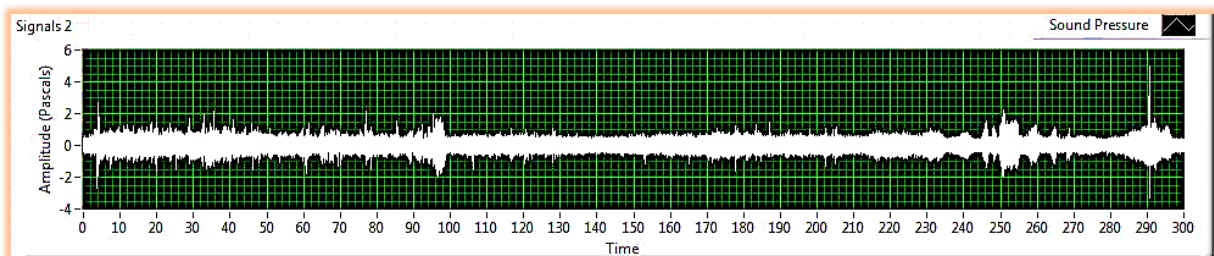
The time domain plots are shown in Figure 4.6, wherein the X-axis represents the time in seconds and the Y-axis the amplitude in Pascals. A total of 300 seconds (the required time to drill 30 mm depth hole for each of the five rock types) time domain data was selected for the analysis. The peak amplitude of FFT was selected for the analysis of 300-second time domain plots, i.e. 262nd second FFT, 225th second FFT, 291st second FFT, 65th second FFT and 189th second FFT were selected corresponding to (a) ochre, (b) bituminous coal, (c) laterite, (d) pink limestone and (e) hematite. This peak amplitude contains the maximum energy carried in the noise spectrum. All spectrogram algorithms were plotted using the Hanning function. The drilling audio recording sampling rate was 51.2 kHz per second.



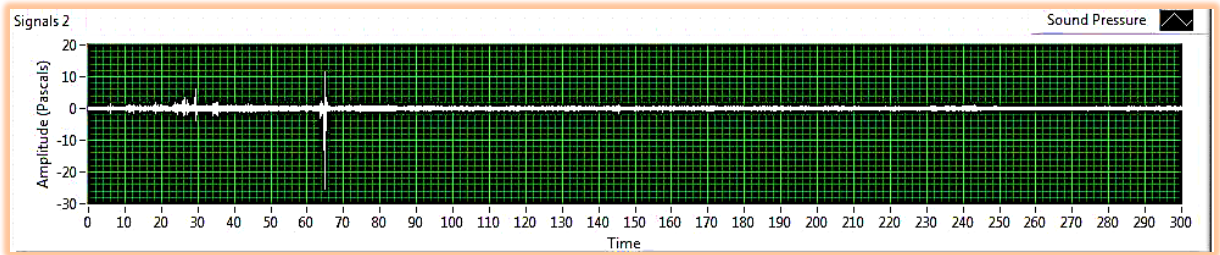
(a)



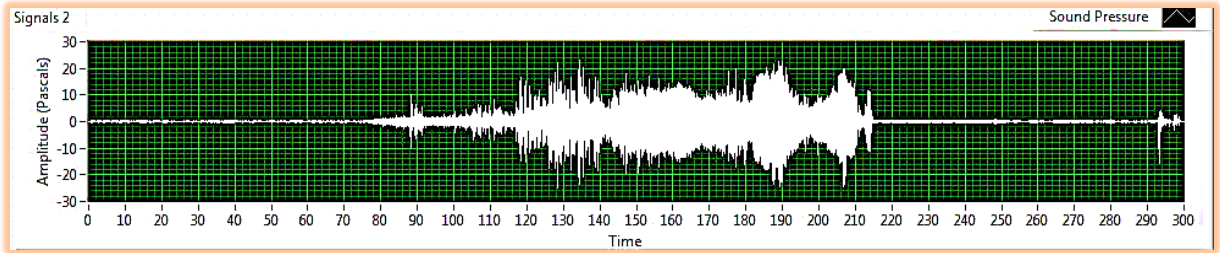
(b)



(c)



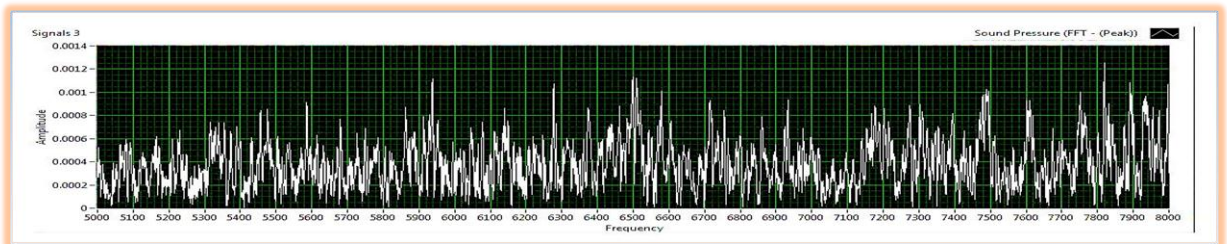
(d)



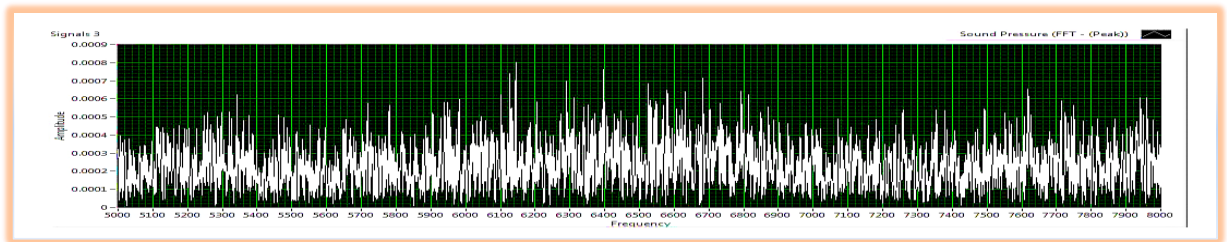
(e)

Figure 4.6: Time domain plots for various rock types i.e. (a) ochre, (b) bituminous coal, (c) laterite, (d) pink limestone and (e) hematite

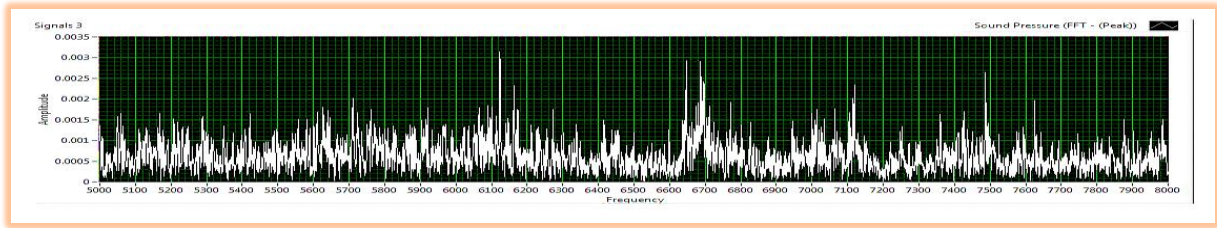
Five dominant frequencies were extracted from the frequency domain of each selected rock, where the highest sound pressure level (dB) was determined, as shown in Figure 4.7a to Figure 4.7e. These frequencies known as dominant frequencies corresponding to every rock type are given in Table 4.13. The results given in Table 4.13 are in line with Zborovjan et al. (2003), wherein it was said that the maximum information contained appropriate signal transfer. The rock drilling acoustic signature can be found between 5000 Hz to 8000 Hz.



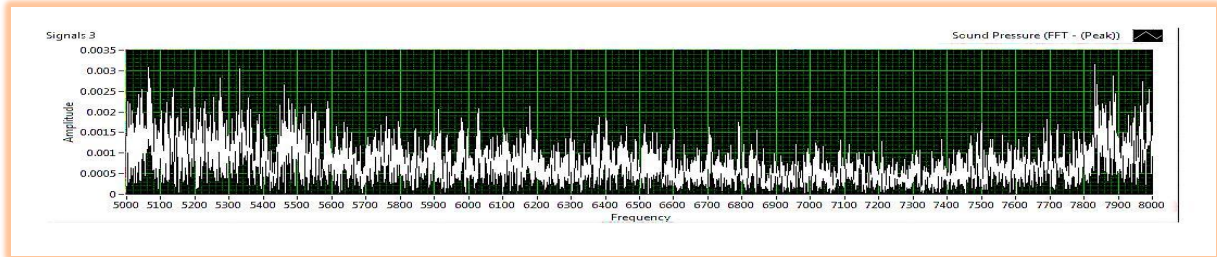
(a)



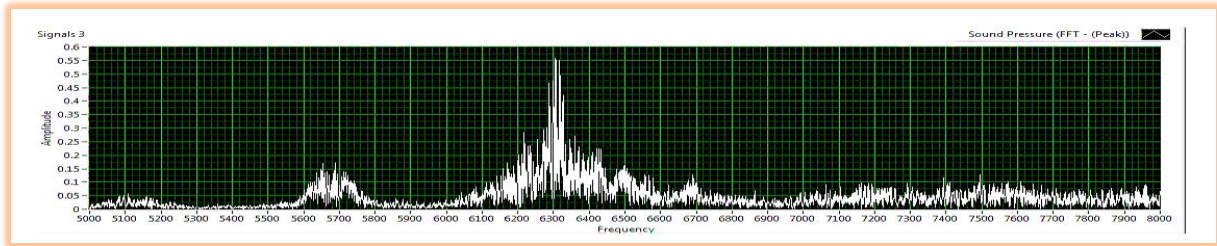
(b)



(c)



(d)



(e)

Figure 4.7: Selected five dominant frequencies between 5000 Hz and 8000 Hz from the FFT results i.e., (a) ochre, (b) bituminous coal, (c) laterite, (d) pink limestone and (e) hematite

Table 4.13: Dominant frequencies for various rock types

Rock type	Frequency- F1 (Hz)	Frequency- F2 (Hz)	Frequency- F3 (Hz)	Frequency- F4 (Hz)	Frequency- F5 (Hz)
Ochre	5476	5938	6499	7494	7820
Bituminous coal	5981	6144	7620	7959	8001
Laterite	5421	6123	6448	6686	7494
Pink limestone	5045	5330	7832	7839	7876
Hematite	6305	6310	6320	6327	6371

4.6.2 Modeling of rock properties

After the extraction of dominant frequency for each rock type, simple linear regression analysis was performed between the physico-mechanical rock properties and dominant frequencies using the SPSS statistics software. For the modelling of UCS, F5 frequency was significant compared to F1, F2, F3 and F4 frequencies. Similarly, in the case of BTS, F5 frequency was significant and, for density, F4

frequency was significant. A set of satisfactory mathematical equations (4.1) to (4.3) were obtained for the quantification of physico-mechanical rock properties, i.e. uniaxial compressive strength (UCS), Brazilian tensile strength (BTS) and density wherein the significant value (Table 4.14, Table 4.15 and Table 4.16) are less than 0.005. The coefficients of predicting the model are shown from Table 4.14 to Table 4.16, where the significant P-value was obtained as 0.021, 0.010 and 0.024 corresponding to UCS, BTS and density, respectively.

$$\text{UCS} = 501.886 - 0.060 \times F5, R^2 = 87.0 \% \quad (4.1)$$

$$\text{BTS} = 32.291 - 0.004 \times F5, R^2 = 92.1 \% \quad (4.2)$$

$$\text{Density} = 9.029 - 0.001 \times F4, R^2 = 85.5 \% \quad (4.3)$$

Table 4.14: The prediction model coefficients for predicting uniaxial compressive strength

Model		Unstandardized coefficients		Standardized coefficients	t-value	Significant value
Linear	(Constant) Frequency-F5	B	Std. Error	Beta		
		501.886	101.333	-	4.953	0.016
		-0.060	0.013	-0.933	-4.487	0.021
Dependent variable: UCS						

Table 4.15: The prediction model coefficients for predicting Brazilian tensile strength

Model		Unstandardized coefficients		Standardized coefficients	t-value	Significant value
Linear	(Constant) Frequency-F5	B	Std. Error	Beta		
		32.291	4.999	-	6.459	0.008
		-0.004	0.001	-0.960	-5.924	0.010
Dependent variable: BTS						

Table 4.16: The prediction model coefficients for predicting density

Model		Unstandardized coefficients		Standardized coefficients	t-value	Significant value
Linear	(Constant)	B	Std.Error	Beta		
		Frequency-F4	9.029	1.525	-	5.921
		-0.001	0.000	-0.925	-4.213	0.024
Dependent variable: Density						

After the development of the prediction model, the data for ten rock types obtained through literature were used for validating the developed prediction model. The data on UCS in Table 4.A17 (Referer Appendix-A) and the Brazilian tensile strength in Table 4.A18 (Referer Appendix-A) are taken from Kalyan et al. (2006) and Masood (2015). Similarly, Table 4.A19 (Referer Appendix-A) data on density are taken from Kahraman et al. (2013) and Kalyan et al. (2016). Tables 4.A17 to Table 4.A19 (Referer Appendix-A) also give the predicted values corresponding to the measured values and the model error. It can be perceived that the constructed models predicted all physico-mechanical properties with less than 15.37% error. The comparison of multiple linear regression models with the corresponding validation model is shown in Figure.4.8.

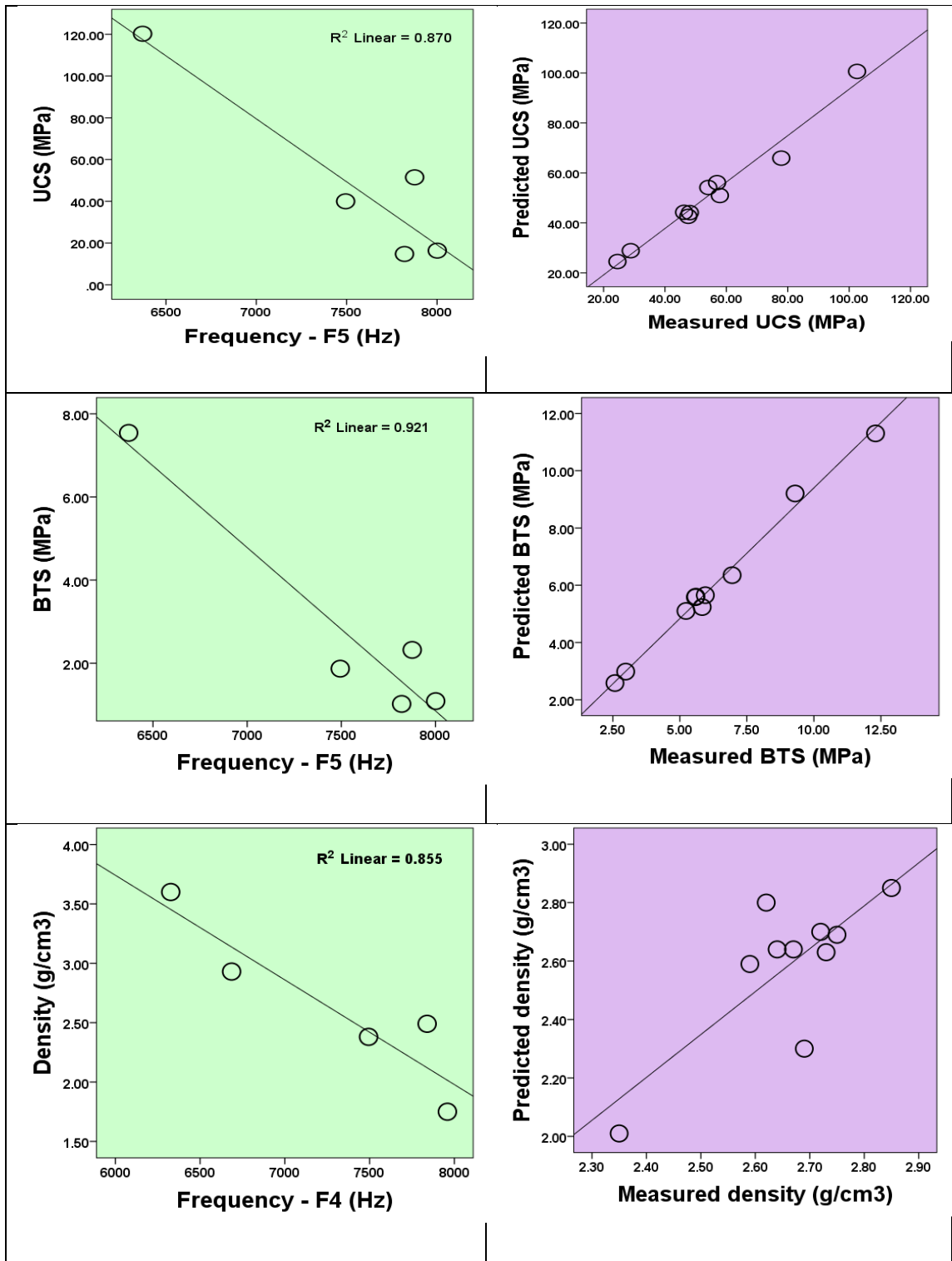


Figure 4.8: Simple linear regression prediction model, and distribution of validation points corresponding UCS, BTS, and density

4.6.3 Excitation frequency (Hz) versus sound pressure level (SPL) for rock blocks

The sound pressure level (dB) and the excitation frequency, one-third octave mid-band frequency (Hz), are shown in Figures 4.9a - Figure.4.9e for various rock blocks. It was observed that the sound pressure level was higher up to the frequency of 5000 Hz for rock blocks, namely ochre (Figure 4.9a), bituminous coal (Figure 4.9b), laterite (Figure 4.9c) and pink limestone (Figure 4.9d). However, for hematite block (Figure 4.9e), the sound pressure level was higher beyond 5000 Hz centre frequency for hematite block. This may be due to the significantly greater uniaxial compressive strength of hematite compared to other rock blocks. The increase in the compressive strength and hence drillability depends on the mineralogical composition and the petrographic features (grain size, grain bindings, weathering and micro-cracking) of the rock Macias (2017) and, hence, increase in the sound level (Vardhan et al. 2009).

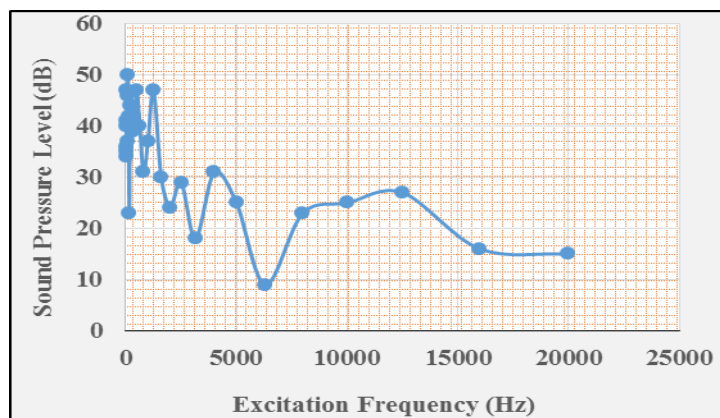


Figure 4.9a: Sound pressure level vs. excitation frequency for ochre rock

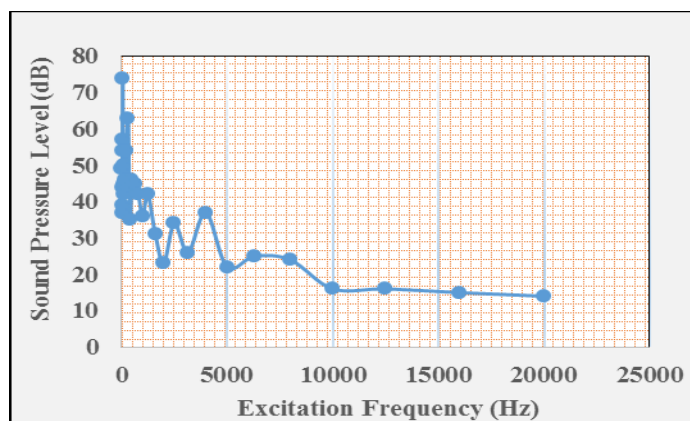


Figure 4.9b: Sound pressure level vs. excitation frequency for bituminous coal

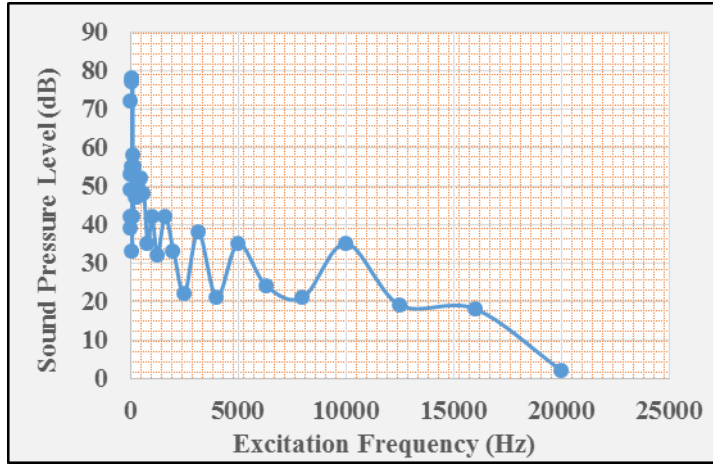


Figure 4.9c: Sound pressure level vs. excitation frequency for laterite

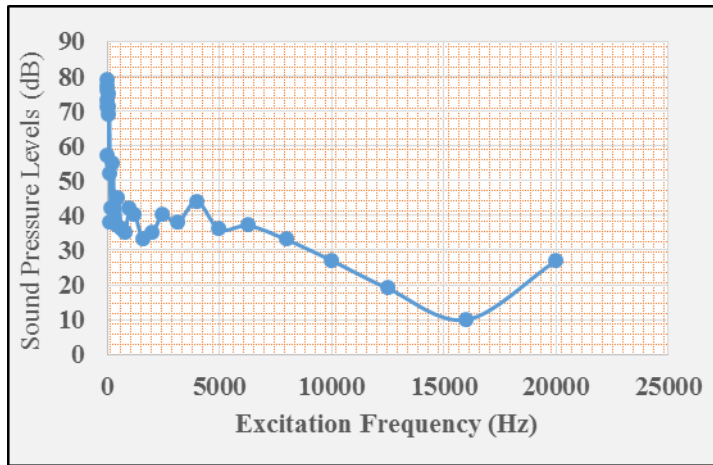


Figure 4.9d: Sound pressure level vs. excitation frequency for pink limestone

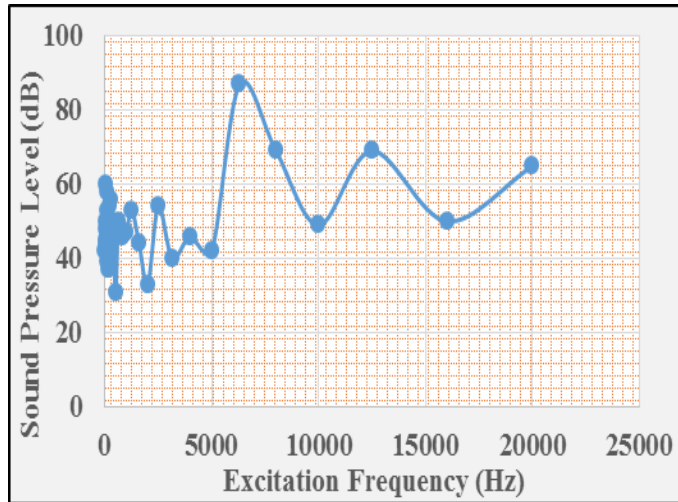


Figure 4.9e: Sound pressure level vs. excitation frequency for hematite

4.7 Development of Rock Properties Predictive Models for varying combinations of Drill bit Diameters, Drill bit Speed, and Penetration rate

4.7.1 Sound pressure level measurement

In this investigation, case - (i) methodology was used to predict rock properties, but for each drilling condition, drilling time was different. For example, a drilling condition of (6, 150, 2) i.e., drill bit diameter = 6 mm, speed = 150 rpm, and penetration rate = 2 mm/ min) was used for ochre to drill for 40 s to obtain frequencies F1- F5, as listed in Table 4.20. Similarly, the cases of bituminous coal, laterite, pink limestone, and hematite used corresponding drilling conditions of (10, 200, 3) to drill for 30 s, (16, 250, 4) to drill for 24 s, (18, 300, 5) to drill for 20 s, and (20, 350, 6) to drill for 17 s to obtain frequencies F1- F5. The standard deviation and uncertainty were within limits to for prediction of UCS, BTS and density using the dominant frequency of sound signals. The extracted dominant frequencies from frequency domain are shown in Table.4.20.

Table 4.20: Five dominant frequencies for selected rock samples

Rock type	Frequenc y- F1 (Hz)	Frequenc y- F2 (Hz)	Frequenc y- F3 (Hz)	Frequenc y- F4 (Hz)	Frequency- F5 (Hz)
Ochre	5579	6900	6941	7994	8000
Bituminous coal	6002	7732	8507	8512	8522
Laterite	5880	5998	6025	6999	7168
Pink limestone	5510	5991	6800	7910	7970
Hematite	4000	4100	5641	6494	7650

4.7.2 Modeling of rock properties

After extraction of each rock dominant frequencies, simple linear regression analysis was performed between the physico-mechanical rock properties and dominant frequencies using SPSS statistics software. For the prediction model, rock properties were selected as a dependent variable and independent variable as frequency. All selected frequency F1 to F5 corresponding rock properties like UCS, BTS, and density were checked. For the modeling of UCS, F2 frequency was significant compared with F1, F3, F4, and F5 frequencies. Similar was the case with BTS, and density. A set of satisfactory mathematical equations (4.4) to (4.6) were derived for the quantification of rock properties, i.e. Uniaxial Compressive Strength (UCS), Brazilian Tensile Strength (BTS) and density where in the significant value (Table 4.22) are less than 0.005 and the R^2 value is 91.4 %, 93.5 %, and 96.0 % as shown in Table 4.21. The coefficients of predicting models are given in Table 4.23 to Table 4.25.

$$\text{UCS} = 235.349 - 0.030 \times \text{F2}, \quad R^2 = 91.4 \% \quad (4.4)$$

$$\text{BTS} = 20.392 - 0.003 \times \text{F1}, \quad R^2 = 93.5 \% \quad (4.5)$$

$$\text{Density} = 8.877 - 0.001 \times \text{F4}, \quad R^2 = 96.0 \% \quad (4.6)$$

Table 4.21 Model summary for the dependent variable

Dependent variable	R value	R Square	Adjusted R Square	Standard error of the estimate
UCS	0.956	0.914	0.885	14.59412
BTS	0.967	0.935	0.913	0.80226
Density	0.980	0.960	0.946	0.15900

Table 4.22 Analysis of variance (ANOVA) for the dependent variable

Dependent variable	Model	Degree of freedom	Sum of Squares	Mean Square	F-value	Significant P-value
UCS	Regression	1	6760.480	6760.480	31.741	0.011
	Residual	3	638.965	212.988	-	-
	Total	4	7399.445	-	-	-
BTS	Regression	1	27.719	27.719	43.068	0.007
	Residual	3	1.931	0.644	-	-
	Total	4	29.650	-	-	-
Density	Regression	1	1.812	1.812	71.657	0.003
	Residual	3	0.076	0.025	-	-
	Total	4	1.887	-	-	-

Table 4.23 Coefficients of proposed model for predicted UCS

Model		Unstandardized coefficients		Standardized coefficients	t-value	Significant value
Linear	(Constant) Frequency-F2	B	Std. Error	Beta		
		235.349	33.788		6.965	0.006
		-0.030	0.005	-0.956	-5.634	0.011

Dependent variable: UCS

Table 4.24 Coefficients of proposed model for predicted BTS

Model		Unstandardized coefficients		Standardized coefficients	t-value	Significant value
Linear	(Constant) Frequency-F1	B	Std.Error	Beta		
		20.392	2.709	-	7.526	0.005
		-0.003	0.000	-0.967	-6.563	0.007

Dependent variable: BTS

Table 4.25 Coefficients of proposed model for predicted density

Model		Unstandardized coefficients		Standardized coefficients	t-value	Significant value
Linear	(Constant) Frequency-F4	B	Std. Error	Beta		
		8.880	0.742	-	11.972	0.001
		-0.001	0.000	-0.980	-8.465	0.003

Dependent variable: density

After the development of the prediction model, three rock types (marble, moon white granite, and basalt) were used for validating the developed prediction model. Table 4.26 to Table 4.28 gives the predicted values corresponding to the measured values, and the model error. It can be seen that, the constructed models predicted all physico-mechanical properties with less than 4.0 % error. The comparison of the simple linear regression model with the corresponding validation model is shown in Figure 4.10.

Table 4.26 Predicted values, measured values from prediction model and model error for uniaxial compressive strength (Three validation rock samples)

Rock sample name	Measured UCS (MPa)	Predicted UCS (MPa)	Error %
Marble	24.05	24.059	3.7422
Moon white granite	28.83	28.859	0.1005
Basalt	54.13	54.149	0.0351

Table 4.27 Predicted values, measured values from prediction model and model error for Brazilian tensile strength (Three validation rock samples)

Rock sample name	Measured BTS (MPa)	Predicted BTS (MPa)	Error %
Marble	2.58	2.581	0.0387
Moon white granite	2.98	2.982	0.0671
Basalt	5.58	5.581	0.0179

Table 4.28 Predicted values, measured values from prediction model and model error for density (Three validation rock samples)

Rock sample name	Measured density (g/cm ³)	Predicted density (g/cm ³)	Error %
Marble	2.59	2.591	0.0386
Moon white granite	2.64	2.641	0.0378
Basalt	2.85	2.851	0.0350

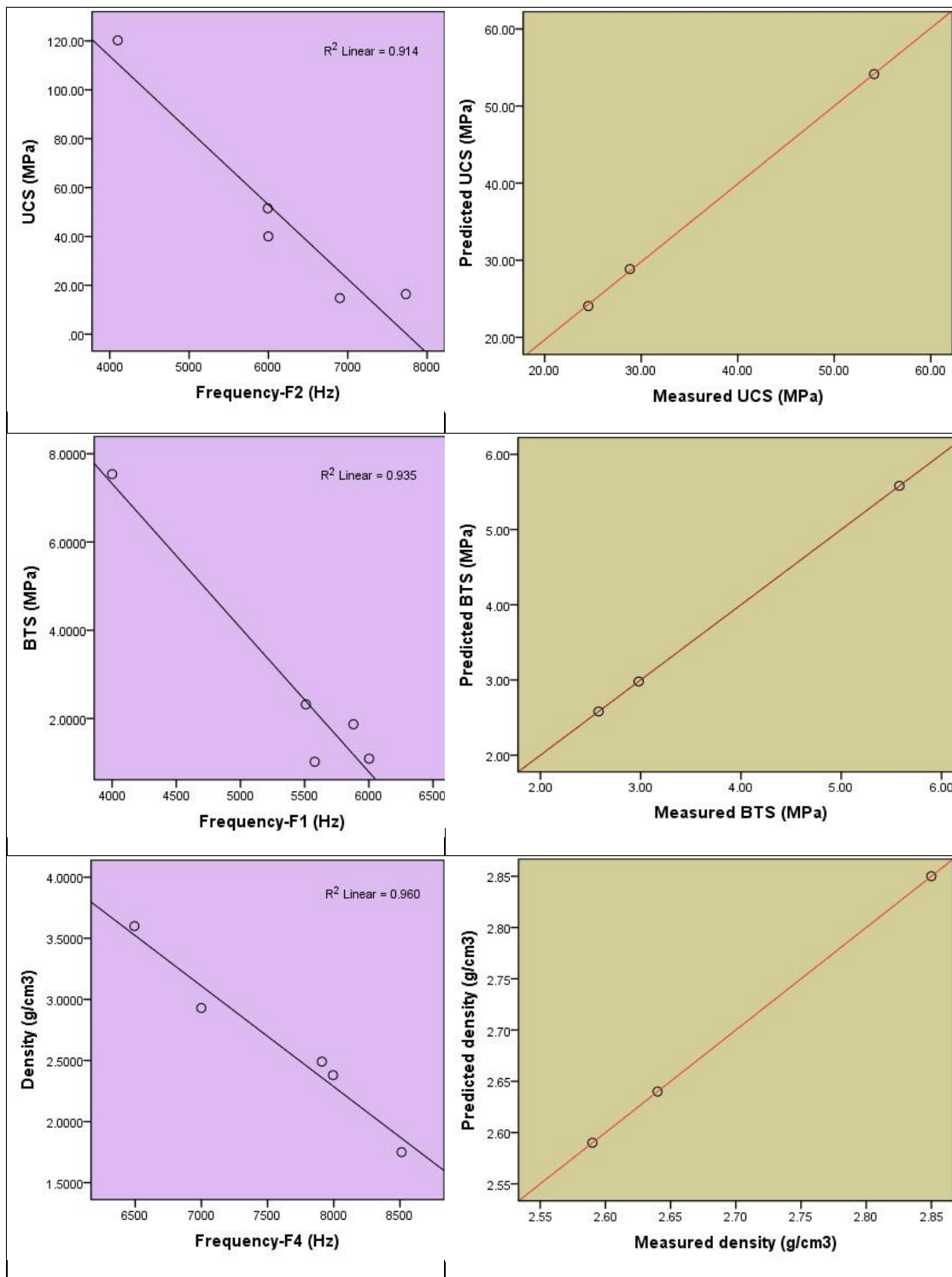


Figure 4.10: Simple linear regression prediction model, and distribution of validation points corresponding UCS, BTS, and density

4.8 Development of Rock Properties Predictive Models for Combinations of the Drill bit Diameters, Drill bit Speed, and Penetration rate

In this investigation case - (i) methodology was used to predict rock properties. The audio signals produced during drilling were measured for 60 seconds for various drill bit conditions, penetration rates, and spindle speeds for selected rock samples. For each test conditions, audio signals were measured for 60 seconds and this 60 seconds data was used for the frequency analysis. The 125 (i.e. combinations of drill bit diameters of 6 mm, 10 mm, 16 mm, 18 mm, and 20 mm at penetration rates of 2 mm/min, 3 mm/min, 4 mm/min, 5 mm/min, and 6 mm/min and speeds of 150 rpm, 200 rpm, 250 rpm, 300 rpm, and 350 rpm, total test conditions: 125×7 rock types = 875 test conditions were arrived) dominant frequencies were extracted from the frequency domain of each selected rock, where the highest sound pressure level (dB) was determined. These frequencies were called dominant frequencies corresponding to each rock block. Table 4.A29 shown in Appendix- A experimental results of 125 dominant frequencies (Hz) for each rock sample.

4.8.1 Modelling of rock properties using multiple regression analysis

A multiple regression model was developed for UCS, BTS, density, and abrasivity considering 60 seconds of drilling, after the penetration of the drill bit into the rock mass, as shown in Equations 4.7 to 4.10. To evaluate the model, a backward elimination method was used as the test procedure. Analysis of variance was performed to observe the essential parameters carried out in the statistical model for UCS, BTS, density, and abrasivity, with significance of 95% confidence interval. Influence of the parametric level of the UCS, BTS, density, and abrasivity were compared using ANOVA with the Minitab17. Where the p-values equal or smaller than 0.005, were considered to be statistically significant, and the corresponding data was noted down, as shown in the regression Table 4.A30 (Appendix-A).

Development of regression models:

Regression equation for UCS:

$$\text{UCS} = -10.5 - 13.035 \text{ DD} - 0.0377 \text{ RPM} + 0.02758 \text{ FR} + 0.7698 \text{ DD} * \text{DD} - 0.000002 \text{ FR} * \text{FR} + 0.000006 \text{ RPM} * \text{FR} \quad (4.7)$$

Regression equation for BTS:

$$\text{BTS} = 0.58 - 1.1561 \text{ DD} - 0.00278 \text{ RPM} + 0.001899 \text{ FR} + 0.06017 \text{ DD} * \text{DD} - 0.000001 \text{ FR} * \text{FR} + 0.000003 \text{ RPM} * \text{FR} \quad (4.8)$$

Regression equation for density:

$$\text{Density} = 2.915 - 0.2413 \text{ DD} - 0.00127 \text{ RPM} + 0.000219 \text{ FR} + 0.011513 \text{ DD} * \text{DD} - 0.000001 \text{ FR} * \text{FR} + 0.000005 \text{ DD} * \text{FR} + 0.000001 \text{ RPM} * \text{FR} \quad (4.9)$$

Regression equation for abrasivity:

$$\text{Abrasivity} = 112.6 - 4.651 \text{ DD} - 0.00527 \text{ FR} + 0.000001 \text{ FR} * \text{FR} + 0.000088 \text{ DD} * \text{FR} \quad (4.10)$$

Where, DD = diameter of the drill bit (mm), SS = spindle speed (rpm), PR = penetration rate (mm/min), FR = dominant frequency (Hz).

4.8.2 Analysis of variance (ANOVA)

Regression analysis was carried out to obtain second-order models for UCS, BTS, density, and abrasivity during diamond core drilling operations. This test helps find the input parameters that considerably affect the desired output response in the model. ANOVA is most the popular analysis tool for studying the significant parameters that influence the quality characteristics and identify the percentage contribution ratio of each process factor on the output response.

Initially, ANOVA was performed between the input parameters i.e. drill bit diameter (mm), penetration rate (mm/min), spindle speed (rpm), dominant frequencies (DF) and rock properties (i.e., UCS, BTS, density, abrasivity). All the insignificant terms ($p > 0.05$) from the obtained model were removed, and the regression analysis was carried out again, this time with significant terms in the model. After performing the experimental analysis of the obtained data, presented in Table 4.31. Whereas the P-value was found to be significantly good, at less than 0.005.

Table 4.31: Results of ANOVA for various rocks

UCS							
	Source	DF	Seq.SS	Adj SS	Adj MS	F-Value	P-Value
Eq.4.7	Regression	6	1308442	1308442	218074	682.00	0.000
	DD	1	1136383	69965	69965	2188.81	0.000
	RPM	1	0	146	146	0.46	0.050
	FR	1	359	2724	2724	8.52	0.004
	DD*DD	1	168212	166496	166496	520.70	0.000
	FR*FR	1	3327	3345	3345	10.46	0.001
	RPM*FR	1	160	160	160	0.50	0.005
	Error	868	277547	277547	320	-	-
	Total	874	1585989	-	-	-	-
BTS							
	Source	DF	Seq.SS	Adj SS	Adj MS	F-Value	P-Value
Eq.4.8	Regression	6	4899.61	4899.6	816.60	525.44	0.000
	DD	1	3854.94	550.35	550.35	354.12	0.000
	RPM	1	0.00	0.80	0.80	0.51	0.054
	FR	1	1.11	12.92	12.92	8.31	0.004
	DD*DD	1	1026.90	1017.06	1017.06	654.43	0.000
	FR*FR	1	15.78	15.88	15.88	10.22	0.001
	RPM*FR	1	0.87	0.87	0.87	0.56	0.055
	Error	868	1348.99	1348.99	1.55	-	-
	Total	874	6248.60	-	-	-	-
Density							
	Source	DF	Seq.SS	Adj SS	Adj MS	F-Value	P-Value
Eq.4.9	Regression	7	230.625	230.625	32.9464	207.41	0.000
	DD	1	191.702	12.852	12.8521	80.91	0.000
	RPM	1	0.000	0.165	0.1655	1.04	0.008
	FR	1	0.355	0.166	0.1664	1.05	0.006
	DD*DD	1	37.353	37.167	37.1675	233.99	0.000
	FR*FR	1	0.488	0.479	0.4791	3.02	0.053
	DD*FR	1	0.549	0.556	0.5560	3.50	0.002
	RPM*FR	1	0.178	0.178	0.1784	1.12	0.007
	Error	867	137.718	137.718	0.1588	-	-
	Total	874	368.343	-	-	-	-
Abrasivity							
	Source	DF	Seq.SS	Adj SS	Adj MS	F-Value	P-Value
Eq.4.10	Regression	4	391573	391573	97893.3	2998.03	0.000
	DD	1	391228	11100	11099.8	339.94	0.000
	FR	1	88	100	100.3	3.07	0.080
	FR*FR	1	67	71	70.7	2.17	0.001
	Error	868	137.718	137.718	0.1588	-	-

	DD*FR	1	191	191	190.8	5.84	0.016
	Error	870	28408	28408	32.7	-	-
	Total	874	419981	-	-	-	-

4.8.3 Validation of the derived models

The statistical results of the UCS, BTS, density, and abrasivity models for various rock types are demonstrated in Figure 4.11. The correlation coefficients of these models i.e. the R^2 values are 82.50%, 78.41%, 70.40%, and 93.24% for UCS, BTS, density, and abrasivity, respectively. Figure.4.8 shows the measured value versus predicted value, corresponding to the UCS, BTS, density, and abrasivity. The scatter plots show that the values obtained from the multiple regression models and the value measured from the experimental work, both are fairly close with less than 10% error. It can be said that the developed models are reasonably good.

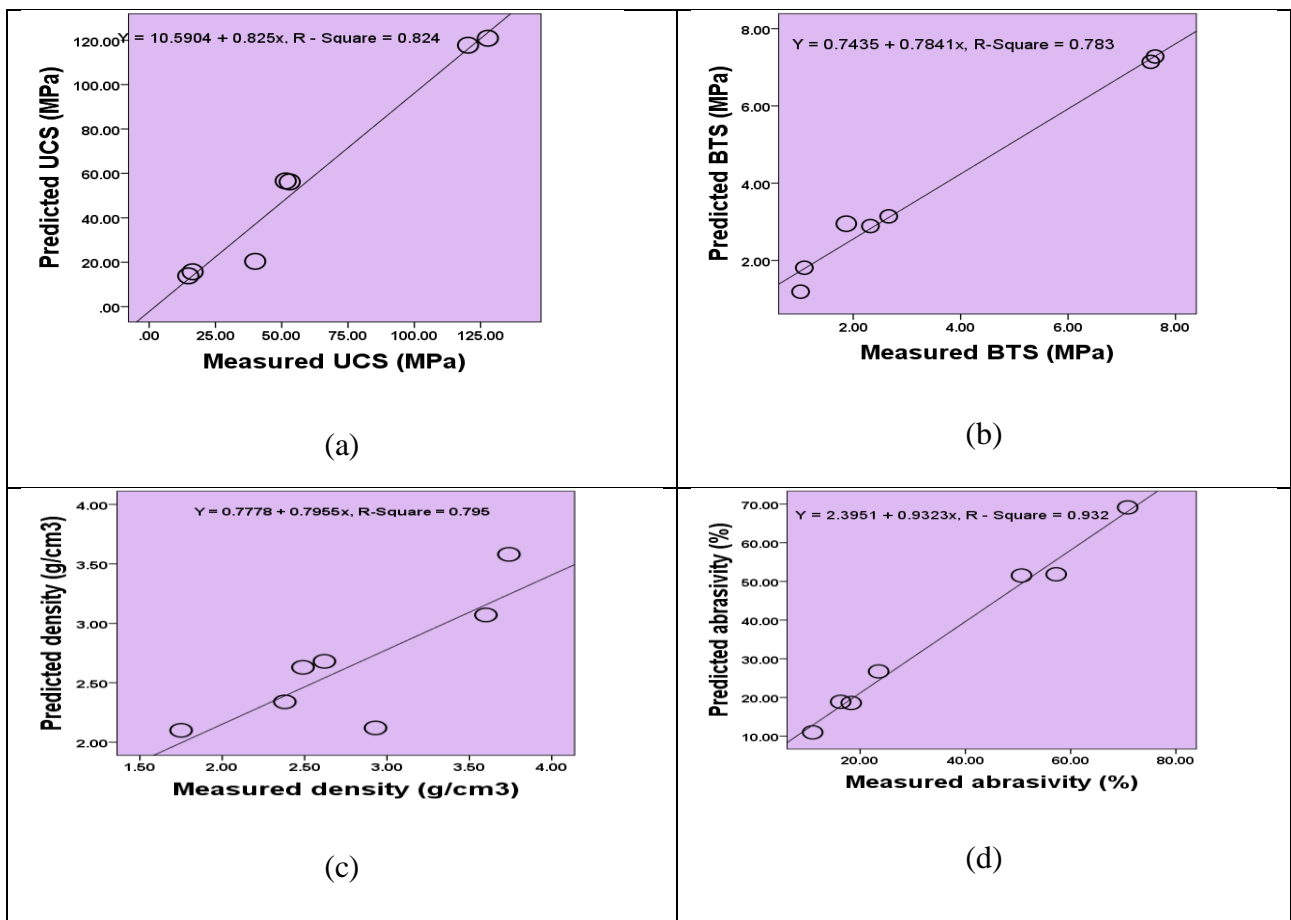


Figure 4.11: Measured UCS, BTS, density, and abrasivity vs. predicted UCS, BTS, density, and abrasivity

4.8.4 Performance prediction of derived models

The prediction of performance is a better indicator for the developed prediction models to assess the coefficient of correlations between the predicted and measured results. The value adjustment factor (VAF) and the root mean square error (RMSE) were calculated for the predictive ability of the models, whereas, y and y_1 and A_i and P_i are the measured and predicted values, as given in Equations (11) to (13). If VAF is equal to 100 and RMSE is equal to zero then the model is considered good. Similarly, the mean absolute percentage error (MAPE) demonstrates the accuracy fit value of the statistics (Kumar et al., 2011b). The performance indices of the developed regression model are shown in Table 4.32.

$$VAF = \left[1 - \frac{Var(y-y_1)}{Var(y)}\right] \times 100 \quad (4.11)$$

$$RMSE = \sqrt{\frac{1}{N} \sum_{i=0}^n (y - y')^2} \quad (4.12)$$

$$MAPE = \frac{1}{N} \sum_{i=1}^N \left| \frac{A_i - P_i}{A_i} \right| \times 100 \quad (4.13)$$

Table 4.32 Performance indices of the developed regression model

Variable	Performance Indices		
	RMSE	VAF (%)	MAPE
UCS	0.102754	82.50008	0.027281
BTS	1.241652	78.41137	0.028388
Density	0.396727	79.40137	0.007817
Abrasivity	0.697889	93.23596	0.00521

4.9 Development of Artificial Neural Network Models

In this analysis, the sound pressure levels recorded for duration of around 60 seconds of drilling was used to determine dominant frequencies using FFT analysis as followed by case-(iii).

Experimental data of total 875 test conditions, were used to predict physic-mechanical rock properties during drilling operations through ANN. Out of these, 70% data (612 test conditions) were used for the training set and the remaining 30% data (263 test conditions) were used to test the models. Figure 4.12 shows the multi-layer perceptron (MLP) generalised structure of the ANN model. The spindle speed,

penetration rate, dominant frequencies and drill bit diameter were employed as input parameters in the model while the output responses were UCS, BTS, dry density and abrasivity. These input parameters are effective for constructing the ANN prediction model and cover the problem of the domain being investigated.

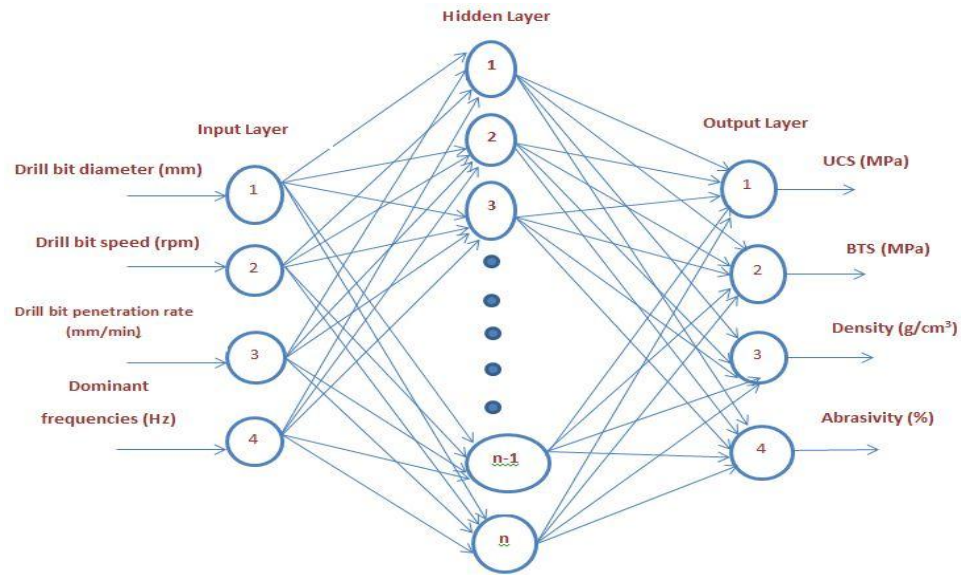


Figure 4.12: Illustration of an artificial neural network model

The multi-layer perceptron network was employed by Matlab 2015 ANN toolbox. Seven types of back-propagation training algorithms were used to train the data sets. These algorithms show the network accuracy and the performance (mean square error-mse) of the plots. The seven algorithms are `trainscg` (scaled conjugate gradient algorithm), `traingda` (gradient descent with adaptive learning back-propagation algorithm), `trainrp` (resilient back-propagation algorithm), `traingdx` (gradient descent with momentum and adaptive learning back-propagation algorithm), `trainlm` (levenberg-marquardt algorithm), `trainbfg` (BFGS quasi-newton back-propagation algorithm), `traincgf` (conjugate gradient back-propagation with fletcher-reeves updates algorithm).

While training the algorithms, the number of neurons in the hidden layer was estimated using the trial and error method. It revealed that 6-35 neurons were used in a hidden layer with the `tansig` transfer function corresponding seven types of back-propagation training algorithms. Primarily several trails were conducted to fix the number of neurons in the hidden layer for every type of algorithm. The minimum

RMSE value and the maximum VAF value was selected for the optimal number of neurons in the hidden layer. The seven types of back-propagation training algorithms performance and network architecture are shown in Table 4.33. This table clarifies that “resilient back-propagation algorithm (trainrp)” was the most significant (fewer epochs and the time take convergence is lesser) of the seven back-propagation training algorithms with 35 neurons and minimum number of epochs - 9 - for the prediction of physico-mechanical rock properties. This is the optimal number because of the low RMSE value with the highest value of regression (R) respectively.

Table 4.33 Schematic representation of network architecture

Sl.no	Training algorithm	Network architecture	Number of epochs	Time taken for convergence (sec)	Neural network training regression	Neural network testing regression
1	Traingda	4:6:4	1000	152 sec	0.83296	0.89346
2	Traingdx	4:10:4	130	120 sec	0.83755	0.88689
3	Trainrp	4:35:4	09	32 sec	0.98428	0.98436
4	Traincgf	4:10:4	132	145 sec	0.833423	0.890522
5	trainglm	4:22:4	08	56 sec	0.83172	0.83299
6	Trainbfg	4:27:4	18	100 sec	0.81411	0.83296
7	Trainscg	4:15:4	37	60 sec	0.827874	0.901181

The errors were calculated by comparing the data of the measured rock properties with the ANN predictions. The resilient back-propagation algorithm (trainrp) predicted rock properties (UCS, BTS, density, and abrasivity) with an error from 2.31% to 10 %. The ANN models were checked by various performance indices, the performance indices show that VAF, RMSE, and MAPE are minimum for the network using trainrp (resilient back-propagation algorithm) corresponding the other types of the algorithms for both testing and training data. The performance indices of the developed neural network model training and testing as shown in Table 4.A34 in the Appendix-A. Hence, the trainrp (resilient back-propagation algorithm) algorithm could be efficiently used as a predictor to estimate the physico-mechanical properties of rocks based on the dominant frequency of acoustic signals during diamond drilling operations.

4.10 Prediction of Specific Energy

A multiple linear regression model was developed for considering 30 mm depth of drilling time after penetration of drill bit into the rock mass as given by Eq. (4.14) to Eq. (4.20). To evaluate the model, analysis of variance was performed to observe the essential parameters carried out in the statistical model for SE with significance of 95% confidence interval. Influence of the parametric level of the SE was compared, using analysis of variance (ANOVA) with Minitab 2017. Where the p-values are equal or smaller than 0.005, they were considered to be statistically significant; corresponding data are noted down as shown in the regression Table 4.B1 (statistical analysis of significant regression models for various rocks) to Table 4.B2 (results of ANOVA for various rocks) as shown in Appendix-B.

4.10.1 Modeling of specific energy using multiple linear regression analysis

Regression equation for ochre:

$$\text{Specific energy (Nm/m}^3\text{)} = 11.20 - 0.8190 \text{ DD} - 0.00077 \text{ SS} - 0.042 \text{ PR} + 0.1175 \text{ A-SPL} + 0.01421 \text{ Thrust} - 2.45 \text{ Torque} \quad (4.14)$$

Contribution percentage (%): DD = 54.05 %, SS = 5.90 %, PR = 5.65 %, A-SPL = 3.57 %, Thrust = 18.72 %, Torque = 1.15 %, Error = 9.96 %

Where, DD = diameter of the drill bit (mm), SS = spindle speed (rpm), PR = penetration rate (mm/min), A-SPL = A-weighted sound level (dB).

Regression equation for coal:

$$\text{Specific energy (Nm/m}^3\text{)} = 5.60 - 0.4309 \text{ DD} + 0.00849 \text{ SS} + 0.129 \text{ PR} - 0.0087 \text{ A-SPL} + 0.01735 \text{ Thrust} - 0.433 \text{ Torque} \quad (4.15)$$

Contribution percentage (%): DD = 50.82 %, SS = 4.00 %, PR = 10.72 %, A-SPL = 7.25 %, Thrust = 13.44 %, Torque = 5.77 %, Error = 8.00 %

Regression equation for laterite:

$$\text{Specific energy (Nm/m}^3\text{)} = 13.82 - 0.5057 \text{ DD} + 0.00607 \text{ SS} - 0.240 \text{ PR} - 0.1127 \text{ A-SPL} + 0.01599 \text{ Thrust} + 0.640 \text{ Torque} \quad (4.16)$$

Contribution percentage (%): DD = 44.68%, SS = 6.72 %, PR = 5.60 %, A-SPL = 15.91 %, Thrust= 9.02 %, Torque = 4.06 %, Error = 14.01 %

Regression equation for pink limestone:

$$\text{Specific energy (Nm/m}^3\text{)} = 22.91 - 1.523 \text{ DD} - 0.00480 \text{ SS} + 0.585 \text{ PR} - 0.0139 \text{ A-SPL} + 0.01305 \text{ Thrust} - 0.228 \text{ Torque} \quad (4.17)$$

Contribution percentage (%): DD = 66.68 %, SS = 0.72 %, PR = 5.60 %, A-SPL = 5.00 %, Thrust = 9.02 %, Torque = 2.07 %, Error=10.91 %

Regression equation for black limestone:

$$\text{Specific energy (Nm/m}^3\text{)} = 14.84 - 1.030 \text{ DD} + 0.00452 \text{ SS} - 2.650 \text{ PR} - 0.00060 \text{ A-SPL} + 0.02991 \text{ Thrust} + 0.040 \text{ Torque} \quad (4.18)$$

Contribution percentage (%): DD = 66.68 %, SS = 0.72 %, PR = 5.60 %, A-SPL = 5.00 %, Thrust = 9.02 %, Torque = 2.07 %, Error = 10.91 %

Regression equation for hematite:

$$\text{Specific energy (Nm/m}^3\text{)} = 25.01 - 1.7078 \text{ DD} - 0.00423 \text{ S} + 0.254 \text{ PR} + 0.0151 \text{ A-SPL} + 0.00842 \text{ Thrust} + 0.158 \text{ Torque} \quad (4.19)$$

Contribution percentage (%): DD = 58.00 %, SS = 7.40 %, PR = 5.60 %, A-SPL = 12.90 %, Thrust = 9.02 %, Torque = 2.07 %, Error=5.01 %

Regression equation for dolomite:

$$\text{Specific energy (Nm/m}^3\text{)} = 26.16 - 1.578 \text{ DD} - 0.00756 \text{ SS} - 1.086 \text{ PR} - 0.00068 \text{ A-SPL} + 0.01578 \text{ Thrust} + 0.132 \text{ Torque} \quad (4.20)$$

Contribution percentage (%): DD = 66.68 %, SS = 0.72 %, PR = 5.60 %, A-SPL = 5.00 %, Thrust = 9.02 %, Torque = 2.07 %, Error = 10.91 %

4.10.2 Analysis of variance (ANOVA)

Regression analysis was carried out to obtain SE predictive models during diamond core drilling operations. This test helps to find out which input parameters considerably affect the desired output response in the model. ANOVA is the most popular analysis tool for studying the significant parameters that influence the quality

characteristics and identify the percentage contribution ratio of each process factors on output response. After performing the experimental analysis of the obtained data presented in Table 4.B2 (Appendix-B) was executed, whereas P-value was significantly good being less than 0.005.

4.10.3 Performance prediction of derived models

The prediction of performance is a better indicator for the developed prediction model to assess the coefficient of correlations between predicted and measured results. Values account for (VAF) and root mean square error (RMSE) were calculated for the predictive ability of the prediction models, whereas y and y' , A_i and P_i are the measured and predicted values are as shown in the Equation (4.21) to Equation (4.23). If VAF is equal to 100 and RMSE is equal to zero, then the model will be good. Similarly mean absolute percentage error (MAPE) shows that accuracy fits value in the statistics (Kumar et al. 2011; Alvarez and Babuska, 1999; Finol et al. 2001; Gokceoglu, 2002; Yilmaz and Yuksek, 2008, 2009; Yilmaz and Oguzkaynar, 2011). The performance indices of the developed regression model are as shown in Table 4.3.

$$\text{VAF} = \left[1 - \frac{\text{Var}(y-y')}{\text{Var}(y)} \right] \times 100 \quad (4.21)$$

$$\text{RMSE} = \sqrt{\frac{1}{N} \sum_{i=0}^n (y - y')^2} \quad (4.22)$$

$$\text{MAPE} = \frac{1}{N} \sum_{i=1}^N \left| \frac{A_i - P_i}{A_i} \right| \times 100 \quad (4.23)$$

Table 4.3 Performance indices of the developed regression models

Rock type	Performance indices		
	RMSE	VAF (%)	MAPE
Ochre	0.074411	72.826808	2.321007
Bituminous coal	0.137019	78.4179	1.302107
Laterite	0.205786	84.155813	3.075358
Pink limestone	0.578601	82.770851	0.061218
Black limestone	0.194082	78.7624	0.330962
Hematite	0.263618	78.0514	0.109818
Dolomite	0.251525	77.246	0.206723

4.10.4 Validation of the specific energy models

The predictive models were verified by considering the behaviour of determination coefficients (R^2), the t-test and the F-test and performance prediction of VAF, RMSE and MAPE. The validation results demonstrate that, at the 95% confidence level, the computed t-values and computed F-values are greater than the tabulated t-value (2.44) and tabulated F-value (2.19), suggesting that the developed models are statistically valid. The figures (Figure 4.13 to Figure 4.19) indicate that the error appears to be at an acceptable degree of accuracy around below 18% from predicted value, confirming the accuracy of the models.

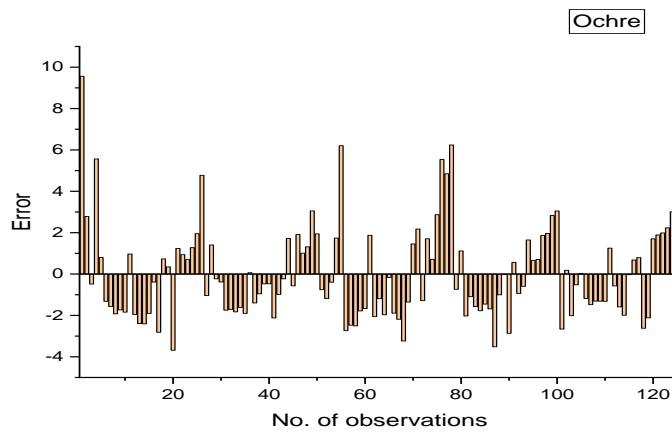


Figure 4.13: Specific energy error graph for ochre

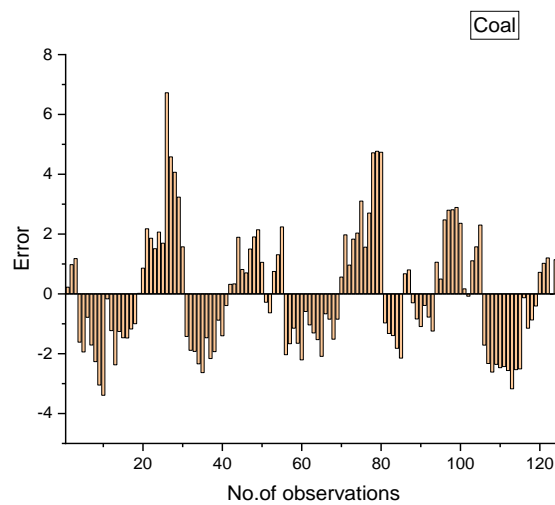


Figure 4.14: Specific energy error graph for coal

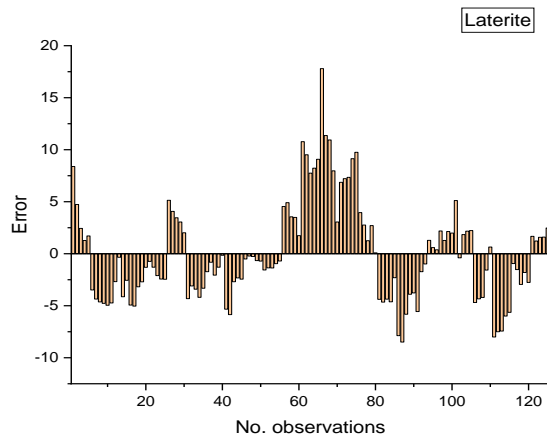


Figure 4.15: Specific energy error graph for laterite

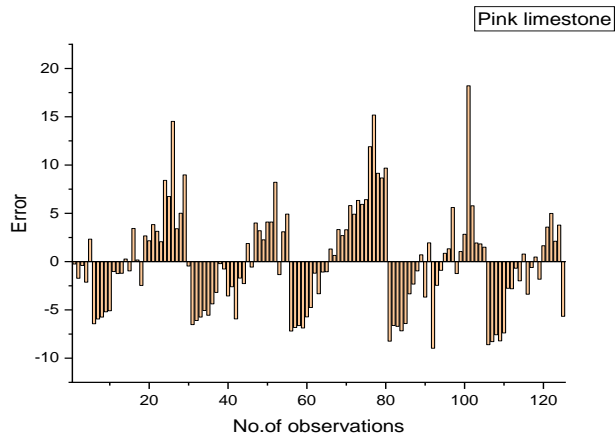


Figure 4.16: Specific energy error graph for pink limestone

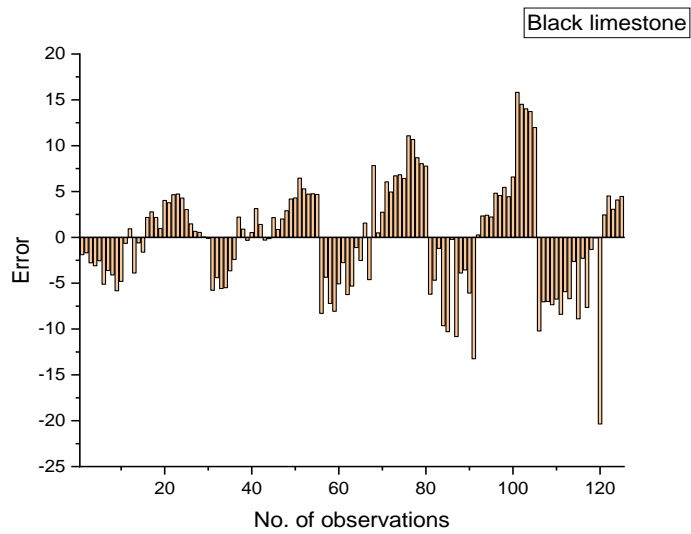


Figure 4.17: Specific energy error graph for black limestone

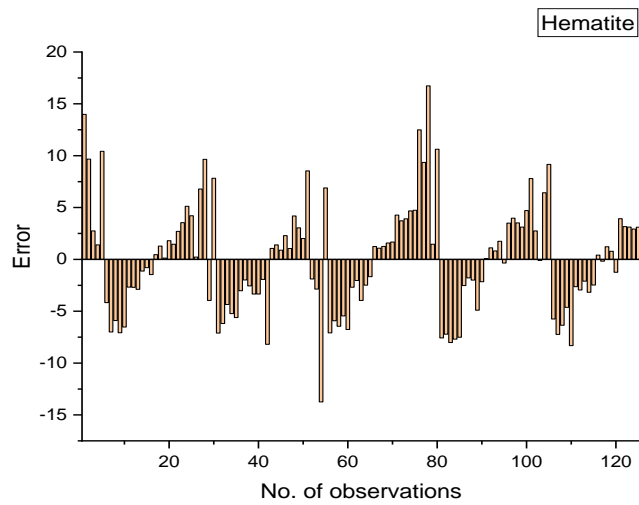


Figure 4.18: Specific energy error graph for hematite

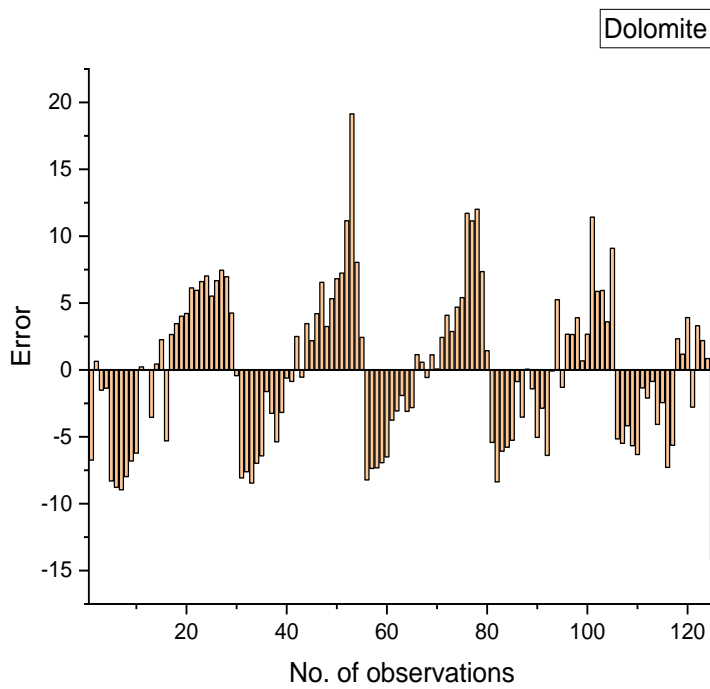


Figure 4.19: Specific energy error graph for dolomite

4.10.5 Effect of physico-mechanical rock properties on specific energy

The relationships between physico-mechanical properties and SE were investigated on the basis of the statistical approach, such as exponential approach and the best relations established are represented in Figure 4.20a to 4.20e and presented in Table

4.4 which indicates that there exist strong correlations between SE and rock properties, except density. It may generally be possible to obtain higher SE values when drilling in the high density hard rocks; due to this reason there may appear moderate correlations between SE and density (Delgado et al. 2005; Xie and Tamaki, 2007). The developed models having R^2 value for all models are around 0.90 % except density, indicating a high degree of relationship between the physico-mechanical properties of rocks and SE. From Figure 4.20a to 4.20e it is observed that the SE increased with increasing UCS, BTS, dry density, and impact strength index (Reddish and Yasar 1996; Coupur et al. 2001; Balci et al. 2014; Tiryaki et al. 2006), whereas, SE decreased with increasing abrasivity (Engin et al. 2013). The experimental 125 test conditions results of thrust, torque and A-SPL, for various (ochre, bituminous coal, laterite, pink limestone, black limestone, hematite, and dolomite) rock samples as shown Table 4.B5 to Table 4.B11 in the Appendix-B.

Table 4.4 Correlations between specific energy and physico-mechanical properties

Physico- mechanical rock properties	Regression equation	R^2 - value
UCS	$SE = 12.2e^{0.003x}$	$R^2 = 92.25$
BTS	$SE = 0.7307e^{0.0029x}$	$R^2 = 90.99$
Density	$SE = 2.0467e^{0.0006x}$	$R^2 = 47.15$
Abrasivity	$SE = 87.665e^{-0.003x}$	$R^2 = 93.90$
Impact strength index	$SE = 52.91e^{0.0005x}$	$R^2 = 82.88$

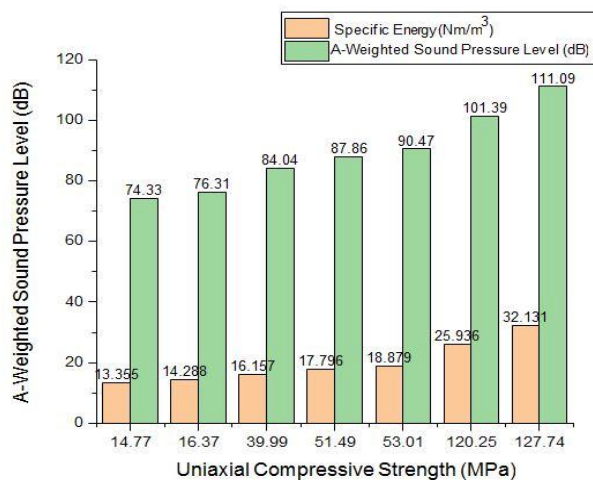


Figure 4.20a: Relationship between uniaxial compressive strength to specific energy

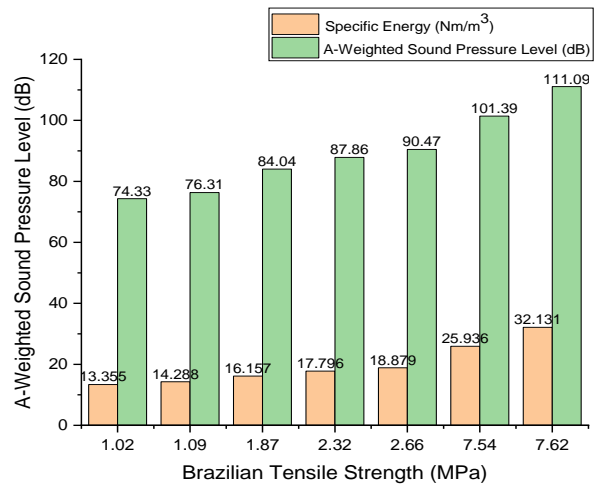


Figure 4.20b Relationship between Brazilian tensile strength to specific energy

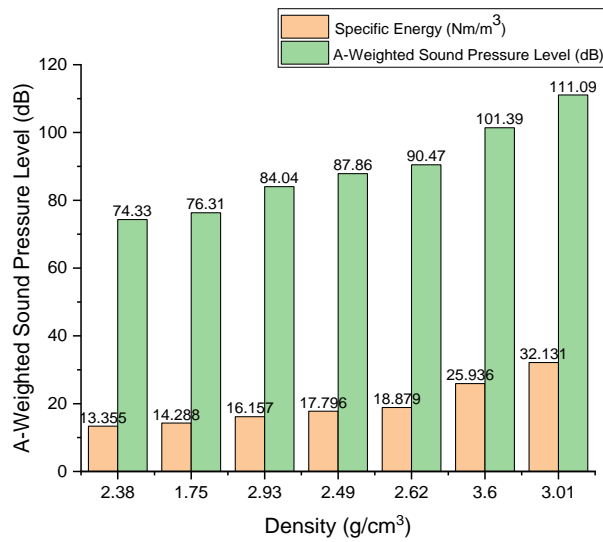


Figure 4.20c: Relationship between density to specific energy

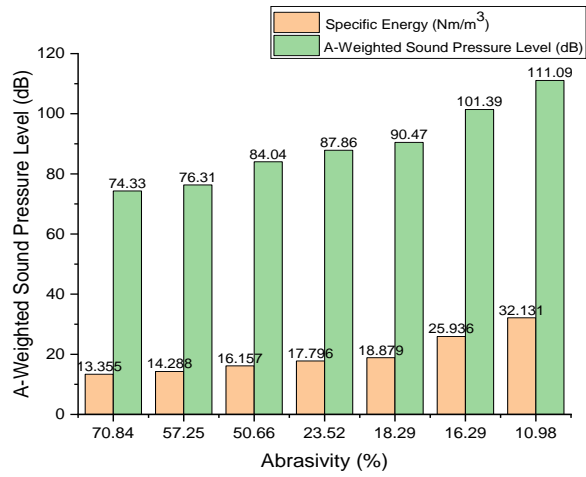


Figure 4.20d: Relationship between abrasivity to specific energy

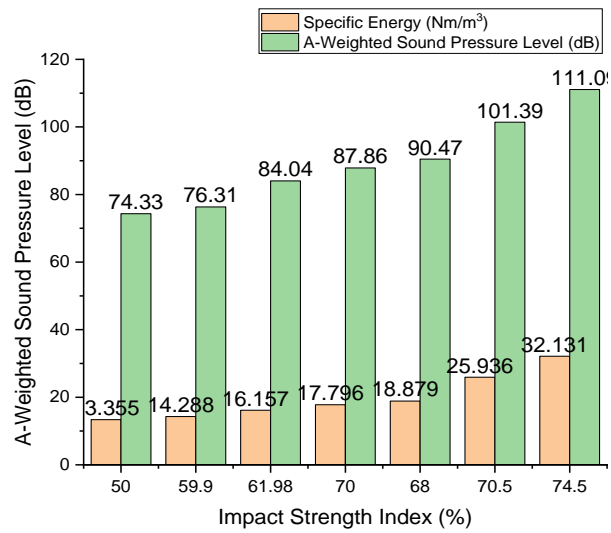


Figure 4.20e: Relationship between impact strength index to specific energy

CHAPTER-5

CONCLUSIONS AND RECOMMENDATIONS

5.1 Conclusions

The following are the conclusions drawn from this research work:

- 1 In relation of operating variables, it was observed that specific energy decreased from 30.381 Nm/m³ to 1.024 Nm/m³ with increasing drill bit diameter, penetration rate and drill bit speed. Similarly, in relation of A-weighted SPL to operating variables it was observed that, A-weighted SPL increased from 71.36 dB to 142.724 dB with increasing drill bit diameter, penetration rate and drill bit speed. The trend of A-weight SPL with the compressive strength is inconsistent which might be due to influences of other rock properties such as abrasivity, mineralogical compositions or petrographic features.
- 2 Thrust and A-weighted sound pressure level increases from 109.23 N to 1001.96 N, 71 dB to 142 dB with an increase in the drill bit diameter, spindle speed, and penetration rate while drilling various rock samples. This may be due to the normal and tangential forces which maintain bit-rock contact frictional forces between diamond drill bit and rock sample. An increase in the drill bit diameter led to increase the thrust forces during diamond drilling operations.
- 3 Torque and A-weighted sound pressure level increased from 2 Nm to 11.88 Nm, 71 dB to 142 dB with an increase in the drill bit diameter, spindle speed, and penetration rate while drilling various rock samples. This may be due to the significant increase in the uniaxial compressive strength of rocks (hardness of the rock). The rock hardness is characterized by a high torque values for hard rock, and also observed that, low torque values for in the soft rocks.
- 4 A-weighted sound pressure level increased corresponding to the rock properties such as UCS, BTS, density, and impact strength index. Higher A-weighted sound pressure level may generally be obtained when drilling in hard rocks having higher UCS and density, which may increase A-weighted sound

pressure level. A-weighted sound pressure level decreased with increasing the abrasivity. It may be the possible the percentage wear loss were observed in the rock samples.

- 5 Simple linear regression model was developed between the rock properties and the sound pressure levels (SPL) measured during diamond drilling. The prediction results show that the developed statistical model prediction has a coefficient of determination (R^2 - value) of 85.5% to 95% with an error from 1.52 % to 10.37 %.
- 6 Multiple regression models were developed between the rock properties and the sound pressure levels measured during diamond drilling. The prediction results show that the developed statistical model has moderate coefficients of determination i.e. R^2 - value of 78.41% to 93.20%, the RMSE value was around zero and the VAF value of 78.41% to 93.23%.
- 7 The multi-layer perceptron (ANN) network was trained using seven types of back-propagation training algorithms i.e. `trainscg`, `traingda`, `trainrp`, `traingdx`, `trainlm`, `trainbfg`, `traingcf`. Their performances were compared in terms of VAF, RMSE and MAPE values. `Trainrp` (resilient back-propagation algorithm) showed better performance than all other algorithms in the prediction of the rock properties.
- 8 A comparison of simple linear, multiple regression models and MLP model using “`trainrp`” algorithm revealed that, simple linear regression, MLP model gave better performance than multiple regression technique with lower MAPE and RMSE values and higher prediction accuracy (VAF value) for all the prediction variables.
- 9 Multiple linear regression models were developed between the rock properties and specific energy using A-weighted equivalent sound level obtained during diamond drilling. The prediction results show that the developed statistical model has moderate coefficients of determination i.e. R^2 - value of 75.58% to 78.76%, the RMSE value was around zero and the VAF value of 72.82% to 84.15%. It was also observed that specific energy increased with increasing UCS, BTS, dry density, and impact strength index, whereas the specific energy decreased with the increase of abrasivity.

5.2 Recommendations for Further Research

1. In the present work, prediction of the rock properties using frequency analysis technique was used in the diamond drilling operation. It is suggested that the future investigation could be carried out using wavelet techniques for quantification of rock properties.
2. In this investigation, the effect of mineralogical composition in rocks on specific energy and noise levels are not reported. It is suggested that further investigation can be carried out in this direction (mineralogical percentage/thin section analysis).
3. In the present work, rock properties and specific energy were predicted using sound pressure levels generated during diamond drilling operations. The same technique can be implemented to predict multiple fracture propagation in rocks, shear strength of rock.
4. This investigation was completely based on laboratory investigations. The same investigation can be conducted at the mining site for estimation of rock properties using dominant frequencies.
5. In field or at drilling site, the drill bit generally goes deeper from the surface, make it difficult to acquire sound pressure levels. To overcome this difficulty, specially designed core drill bits that can be possibly allow to insert microphone/sensors in the core drill bits for acquiring the sound pressure levels.
6. The structure of rocks was not considered in the present research work for measuring noise level/sound levels. It is suggested that further investigation can be carried out in this direction.
7. The texture, structure, size of minerals grains, and bonding between various minerals grains present in the rock will have influence on physico – mechanical properties of rock and hence on sound pressure levels. The same problem is suggested for future investigation.
8. The presence of silicate will have influence on sound pressure level. It is suggested that further investigation can be carried out in this direction.

REFERENCES

Abdi, Y., Garavand, A. T. and Sahamieh, R. Z. (2018). "Prediction of strength parameters of sedimentary rocks using artificial neural networks and regression analysis." *Arabian Journal of Geosciences*, 11 (19), 587 - 592.

Acaroglu, O., Ozdemir, L. and Asbury, B. (2008). "A fuzzy logic model to predict specific energy requirement for tunnel boring machine performance prediction." *Tunneling and Underground Space Technology*, 23 (5), 600 - 608.

Aldeeky, H. and Al Hattamleh, O. (2018). "Prediction of Engineering Properties of Basalt Rock in Jordan Using Ultrasonic Pulse Velocity Test." *Geotechnical and Geological Engineering*, 36 (6), 3511 - 3525.

Altindag, R. (2003). "Correlation of specific energy with rock brittleness concepts on rock cutting." *The Journal of the South Africa Institute of Mining and metallurgy*, 103 (3), 163-171.

Alvarez, G.M. and Babuska, R. (1999). "Fuzzy model for the prediction of unconfined compressive strength of the rock samples." *The Journal of Rock Mechanics Mining Sciences*, 36 (3), 339 - 349.

Atici, U. and Ersoy, A. (2009). "Correlation of specific energy of cutting saws and drilling bits with rock brittleness and destruction energy." *Journal of Materials Processing Technology*, 209 (5), 2602 - 2612.

Aydin, G., Karakurt, I. and Aydiner, K. (2012). "Development of predictive models for specific energy of diamond saw blades concerning operating variables." *JESTECH*, 15(4), 155-161.

Aydin, G., Karakurt, I. and Aydiner, K. (2013). "Development of predictive models for the specific energy of circular diamond sawblades in the sawing of granitic rocks." *Rock Mechanics Rock Engineering*, 46 (4), 767-783.

Balci, C., Demircin, M.A., Copur, H. and Tuncdemir, H. (2004). "Estimation of optimum specific energy based on rock properties for assessment of roadheader performance." *The Journal of the South African Institute of Mining and Metallurgy*, 104 (11), 633-641.

Banks, S. (2013). "Minimizing the mechanical specific energy while drilling using extreme seeking control." 11th International Conference on Vibration Problems, Lisbon, Portugal, September 2013, 9-12.

Becker, H., Lemmes, F. and Schommer, M. (1984). "Testing of rock mechanics as a basis for improved cutting technology." *Gluckauf translation*, 120 (8), 122-124.

Bhatnagar, A. and Khandelwal, M. (2012). "An intelligent approach to evaluate drilling performance." *Neural Computing and Applications*, 21(4), 763-770.

Brown, E.T. (1981). "Rock Characterization testing and monitoring." International society for rock mechanics (ISRM) suggested methods, *Pergamon*, Oxford.

Cao, Q. J., Wiercigroch, M., Pavlovskaja, E. and Yang, S. P. (2010). "Bifurcations and the penetrating rate analysis of a model for percussive drilling." *Acta Mechanica Sinica*, 26 (3), 467-475.

Chiang, L. and Stamm, E. (1998). "Design Optimization of Valveless DTH Pneumatic Hammers by a Weighted Pseudo-Gradient Search Method." *Journal of Mechanical Design*, 120, 687-694.

Copur, H., Tuncdenir, H., Bilgin, N. and Dincer, T. (2001). "Specific Energy as a Criterion for Use of Rapid Excavation Systems in Turkish Mines." *Mining Technology*, 110 (3), 149-157.

Curry, D., Fear, M., Govzitch, A. and Aghazada, L. (2005). "Technical Limit Specific Energy-An Index to Facilitate Drilling Performance Evaluation." *paper SPE/IADC 92318 presented at the SPE/IADC Drilling Conference, Amsterdam, The Netherlands, 23-25 February.*

Clark, B.G. (1982). "Principles of rock drilling and bit wear." *Colorado School of Mines quarterly*, 77(1), 1-12.

Dehghan, S., Sattari, G. H., Chelgani, S. C. and Aliabadi, M. A. (2010). "Prediction of uniaxial compressive strength and modulus of elasticity for Travertine samples using regression and artificial neural networks." *Mining Science and Technology (China)*, 20(1), 41-46.

Delgado, N. S. Rey, A.R., Rio, L.M.S., Sarriá, I.D., Calleja, L. and Argandona.V.G.R. (2005). "The influence of rock micro hardness on the saw ability of Pink Porrino granite (Spain)." *International Journal of Rock Mechanics and Mining Sciences*, 42 (1), 161-166.

Delibalta, M.S., Kahraman, S. and Comakli, R. (2015). "The usability of noise level from rock cutting for the prediction of physico – mechanical properties of rocks." *World Scientific*, 14(1), 1-12.

Dupriest, F. E. and Koederitz, W. L. (2005). "Maximizing Drill Rate with Real-Time Surveillance of Mechanical Specific Energy." *paper SPE/IADC 92194 presented at the SPE/IADC Drilling Conference, Amsterdam, Netherlands.*

Engin, I.C., Bayam, F. and Yasitli, N.E. (2013). "Experimental and statistical evaluation of cutting methods in relation to specific energy and rock properties." *Rock Mechanics and Rock Engineering*, 46 (4), 755-766.

Erosy, A. and Atici, U. (2007). "Correlation of P and S waves with cutting specific energy and dominant properties of volcanic and carbonate rocks." *Rock Mechanics and Rock Engineering*, 40 (5), 491-504.

Ersoy, A., Atici, U. (2004). "Performance characteristic of circular diamond saws in cutting different types of rocks." *Diamond and related Materials*, 13 (1), 22-37.

Ersoy, A. (2003). "Automatic drilling control based on minimum drilling specific energy using PDC and WC bits." *Mining Technology*, 112 (2), 86-96.

Evans, I. (1962). "A theory of the basic mechanics of coal ploughing." *International Symposium on Mining Research*, 2, 761-798.

Evans, I. (1984). "Basic mechanics of the point-attack pick". *Colliery Guardian*, 232 (5), 111-113.

Faisal, S. I., Cording, E. J. and Al-Hattamleh, O. H. (2007). "Estimation of rock engineering properties using hardness tests." *Engineering Geology*, 90 (3-4), 138-147.

Feng, X. T., Young, R. P., Reyes-Montes, J. M., Aydan, Ö., Ishida, T., Liu, J. P. and Liu, H. J. (2019). "ISRM Suggested method for in situ acoustic emission monitoring of the fracturing process in rock masses." *Rock Mechanics and Rock Engineering*, 52 (5), 1395 - 1414.

Field, A. (2009). "Discovering statistics using SPSS." *SAGE Publication Ltd.*, London, 821.

Finol, J., Guo, Y.K. and Jing, X.D. (2001). "A rule based fuzzy model for the prediction of petro physical rock parameters." *J.Pet.Sci.Eng*, 29 (2), 97-113.

Flegner, P., Kacur, J., Durdan, M. and Laciak, M. (2019). "Evaluating noise sources in a working environment when disintegrating rocks by rotary drilling." *Polish Journal of Environmental Studies*, 28 (5), 1-10.

Flegner, P., Kačur, J., Durdán, M., Laciak, M. (2019). "Processing a measured vibroacoustic signal for rock type recognition in rotary drilling technology." *Measurement*, 134, 451-467.

Flegner, P., Kačur, J., Durdán, M., Leško, I., Laciak, M. (2014). Measurement and processing of vibro-acoustic signal from the process of rock disintegration by rotary drilling." *Measurement*, 56, 178-193.

Forouharmajd, F., Mohammadi, Z., Ahmadvand, M. and Forouharmajd, F. (2015). "Sound pressure level tools design used in occupational health by means of labview software." *International Journal of Environmental Health Engineering*, 4 (1), 1-6.

Fowell, R.J. and McFeat-Smith, I. (1976). "Factors influencing the cutting performance of a selective tunnelling machine. In: Jones JM, editor. *Proceedings of the First International Symposium on Tunnelling '76*. London: IMM, 301–309.

Ghaboussi, J., Garrett Jr, J. H. and Wu, X. (1991). "Knowledge-based modeling of material behavior with neural networks." *Journal of engineering mechanics*, 117 (1), 132-153.

Gokceoglu, C. (2002). "A fuzzy triangular chart to predict the uniaxial compressive strength of the Ankara agglomerates from their petrographic composition," *Eng.Geol*, 66 (1), 39-51.

Goktan, R.M. (1991). “Brittleness and micro-scale rock cutting efficiency.” *Mining Science and Technology*, 13 (3), 237–241.

Gradl, C., EustesIII, A.W. and Thonhauser, G. (2007). “An analysis of noise characteristics of drill bits.” *Journal of Energy Resources Technology, ASME*, 134 (1), 1-6.

Hardy, H.R. (1972). “Application of acoustic emission technique to rock mechanics research.” *Acoustic Emission, ASTM STP 505, American Society for Testing and Materials*: 41-83.

Hassanpour, J., Rostami, J., Zhao, J. (2011). “A new hard rock TBM performance prediction model for project planning.” *Tunnelling and Underground Space Technology*, 26 (5), 595-603.

Haykin, S. (1998). “Neural Networks: A Comprehensive Foundation, Prentice Hall PTR.” *Upper Saddle River, NJ, USA*.

He, S., Song, D., Li, Z., He, X., Chen, J., Li, D. and Tian, X. (2019). “Precursor of spatio-temporal evolution law of MS and AE activities for rock burst warning in steeply inclined and extremely thick coal seams under caving mining conditions.” *Rock Mechanics and Rock Engineering*, 52 (7), 2415-2435.

He, M., Li, N., Zhu, J. and Chen, Y. (2020). “Advanced prediction for field strength parameters of rock using drilling operational data from impregnated diamond bit.” *Journal of Petroleum Science and Engineering*, 187, 106847, 1-11.

Hu, X., Su, G., Chen, G., Mei, S., Feng, X., Mei, G. and Huang, X. (2019). “Experiment on rock burst process of borehole and its acoustic emission characteristics.” *Rock Mechanics and Rock Engineering*, 52 (3), 783-802.

Javier, M. (2017). “Optimal operational TBM parameters for efficient hardrock tunnel boring on the basis of rock boreability and on-site testing.” *International Conference on Tunnel boring machines in difficult Grounds (TBM DiGS)*.” Wuhan: 16-18 November 2017.

Jia, S. Q., Wong, R. C. K., Eaton, D. W. and Eyre, T. S. (2018). “Investigating fracture growth and source mechanisms in shale using acoustic emission technique.” In *52nd US Rock Mechanics/Geomechanics Symposium, American Rock Mechanics Association, August*.

Kahraman, S., Delibalta, M.S. and Comakli, R. (2013). “ Noise level measurement test to predict the abrasion resistance of rock aggregates.” *Fluctuation and Noise Letters*, 12 (4), 1350001-1350021.

Kahraman, S., Ucurum, M., Yogurtcuoglu, E. and Fener, M. (2019). “Evaluating the grinding process of granites using the physic - mechanical and mineralogical properties.” *Journal of Metals, Materials and Minerals*, 29(2), 51-57.

Kalyan, B. (2016). “Experimental investigations on assessment and prediction of specific energy in rock indentation tests.” Un published Ph.D thesis, NITK Surathkal.

Kalyan, B., Murthy, Ch.S.N. and Choudhary, R.P. (2016). “Development of predictive models for the specific energy in indentation of rocks.” *Recent Advances in Rock Engineering (RARE)*, Atlantis Press, 530–535.

Karakus, M. and Perez, S. (2014). “Acoustic emission analysis for rock–bit interactions in impregnated diamond core drilling.” *International Journal of Rock Mechanics and Mining Sciences*, 68, 36-43.

Katz, O., Reches, Z. and Roegiers, J. C. (2000). "Evaluation of mechanical rock properties using a Schmidt Hammer." *International Journal of rock mechanics and mining sciences*, 37 (4), 723-728.

Kılıç, A. and Teymen, A. (2008). "Determination of mechanical properties of rocks using simple methods." *Bulletin of Engineering Geology and the Environment*, 67 (2), 237-244.

Kim, K. and Gao, H. (1995). "Probabilistic approaches to estimating variation in the mechanical properties of rock masses." *International journal of rock mechanics and mining sciences & geomechanics abstracts*, 32 (2), 111-120.

Kivade, S.B., Murthy, Ch.S.N. and Vardhan, H. (2015). "ANN models for prediction of sound and penetration rate in percussive drilling." *Journals of Institution of Engineers, India, series D*, 96 (2), 93 - 103.

Kivade, S.B., Murthy, Ch.S.N. and Vardhan, H. (2012a). "Prediction of penetration rate and sound level produced during percussive drilling using regression and artificial neural networks." *International Journal of Earth Science and Engineering*, 5 (6), 1639-1644.

Kivade, S.B., Murthy, Ch.S.N. and Vardhan, H. (2013) "Laboratory investigations on percussive drilling." *The Journal of Institute of Engineers*, 94 (2), 81-87.

Kivade, S.B., Murthy, Ch.S.N. and Vardhan, H. (2012b). "The use of dimensional analysis and optimization of pneumatic drilling operations and operating parameters." *The Journal of Institute of Engineers*, 93 (1), 31-36.

Krepelka, F. and Futo, J. (2007). "Acoustics aspects of technology process in the rock disintegration." *Acta montanistica slovacca*, 12 (1), 25-28.

Krúpa, V., Kruľáková, M., Lazarová, E., Labaš, M., Feriančíková, K. and Ivaničová, L. (2018). “Measurement, modeling and prediction of penetration depth in rotary drilling of rocks.” *Measurement*, 117, 165-175.

Kumar, B.R., Vardhan, H. and Govindaraj, M. (2011a). “A new approach for estimation of rock properties of metamorphic rocks.” *The International Journal of Mining and Mineral Engineering*, 3(2), 109-123.

Kumar, B.R., Vardhan, H. and Govindaraj, M. (2011b). “Prediction of uniaxial compressive strength, tensile strength, and porosity of sedimentary rocks using sound level produced during rotary drilling.” *Rock Mechanics and Rock Engineering*, 44 (5), 613-620.

Kumar, B.R., Vardhan, H. and Govindaraj, M. (2011c). “Sound level produced during rock drilling Vis-à-vis rock properties.” *Engineering Geology*, 123 (4), 333-337.

Kumar, B.R., Vardhan, H., Govindaraj, M. and Saraswathi, P.S. (2013a). “Artificial neural network model for Prediction of rock properties from sound levels produced during drilling.” *An International Journal of Geomechanics and Geoengineering*, 8 (1), 53-61.

Kumar, B.R., Vardhan, H., Govindaraj, M. and Vijay, M. (2013b). “Regression analysis and ANN models to predict rock properties from sound levels produced during drilling.” *Intrnational Journal of Rock mechanics and Mining Sciences*, 58, 61-72.

Li, N., Zhang, S., Zou, Y., Ma, X., Zhang, Z., Li, S. and Sun, Y. (2018). “Acoustic emission response of laboratory hydraulic fracturing in layered shale.” *Rock Mechanics and Rock Engineering*, 51 (11), 3395-3406.

Liao, M., Liu, Y., Chávez, J. P., Chong, A. S. and Wiercigroch, M. (2018). “Dynamics of vibro-impact drilling with linear and nonlinear rock models.” *International Journal of Mechanical Sciences*, 146, 200-210.

Liu, S., Li, X., Li, Z., Chen, P., Yang, X. and Liu, Y. (2019). “Energy distribution and fractal characterization of acoustic emission (AE) during coal deformation and fracturing.” *Measurement*, 136, 122-131.

Luis, E., Izquierdo, and Chiang, L. (2004). “A methodology for estimation of the specific rock energy index using corrected down-the-hole drill monitoring data.” *Mining Technology*, 113 (4), 225 - 236.

Luo, Y., Collins, C., Qi, B. and Li, M.M. (2014). “Experimental studies on controlling drilling parameters to reduce roof bolt-hole drilling noise.” *The Journal of Mining Engineering*, 66 (5), 54 - 61.

Lundberg, B. (1971). “Some basic problems in percussive rock destruction.” Ph.D. Thesis. Chalmers University Technology, Gothenburg, Sweden.

Mahdiabadi, N. and Khanlari, G. (2019). “Prediction of Uniaxial Compressive Strength and Modulus of Elasticity in Calcareous Mudstones Using Neural Networks, Fuzzy Systems, and Regression Analysis.” *Periodica Polytechnica Civil Engineering*, 63 (1), 104 - 114.

Madhubabu, N., Singh, P. K., Kainthola, A., Mahanta, B., Tripathy, A. and Singh, T. N. (2016). “Prediction of compressive strength and elastic modulus of carbonate rocks.” *Measurement*, 88, 202-213.

Masood. (2015). “Estimation of sound level produced during drilling of igneous rock samples using a portable drill set-up.” Global challenges policy frame work & sustainable development for mining of mineral and fossil energy resources (GCPF), *Procedia Earth and Planetary Science*, 11, 469–482.

McNally, G.H. (1990). "The prediction of geotechnical rock properties from sonic and neutron logs." *Australian Society of Exploration Geophysics (ASEG)*, 21 (1/2), 65-71.

Meireles, M. R., Almeida, P. E. and Simões, M. G. (2003). "A comprehensive review for industrial applicability of artificial neural networks." *IEEE transactions on industrial electronics*, 50 (3), 585-601.

Mellor, M. and Hawkes, I. (1971). "Measurement of tensile strength by diametral compression of discs and annuli." *Engineering Geology*, 5 (3), 173-225.

Meulenkamp, F. and Grima, M. A. (1999). "Application of neural networks for the prediction of the unconfined compressive strength (UCS) from Equotip hardness." *International Journal of rock mechanics and mining sciences*, 36 (1), 29-39.

Miklusova, V., Usalova, L., Ivanicova, L. and Krepelka, F. (2006). "Acoustic signals - new feature in monitoring of rock disintegration process." *Contribution to Geophysics Geodesy*, 36, 125-133.

Miller, D. and Ball, A. (1990). "An instrumented laboratory machine for the evaluation of drill bit performance." *Journal of the south African Institute of Mining and metallurgy*, 90 (10), 283-288.

Momeni, E., Armaghani, D. J., Hajihassani, M. and Amin, M. F. M. (2015). "Prediction of uniaxial compressive strength of rock samples using hybrid particle swarm optimization-based artificial neural networks." *Measurement*, 60, 50-63.

Yurdakul, M. and Akdas, H. (2012). "Prediction of Specific Cutting Energy for Large Diameter Circular Saws during Natural Stone Cutting." *International Journal of Rock Mechanics and Mining Science*, 53, 38-44.

Neves, F.P., costaesilva, M. and Navarro torres, V.F. (2012). "Evaluation of elastic deformation energy in stone cutting of Portuguese marbles with a diamond saw." *The Journal of the African Institute of Mining and Metallurgy*, 112 (3), 413-417.

Obert, L. (1941). "Use of sub audible noises for prediction of rock bursts - Part I. U.S." *Bureau of Mines*, R.I.3555.

Obert, L. and Duvall W.I. (1942). "Use of sub audibility noise for prediction of rock bursts - Part II.U.S." *Bureau of Mines*, R.I.3654.

Ocak, I. and Seker, S. E. (2012). "Estimation of elastic modulus of intact rocks by artificial neural network." *Rock mechanics and rock engineering*, 45 (6), 1047-1054.

Omar, H., Ahmad, J., Nahazanan, H., Mohammed, T. A. and Yusoff, Z. M. (2018). "Measurement and simulation of diametrical and axial indirect tensile tests for weak rocks." *Measurement*, 127, 299-307.

Pessier, R.C. and Fear, M.J. (1992). "Quantifying Common Drilling Problems With Mechanical Specific Energy and a Bit-Specific Coefficient of Sliding Friction." *paper SPE 24584 presented at the 1992 SPE 67th Annual Technical Conference and Exhibition*, Washington, DC.

Qin, M., Wang, K., Pan, K., Sun, T. and Liu, Z. (2018). "Analysis of signal characteristics from rock drilling based on vibration and acoustic sensor approaches." *Applied Acoustics*, 140, 275-282.

Rafavich, F., Kendall, C.H. and Todd, T.P. (1984). "The relation between acoustic properties and the petrographic character of carbonate rocks." *Geophysics*, 49 (10), 1622-1636.

Rastegarnia, A., Teshnizi, E. S., Hosseini, S., Shamsi, H. and Etemadifar, M. (2018). "Estimation of punch strength index and static properties of sedimentary rocks using neural networks in south west of Iran." *Measurement*, 128, 464-478.

Reddish, D.J. and Yasar, E. (1996). "A new portable rock strength index test based on specific energy." *International Journal of Rock Mechanics Mining Science & Geo mechanics*, 33 (5), 543-548.

Rostami, J., Kahraman, S., Naeimipour, A. and Collins, C. (2015). "Rock characterization while drilling and application of roof bolter drilling data for evaluation of ground conditions." *Journal of Rock Mechanics and Geotechnical Engineering*, 7 (3), 273-281.

Rumelhart, D. E. and McClelland, J. L. (1986). "PDP Research Group. Parallel distributed processing." *Exploration in the microstructure of cognition*, 1, 3 - 44.

Salimia, A., Moormanna, C., Singh, T. N. and Jain, P. (2015). TBM performance prediction in rock tunneling using various artificial intelligence algorithms." *In Proceeding 11th Iranian and 2nd Regional Conference Tunnels and the Future*, Stuttgart, Germany.

Sarkar, K., Tiwary, A. and Singh, T. N. (2010). "Estimation of strength parameters of rock using artificial neural networks." *Bulletin of engineering geology and the environment*, 69 (4), 599 - 606.

Sachpazis, C. I. (1990). "Correlating schmidt hardness with compressive strength and young's modulus of carbonate rocks." *Bulletin of the International Association of Engineering Geology*, 42 (1), 75 - 83.

Selmer-Olsen, R. and Blindheim, D.T. (1970). "On the drillability of rocks by percussive drilling." *In proceeding of second congress of the international society for rock mechanics, Belgrade*, 65-70.

Sheng, M., Tian, S., Zhang, B. and Ge, H. (2019). "Frequency analysis of multi-sources acoustic emission from high-velocity waterjet rock drilling and its indicator to drilling efficiency." *International Journal of Rock Mechanics and Mining Sciences*, 115, 137-144.

Shewalla, M. and Smith, J. (2015) "Measurement of specific energy during drilling of rocks." *The Journal of EJGE*, 20 (16), 123 - 129.

Shreedharan, S., Hegde, C., Sharma, S. and Vardhan, H. (2014). "Acoustic finger printing for rock identification during drilling." *International Journal of Mining and Mineral Engineering*, 5(2), 89-105.

Simpson, P.K. (1990). "Artificial neural systems: foundations, paradigms, applications, and implementations." Pergamon.

Singh, T. N., Kanchan, R., Verma, A. K. and Singh, S. (2003). "An intelligent approach for prediction of triaxial properties using unconfined uniaxial strength." *Min Eng. J.* 5 (4), 12-16.

Sinkala, T. (1991). "Relating drilling parameters at the bit-rock interface: theoretical and field studies." *Mining Science and Technology*, 12, 67-77.

Singh, V. K., Singh, D. and Singh, T. N. (2001). "Prediction of strength properties of some schistose rocks from petrographic properties using artificial neural networks." *International Journal of Rock Mechanics and Mining Sciences*, 38 (2), 269 - 284.

Sonmez, H., Gokceoglu, C., Nefeslioglu, H. A. and Kayabasi, A. (2006). "Estimation of rock modulus: for intact rocks with an artificial neural network and for rock masses with a new empirical equation." *International Journal of Rock Mechanics and Mining Sciences*, 43 (2), 224 - 235.

Teale, R. (1965). "The concept of specific energy in rock drilling." *International Journal of Rock Mining Sciences*, 2 (1), 57 - 73.

Teymen, A. (2019). "Estimation of Los Angeles abrasion resistance of igneous rocks from mechanical aggregate properties." *Bulletin of Engineering Geology and the Environment*, 78 (2), 837 - 846.

Tiryaki, B. (2008a). "Application of artificial neural networks for predicting the cuttability of rocks by drag tools." *Tunneling and Underground Space Technology*, 23 (3), 273 -280.

Tiryaki, B. (2008b). "Predicting intact rock strength for mechanical excavation using multivariate statistics, artificial neural networks, and regression trees." *Engineering Geology*, 99 (1-2), 51 - 60.

Tiryaki, B. and Dikmen, A. (2006). "Effects of rock properties on specific cutting energy in linear cutting of sandstones by picks." *Rock Mech. Rock Engineering.*" 39 (2), 89 - 120.

Tiryaki, B., Ayhan, M. and Hekimoglu, O. Z. (2001). "A new computer program for cutting head design of roadheaders and drum shearers." *In 17th International Mining Congress and Exhibition of Turkey-IMCET*, 655 - 662.

Tripathy, A., Singh, T. N. and Kundu, J. (2015). "Prediction of abrasiveness index of some Indian rocks using soft computing methods." *Measurement*, 68, 302 - 309.

Ulusay, R. and Hudson, J.A. (2007). "The complete ISRM suggested methods for rock characterization testing and monitoring 1947-2006." *Compilation arranged by the ISRM Turkish national group*, Ankara, Turkey: 628, ISBN: 978-975-93675-4-4.

Vardhan, H. and Murthy, Ch.S.N. (2007). "An experimental investigation of jack hammer drill noise with special emphasis on drilling in rocks of different compressive strength." *Noise Control Engineering Journal*, 55 (3), 282 - 293.

Vardhan, H., Adhikari G.R. and Govindaraj M. (2009). "Estimating rock properties using sound levels produced during drilling." *International Journal of Rock Mechanics & Mining Sciences*, 46 (3), 604 - 612.

Waughman, R.J., Kenner, J.V. and Moore, R.A. (2002). "Real-Time Specific Energy Monitoring Reveals Drilling Inefficiency and Enhances the Understanding of When to Pull Worn PDC Bits." *paper IADC/SPE 74520 presented at the IADC/SPE Drilling Conference, Dallas, Texas, and 26 - 28 February*.

Wijk, G. (1982). "Indexation effects on mechanical rock destruction efficiency. SveDeFo Rep. DS 1982; 2, Stockholm.

Xiao, Y., Hurich, C., Molgaard, J. and Butt, S. D. (2018). "Investigation of active vibration drilling using acoustic emission and cutting size analysis." *Journal of Rock Mechanics and Geotechnical Engineering*, 10 (2), 390-401.

Xie, J. and Tamaki, J. (2007). "Parameterization of micro-hardness distribution in granite related to abrasive machining performance." *Journal of Materials Processing Technology*, 186 (1-3), 253 - 258.

Yaşar, E. and Erdoğan, Y. (2004). "Estimation of rock physicochemical properties using hardness methods." *Engineering Geology*, 71 (3-4), 281 - 288.

Yilmaz, I. (2009). "Prediction of the strength and elasticity modulus of gypsum using multiple regression, ANN, and ANFIS models." *Int. J. Rock Mech. Min. Sci.* 46, 803-810.

Yilmaz, I. (2010). "Comparison of landslide susceptibility mapping methodologies for Koyulhisar, Turkey: conditional probability, logistic regression, artificial neural networks, and support vector machine." *Environmental Earth Sciences*, 61 (4), 821-836.

Yilmaz, I. and Oguz Kaynar. (2011). "Multiple regression, ANN (RBF, MLP), and ANFIS models for prediction of swell potential of clayey soils." *Expert systems with application*, 38 (5), 5958 - 5966.

Yilmaz, I. and Yuksek, A.G. (2008). "Technical note an example of artificial neural network (ANN) application for indirect estimation of rock parameters." *Rock Mech Rock.Engg.* 41 (5), 781-795.

Yilmaz, I. and Yuksek, A.G. (2009). "Prediction of the strength and elasticity modulus of gypsum using multiple regression, ANN, ANFIS models and their comparison." *Int.J.Rock Mech.Min.Sci.* 46 (4), 803 - 810.

Yilmaz, I. and Kaynar, O. (2011). "Multiple regression, ANN (RBF, MLP) and ANFIS models for prediction of swell potential of clayey soils." *Expert systems with applications*, 38 (5), 5958 - 5966.

Yilmaz, I. and Sendir, H. (2002). "Correlation of Schmidt hardness with unconfined compressive strength and Young's modulus in gypsum from Sivas (Turkey)." *Engineering Geology*, 66 (3-4), 211 - 219.

Yılmaz, I. and Yuksek, A. G. (2008). “An example of artificial neural network (ANN) application for indirect estimation of rock parameters.” *Rock Mechanics and Rock Engineering*, 41 (5), 781 - 795.

Zborovjan, M. (2001). “Identification of minerals during drilling process via acoustic signal.” *Metallurgy and Foundry*, Krakow, Poland, 26 (4), 367 - 374.

Zborovjan, M. (2002). “Identification of Minerals from Sound during Drilling.” *Semestral Project*, TU-Kosice, Poland.

Zborovjan, M., Lesso, I. and Dorcak, L. (2003). “Acoustic identification of rocks during drilling process.” *Acta Montanistica Slovaca*, 8 (4), 191-193.

Zhang, J., Ai, C., Li, Y. W., Che, M. G., Gao, R. and Zeng, J. (2018a). “Energy-based brittleness index and acoustic emission characteristics of anisotropic coal under triaxial stress condition.” *Rock Mechanics and Rock Engineering*, 51 (11), 3343 - 3360.

Zhang, R., Ai, T., Ren, L. and Li, G. (2018b). “Failure characterization of three typical coal-bearing formation rocks using acoustic emission monitoring and X-ray computed tomography techniques.” *Rock Mechanics and Rock Engineering*, 52 (6), 1945 - 1958.

Zorlu, K., Gokceoglu, C., Ocakoglu, F., Nefeslioglu, H. A. and Acikalin, S. (2008). “Prediction of uniaxial compressive strength of sandstones using petrography-based models.” *Engineering Geology*, 96 (3-4), 141 - 158.

APPENDIX-A

Table 4.A1: A-weighted sound pressure level of ochre, bituminous coal, laterite, pink limestone, black limestone, hematite, and dolomite for different drill bit diameter

	A-weighted sound pressure level (dB)						
Drill bit diameter (mm)	Ochre	Bituminous coal	Laterite	Pink limestone	Black limestone	Hematite	Dolomite
6	75.548	75.036	81.120	77.544	73.972	82.908	82.864
10	77.20	78.372	83.884	77.736	77.768	84.68	86.08
16	79.088	79.552	86.452	83.964	111.908	85.824	116.43
18	84.188	82.108	87.256	90.868	116.028	89.008	124.5
20	85.648	86.524	89.608	94.212	117.712	107.572	135.908

Table 4.A2: A-weighted sound pressure level of ochre, bituminous coal, laterite, pink limestone, black limestone, hematite, and dolomite for different penetration rate

	A-weighted sound pressure level (dB)						
Penetration rate (mm/min)	Ochre	Bituminous coal	Laterite	Pink limestone	Black limestone	Hematite	Dolomite
2	71.336	75.972	81.148	80.004	81.412	88.996	87.204
3	73.764	77.552	84.184	84.496	86.632	89.46	88.8
4	74.896	79.888	84.336	86.808	107.956	90.896	91.368
5	76.68	81.564	85.24	89.948	114.052	92.672	125.564
6	79.996	83.616	87.292	85.068	113.336	101.968	132.548

Table 4.A3: A-weighted sound pressure level of ochre, bituminous coal, laterite, pink limestone, black limestone, hematite, and dolomite for different drill bit speed

	A-weighted sound pressure level (dB)						
Drill bit speed (rpm)	Ochre	Bituminous coal	Laterite	Pink limestone	Black limestone	Hematite	Dolomite
150	71.888	71.36	79.204	79.496	109.936	85.512	88.984
200	73.932	72.8	80.64	83.452	112.376	89.932	89.432
250	74.404	75.996	82.812	84.228	121.332	97.084	120.212
300	74.924	78.688	85.256	86.912	122.44	100.564	126.132
350	79.924	81.748	87.288	93.236	131.304	123.910	142.724

Table 4.A4: Specific energy of ochre, bituminous coal, laterite, pink limestone, black limestone, hematite, and dolomite for different drill bit diameter

	Specific energy (Nm/m ³)						
Drill bit diameter (mm)	Ochre	Bituminous coal	Laterite	Pink limestone	Black limestone	Hematite	Dolomite
6	10.527	10.360	12.043	28.229	30.213	29.354	30.381
10	7.1281	9.543	8.137	18.572	18.042	13.490	17.829
16	5.251	7.112	5.636	12.785	12.826	12.838	13.061
18	3.199	5.886	4.680	9.662	6.040	8.853	12.452
20	1.672	2.540	2.289	4.732	3.273	3.115	5.931

Table 4.A5: Specific energy of ochre, bituminous coal, laterite, pink limestone, black limestone, hematite, and dolomite for different penetration rate

	Specific energy (Nm/m ³)						
Penetration rate (mm/min)	Ochre	Bituminous coal	Laterite	Pink limestone	Black limestone	Hematite	Dolomite
2	6.929	9.084	15.864	21.174	19.296	15.594	25.076
3	4.703	7.029	12.677	16.431	11.376	13.465	18.644
4	3.614	5.434	7.595	11.692	8.675	10.314	13.200
5	2.029	2.819	5.562	8.128	5.063	8.284	8.729
6	1.502	2.075	4.088	6.554	3.984	7.993	5.006

Table 4.A6: Specific energy of ochre, bituminous coal, laterite, pink limestone, black limestone, hematite, and dolomite for different drill bit speed

	Specific energy (Nm/m ³)						
Drill bit speed (rpm)	Ochre	Bituminous coal	Laterite	Pink limestone	Black limestone	Hematite	Dolomite
150	6.859	8.187	14.001	17.476	10.256	12.456	16.417
200	4.472	7.227	11.677	10.364	9.261	11.008	11.155
250	3.300	6.532	9.562	9.187	8.293	10.044	9.271
300	2.123	3.228	9.595	8.157	8.428	9.998	9.459
350	1.024	2.267	5.088	7.796	8.156	7.145	9.353

Table 4.A7: Thrust for different drill bit diameters while drilling ochre, bituminous coal, laterite, pink limestone, black limestone, hematite, and dolomite samples

Drill bit diameter (mm)	Thrust (N)						
	Ochre	Bituminous coal	Laterite	Pink limestone	Black limestone	Hematite	Dolomite
6	213.64	173.92	340.52	528.16	514.24	629.96	729
10	305.68	218.32	464.56	673.24	601.6	702.44	754.92
16	401.68	323.64	494.24	710	768.36	871.84	815.56
18	455.28	355.52	585.52	757.48	799.12	926.16	824.12
20	511.36	573.84	631.48	804.2	950.16	994.52	906.88

Table 4.A8: Thrust for different penetration rates while drilling ochre, bituminous coal, laterite, pink limestone, black limestone, hematite, and dolomite samples

Penetration rate (mm/min)	Thrust (N)						
	Ochre	Bituminous coal	Laterite	Pink limestone	Black limestone	Hematite	Dolomite
2	237.61	191.68	313.84	568.92	213.2	485.24	320.2
3	286.24	221.28	372.64	674.88	381.12	694.4	569.6
4	329.92	251.32	432.26	758.04	569.92	767.6	640.08
5	406.64	343.28	570.24	793.72	753.08	827.12	792.88
6	499.24	587.68	677.24	897.52	1001.96	940.56	897.72

Table 4.A9: Thrust for different drill bit speeds while drilling ochre, bituminous coal, laterite, pink limestone, black limestone, hematite, and dolomite samples

Drill bit speed (rpm)	Thrust (N)						
	Ochre	Bituminous coal	Laterite	Pink limestone	Black limestone	Hematite	Dolomite
150	109.23	264.16	352.2	511.96	666.4	744.24	568.4
200	216.04	364.16	380.76	612.96	699.4	818.28	794.88
250	293.04	558.92	399.32	691.96	755.12	844.96	892.44
300	532.64	603.72	462.72	898.52	863.8	887.2	917.64
350	589.92	794.32	781.32	997.68	970.76	992.2	947.12

Table 4.A10: Torque for different drill bit diameters of ochre, bituminous coal, laterite, pink limestone, black limestone, hematite, and dolomite samples

	Torque (Nm)						
Drill bit diameter (mm)	Ochre	Bituminous coal	Laterite	Pink limestone	Black limestone	Hematite	Dolomite
6	2	3.6	3.6	3.72	4.12	6.92	7.64
10	3	4.8	4.24	5.8	5.2	7.64	7.99
16	4	5.8	4.88	5.98	6.92	8.04	8.92
18	4.5	6	4.52	6.64	7.96	8.68	9.4
20	5	7.2	6.84	7.2	8.88	9.96	9.72

Table 4.A11: Torque for different penetration rates while drilling ochre, bituminous coal, laterite, pink limestone, black limestone, hematite, and dolomite samples

	Torque (Nm)						
Penetration rate (mm/min)	Ochre	Bituminous coal	Laterite	Pink limestone	Black limestone	Hematite	Dolomite
2	3.04	4.72	3.84	4.72	3.2	7.2	4.96
3	4.01	5	4.72	5.08	4.56	7.6	5.72
4	4.44	5.9	6.64	6.84	5.56	8.2	6.52
5	5.04	6.2	7.04	7.52	6.92	8.8	8.28
6	6.19	7.02	7.84	8.68	7.44	9.36	9.6

Table 4.A12: Torque for different drill bit speeds while drilling of ochre, bituminous coal, laterite, pink limestone, black limestone, hematite, and dolomite samples

	Torque (Nm)						
Drill bit speed (rpm)	Ochre	Bituminous coal	Laterite	Pink limestone	Black limestone	Hematite	Dolomite
150	2.6	4.52	2.12	5.52	5	4.23	5.12
200	3.4	5.52	2.78	6.76	6.96	6.04	5.96
250	3.9	5.92	4.92	6.94	7.8	6.36	7.84
300	4.4	6.48	5.96	8.18	9.52	7.08	8.28
350	6.4	6.95	6.8	8.57	10.4	9.76	11.88

Table 4.A17: Predicted values, measured values, and model error from the prediction model for uniaxial compressive strength (ten rock samples for validation)

Sl.no	Rock sample name	UCS (MPa)*	Predicted UCS (MPa)	Error %
1	Marble	24.52	24.526	0.0244
2	Moon white granite	28.83	28.846	0.0555
3	Basalt	54.13	54.166	0.0665
4	Black galaxy granite	56.977	56.108	1.5251
5	Granite grey	46.23	44.246	4.2915
6	Felsite mysore	47.60	42.626	10.4984
7	Syenite	48.1	44.106	8.3035
8	Diorite porphyry	57.9	50.946	12.0103
9	Granite karnataka	77.9	65.926	15.3709
10	Gabbro madduru	102.6	100.646	1.9044

* The data on UCS presented in Table 4.A17 have been taken from Kalyan et al., (2016) & Masood (2015) for the purpose of model validation.

Table 4.A18: Predicted values, measured values, and model error from the prediction model for Brazilian tensile strength (ten rock samples for validation)

Sl.no	Rock sample name	BTS (MPa)*	Predicted BTS (MPa)	Error %
1	Marble	2.58	2.583	0.2325
2	Moon white granite	2.98	2.983	0.1006
3	Basalt	5.58	5.583	0.0537
4	Black galaxy granite	5.831	5.236	10.2040
5	Granite grey	5.23	5.101	2.4856
6	Felsite mysore	5.60	5.603	0.0535
7	Syenite	5.95	5.651	5.0252
8	Diorite porphyry	6.95	6.351	8.6187
9	Granite karnataka	9.30	9.204	1.0322
10	Gabbro madduru	12.3	11.303	8.1056

* The data on Brazilian tensile strength presented in Table 4.A18 have been taken from Kalyan et al., (2016) & Masood (2015) for the purpose of model validation.

Table 4.A19: Predicted values, measured values, and model error from the prediction model
for density (ten rock samples for validation)

Sl.no	Rock sample name	Density (gm/cm ³)*	Predicted density (gm/cm ³)	Error %
1	Marble	2.59	2.59	0.0000
2	Moon white granite	2.64	2.64	0.0000
3	Basalt	2.85	2.85	0.0000
4	Marble(kulahya yesili)	2.67	2.64	1.1235
5	Marble (afyon sekeri)	2.62	2.80	6.8702
6	Serpentinite	2.73	2.63	3.6630
7	Amphibole schist	2.69	2.30	14.4981
8	Quartzite	2.72	2.70	0.7353
9	Micaschist	2.75	2.69	3.6363
10	Travertine (limra)	2.35	2.01	14.4680

* Table 4.A19 data on density have been taken from Kahraman et al., (2013) & Kalyan et al., (2016) for the purpose of validation of the developed model

Table 4.A29: Experimental results of 125 dominant frequencies (Hz) for each rock sample

Test conditions	Drill bit diameter (mm)	Penetration rate (mm/min)	Drill bit Speed (rpm)	Ochre	Bituminous Coal	Laterite	Pink limestone	Black limestone	Ironstone	Dolomite
1	6	2	150	5047	7360	6238	8000	5127	7313	7911
2	6	2	200	6024	8000	6000	7500	8000	7845	5401
3	6	2	250	5024	6520	6258	7412	6347	7680	5874
4	6	2	300	7014	7251	6741	8000	7541	7845	7004
5	6	2	350	5092	7529	6852	5214	7935	7999	6458
6	6	3	150	6000	5241	7000	6894	6012	7890	5252
7	6	3	200	5791	7899	5012	7553	5154	6201	7000
8	6	3	250	8000	6894	7285	5213	7899	7589	7676
9	6	3	300	7922	7836	7341	5000	6000	7845	8000
10	6	3	350	7500	7856	7417	6471	7985	7001	5250
11	6	4	150	8000	8000	7108	8000	5246	7685	7714
12	6	4	200	7771	5478	8000	5445	6999	7000	7685

13	6	4	250	5214	6998	7561	7456	5892	6993	7000
14	6	4	300	6999	6548	8001	7534	6007	8000	7891
15	6	4	350	8000	7993	7985	7641	7262	6457	7245
16	6	5	150	6247	7854	8000	7648	7856	7000	7658
17	6	5	200	5693	7841	7532	8000	7977	7498	7999
18	6	5	250	7958	5001	7214	7412	8000	7741	5879
19	6	5	300	8000	6641	8000	8000	5213	7769	6457
20	6	5	350	7142	8642	8001	5798	7845	8000	5281
21	6	6	150	5190	5731	5169	6000	5213	6589	6447
22	6	6	200	5999	6521	5214	7417	7008	7894	8001
23	6	6	250	5097	7854	5000	7888	7104	7733	7451
24	6	6	300	5896	5411	5891	8001	5998	8000	7481
25	6	6	350	7982	8000	5899	7885	5276	7450	8000
26	10	2	150	8000	8000	5201	7905	5782	6793	7704
27	10	2	200	7862	6987	8000	6451	5841	6000	4751
28	10	2	250	6807	8000	6208	6001	6089	6854	6652
29	10	2	300	7891	7541	6985	5214	6974	5689	8002

30	10	2	350	5240	7629	5525	7789	7943	6735	6975
31	10	3	150	7856	6471	8000	6008	7048	6214	8000
32	10	3	200	8000	5412	6259	6471	6998	5648	5481
33	10	3	250	7894	7814	6009	7401	6854	7474	5278
34	10	3	300	8000	7992	6785	5158	5047	5234	5894
35	10	3	350	6899	5689	6456	6320	7852	5000	8000
36	10	4	150	5446	5155	7031	7000	6689	7458	5417
37	10	4	200	8000	7451	7008	7412	8000	5234	6000
38	10	4	250	8000	6560	7496	7652	7548	7000	7412
39	10	4	300	7900	8000	8000	7810	8000	7897	7869
40	10	4	350	5408	6014	5689	7691	5214	5200	7568
41	10	5	150	6897	6475	6841	7891	7994	5940	7914
42	10	5	200	5286	5412	6001	7941	6568	6000	7365
43	10	5	250	8001	8974	8007	8001	6389	5412	7856
44	10	5	300	5031	7986	5687	6990	5133	6692	6874
45	10	5	350	6589	5641	6003	8000	8000	8000	8000
46	10	6	150	8000	6531	6999	7121	7854	5285	6987

47	10	6	200	7894	7894	7074	7235	5489	5867	7000
48	10	6	250	5442	7891	8000	7452	5989	7000	7104
49	10	6	300	7214	6457	6741	7861	6000	7984	7689
50	10	6	350	8000	6812	7187	6002	7977	7614	7467
51	16	2	150	6899	5481	5257	5474	5899	5006	7900
52	16	2	200	7086	8546	5332	6000	8000	7689	7842
53	16	2	250	7952	8000	5623	5789	7451	7771	7800
54	16	2	300	8000	7541	5404	6014	7823	8000	6987
55	16	2	350	8000	5017	5051	6741	6458	7568	6589
56	16	3	150	6948	6587	8000	6589	6004	7999	6325
57	16	3	200	7856	8000	5813	6984	8000	7025	6985
58	16	3	250	6852	6891	5974	7000	6241	7001	6999
59	16	3	300	7992	5142	5009	7456	5182	6541	7458
60	16	3	350	8005	8012	5278	8000	8000	6741	7986
61	16	4	150	7899	5004	5382	6201	6503	8000	7327
62	16	4	200	5269	7412	6007	5641	7856	7892	7958
63	16	4	250	6589	7059	6102	5894	6247	6845	7800

64	16	4	300	7009	7999	8000	5987	8000	8000	8000
65	16	4	350	8000	5033	5014	5999	8001	7965	6589
66	16	5	150	8001	6548	8000	6000	7923	7999	8001
67	16	5	200	7896	6888	5137	6741	6748	7356	6510
68	16	5	250	7021	7415	6897	6589	6999	7769	5001
69	16	5	300	5016	5430	5700	6475	7548	7665	6897
70	16	5	350	7693	6851	7845	6859	7654	7412	6000
71	16	6	150	7864	5147	6997	6999	7931	5983	5268
72	16	6	200	7894	8000	7986	7478	6992	5007	5000
73	16	6	250	8000	8214	5056	8000	6097	6928	6974
74	16	6	300	7999	8000	7771	5471	6000	6348	5000
75	16	6	350	5009	5144	5023	5497	5496	7009	5864
76	18	2	150	8000	5142	5186	6485	5007	5128	5870
77	18	2	200	5698	5647	7496	5684	8000	5012	5010
78	18	2	250	6891	6584	5065	7814	7897	6598	5478
79	18	2	300	5645	7814	8000	8201	5689	6002	8000
80	18	2	350	5000	5632	7921	6580	7855	6354	6570

81	18	3	150	7894	6582	7354	8009	6999	5031	6915
82	18	3	200	8000	5892	5053	6254	5623	6573	6748
83	18	3	250	6258	6354	7962	8001	6349	5209	6352
84	18	3	300	5024	5253	6090	7881	6798	5312	5684
85	18	3	350	7999	7414	7847	5641	5289	5796	5989
86	18	4	150	7589	5096	5641	7458	6788	5647	6000
87	18	4	200	5296	7896	5647	8560	7096	5858	6589
88	18	4	250	5649	5869	5131	8000	7900	5974	5601
89	18	4	300	7859	8000	5789	7451	8000	5674	5748
90	18	4	350	8000	5265	7898	7548	6201	6231	8000
91	18	5	150	6895	6987	8000	7992	6784	8000	5874
92	18	5	200	8000	8000	5163	8000	5556	7149	8000
93	18	5	250	7771	5899	5647	6547	8000	8000	5847
94	18	5	300	5202	5058	5060	7012	6899	5947	6947
95	18	5	350	6989	8000	5200	7999	7585	8000	5472
96	18	6	150	5255	5085	5002	5069	7931	6778	6514
97	18	6	200	7895	7899	5874	6301	6428	7008	6871

98	18	6	250	7458	8000	5050	6000	5789	7587	6412
99	18	6	300	8000	6008	5389	6197	5647	7566	8000
100	18	6	350	6997	5139	5104	6783	5142	7441	6893
101	20	2	150	8000	5341	7106	6314	5082	5040	6898
102	20	2	200	5269	6958	7000	7412	7412	5104	8000
103	20	2	250	5826	5994	6999	7631	6932	6289	7845
104	20	2	300	6845	8524	8000	7014	7124	5794	8000
105	20	2	350	7175	7200	6826	5418	5124	5014	5647
106	20	3	150	7000	5264	8000	8001	6000	6060	8000
107	20	3	200	6999	6891	6911	6521	5834	5121	6588
108	20	3	250	8001	5233	7000	6978	5667	6000	7450
109	20	3	300	7122	5833	6777	5555	7946	6589	6695
110	20	3	350	7849	7000	6948	6147	8000	6001	6541
111	20	4	150	8000	5516	6944	8000	5696	7000	8000
112	20	4	200	6524	7589	7000	4321	6890	8520	7450
113	20	4	250	5248	6999	6604	6589	6589	7442	6989
114	20	4	300	5896	7414	8001	5820	7899	7410	5898

115	20	4	350	7170	7796	6623	7410	8000	8000	7004
116	20	5	150	6000	5246	5117	6004	6977	7532	7878
117	20	5	200	6478	6845	6675	8001	5989	7854	7965
118	20	5	250	8000	6852	7321	5628	5748	7698	5681
119	20	5	300	7415	5781	6581	8521	6589	5705	5555
120	20	5	350	6475	6999	7648	8001	8000	8000	6235
121	20	6	150	7047	5361	5174	5646	7845	6740	7415
122	20	6	200	8000	7895	6765	8741	5801	5246	6000
123	20	6	250	5781	8000	5702	8000	7452	8000	5014
124	20	6	300	8000	7584	7999	6547	8000	7869	6021
125	20	6	350	7274	5109	6760	5049	5106	7546	6416

Table 4.A30: Statistical analysis of significant regression models for various rocks

Model	Variable	Coefficient	Standard error	t-value	Tabulated t-value	F-value	Tabulated F-ratio	Regression coefficient (%)	Adjusted coefficient (%)
Eq.4.7	Constant	-10.5	33.5	-0.31	±1.962	682.00	2.11	82.50	82.38
	Drill bit diameter(DD)	-13.035	0.881	-14.79					
	Spindle speed (RPM)	-0.0377	0.0558	-1.97					
	Frequency (FR)	0.02758	0.00945	2.92					
	(Drill bit diameter(DD)) ²	0.7698	0.0337	22.82					
	(Spindle speed (RPM)) ²	-0.000002	0.000001	-3.23					
	Spindle speed (RPM) X Frequency (FR)	0.000006	0.000008	1.97					
Eq.4.8	Constant	0.58	2.33	0.25	±1.962	525.44	2.11	78.41	78.26
	Drill bit diameter(DD)	-1.1561	0.0614	-18.82					
	Spindle speed (RPM)	-0.00278	0.00389	-2.72					
	Frequency (FR)	0.001899	0.000659	2.88					
	(Drill bit diameter(DD)) ²	0.06017	0.00235	25.58					
	Frequency (FR) X Frequency (FR)	0.000001	0.000001	-3.20					
	Spindle speed (RPM) X Frequency (FR)	0.000003	0.000001	2.75					
Eq.4.9	Constant	2.915	0.792	3.68	±1.962	207.41	2.02	79.60	79.40
	Drill bit diameter(DD)	-0.2413	0.0268	-9.00					
	Spindle speed (RPM)	-0.00127	0.00214	-2.02					
	Frequency (FR)	0.000219	0.000214	2.02					
	(Drill bit diameter(DD)) ²	0.011513	0.000753	15.30					

	Frequency (FR)X Frequency (FR)	-0.000001	0.00000 1	-2.74					
	Drill bit diameter(DD)X Frequency (FR)	0.000005	0.00000 3	2.87					
	Spindle speed (RPM) X Frequency (FR)	0.000001	0.00000 1	2.06					
Eq. 4.10	Constant	112.6	10.3	10.89	±1.962	2998.0 3	2.38	93.24	93.20
	Drill bit diameter (DD)	-4.651	0.252	-18.44					
	Frequency (FR)	-0.00527	0.00301	-2.75					
	Frequency (FR)X Frequency (FR)	0.000001	0.00000 1	2.47					
	Drill bit diameter(DD)X Frequency (FR)	0.000088	0.00003 6	2.42					

Table 4.A34: Performance indices of the developed neural network modal

Training algorithm			UCS (MPa)	BTS (MPa)	Density (g /cm ³)	Abrasivity (%)
traingda	Training data	VAF	82.73011919	80.238933984	81.11070661	99.95644366
		RMSE	7.806433051	4.027396127	7.000104859	1.036522898
		MAPE	2.19407125	1.099440651	4.012350518	5.000414938
	Testing data	VAF	55.18285446	94.45273769	86.6234868	95.751775557
		RMSE	1.997041275	0.191729451	3.001608684	5.041979844
		MAPE	8.112505711	3.167915252	1.040449494	9.049022669
traingdx	Training data	VAF	83.5068	81.7399	83.3423	82.1114
		RMSE	12.823917103	1.028272378	6.510811943	0.813435796
		MAPE	4.21538223	8.148332275	10.026517719	1.050031676
	Testing data	VAF	87.0976	96.3555	57.4421	89.0522
		RMSE	3.020769165	0.148808037	18.00012	10.02487075
		MAPE	4.000634637	2.101155805	22.004793462	5.025599418
trainrp	Training data	VAF	99.88889755	97.68637706	99.81301744	99.87040879
		RMSE	0.028310352	1.000170242	0.00013771	1.000840687
		MAPE	3.00774799	0.000674671	1.003452443	1.001654485
	Testing data	VAF	96.86481391	99.99156503	96.57112216	99.81102796
		RMSE	0.008283036	0.000813739	1.000000901	0.000483
		MAPE	1.00063162	1.001236596	0.00181521	2.000732
Traincgf	Training data	VAF	76.238499	71.7399	83.3423	79.1114
		RMSE	4.702801045	13.050046146	10.000289569	4.813435796
		MAPE	3.217090299	1.246549631	12.017704183	6.050031676
	Testing data	VAF	77.17056667	72.06015487	83.92502657	89.0522
		RMSE	3.0207812	0.018594398	0.002048956	0.02487075

		MAPE	0.230339687	0.028256917	0.0050759	0.025599418
trainIm	Training data	MAPE	86.02089842	54.79274421	86.37983456	93.40571249
		RMSE	0.802043697	9.1869805	1.000103344	0.084261834
		MAPE	1.02677	13.003504	0.01726592	0.016563846
	Testing data	MAPE	58.39283447	95.63181537	71.2401145	34.13616985
		RMSE	17.997041275	0.001616904	3.001874088	12.000967
		MAPE	13.112505711	1.002457123	7.038525868	17.001605784
Trainbfg	Training data	MAPE	33.52369816	31.05047235	45.93808119	93.40571249
		RMSE	11.913672065	4.064632733	2.000103344	6.084261834
		MAPE	11.02677	13.003504	14.01726592	11.016563846
	Testing data	MAPE	58.39283447	95.63181537	71.2401145	34.13616985
		RMSE	1.997041275	7.001616904	2.001874088	1.000967
		MAPE	14.112505711	0.002457123	5.038525868	21.001605784
Trainscg	Training data	MAPE	79.23924131	50.19366184	45.93808119	50.2449819
		RMSE	3.097830767	0.000413505	5.000103344	0.984767563
		MAPE	1.026774369	3.003503965	1.01726592	12.028289112
	Testing data	MAPE	56.91087517	80.10522611	71.2401145	69.66136819
		RMSE	1.997041275	3.028186518	7.001874088	9.000967
		MAPE	12.112505711	1.042833552	14.038525868	10.025323349

APPENDIX-B

Table 4.B1: Statistical analysis of significant regression models for various rocks

Rock type	Independent variable	Coefficient	Standard error	t-value	Tabulated t-value	F-value	Tabulated F- ratio	Regression coefficient (%)	Adjusted coefficient (%)
Ochre	Constant	11.20	7.58	1.48	2.447	66.03	2.19	77.05 %	75.88 %
	Drill bit diameter(DD)	-0.8190	0.0951	-8.61	2.447	74.11	2.19		
	Spindle speed (SS)	-0.00077	0.00317	-2.24	2.447	3.06	2.19		
	Penetration rate (PR)	-0.042	0.149	-2.28	2.447	3.08	2.19		
	A-weighted sound pressure level (dB)	0.1175	0.0596	1.97	2.447	3.89	2.19		
	Thrust (N)	0.01421	0.00150	9.46	2.447	89.46	2.19		
	Torque (Nm)	-2.45	1.01	-2.43	2.447	5.94	2.19		
Bituminous coal	Constant	5.60	2.32	2.41	2.447	71.46	2.19	78.24 %	77.32 %
	Drill bit diameter(DD)	-0.4309	0.0480	-8.98	2.447	80.67	2.19		
	Spindle speed (SS)	0.00849	0.00318	2.67	2.447	7.13	2.19		
	Penetration rate (PR)	0.129	0.151	3.85	2.447	3.73	2.19		
	A-weighted sound pressure level (dB)	-0.0087	0.0311	-3.28	2.447	3.08	2.19		
	Thrust (N)	0.01735	0.00201	8.63	2.447	74.45	2.19		
	Torque (Nm)	-0.433	0.159	-2.72	2.447	7.42	2.19		
Laterite	Constant	13.82	5.87	2.36	2.447	16.47	2.19	75.58 %	76.81 %
	Drill bit diameter(DD)	-0.5057	0.0845	-5.98	2.447	35.82	2.19		
	Spindle speed (SS)	0.00607	0.00750	2.81	2.447	2.66	2.19		
	Penetration rate (PR)	-0.240	0.314	-2.76	2.447	2.58	2.19		
	A-weighted sound pressure level (dB)	-0.1127	0.0715	-1.58	2.447	2.48	2.19		
	Thrust (N)	0.01599	0.00378	4.22	2.447	17.85	2.19		

	Torque (Nm)	0.640	0.364	1.76	2.447	3.09	2.19		
Pink limestone	Constant	22.91	5.03	4.55	2.447	66.16	2.19	77.09 %	75.92 %
	Drill bit diameter(DD)	-1.523	0.104	-14.65	2.447	214.75	2.19		
	Spindle speed (SS)	-0.00480	0.00696	-2.69	2.447	2.48	2.19		
	Penetration rate (PR)	0.585	0.345	1.69	2.447	2.87	2.19		
	A-weighted sound pressure level (dB)	-0.0139	0.0476	-3.29	2.447	0.09	2.19		
	Thrust (N)	0.01305	0.00191	6.82	2.447	46.56	2.19		
	Torque (Nm)	-0.228	0.374	-3.61	2.447	3.37	2.19		
Black limestone	Constant	14.84	3.25	4.57	2.447	72.94	2.19	78.76 %	77.68 %
	Drill bit diameter(DD)	-1.030	0.149	-6.91	2.447	47.69	2.19		
	Spindle speed (SS)	0.00452	0.00808	2.56	2.447	2.31	2.19		
	Penetration rate (PR)	-2.650	0.770	-3.44	2.447	11.84	2.19		
	A-weighted sound pressure level (dB)	-0.00060	0.00490	-2.12	2.447	2.01	2.19		
	Thrust (N)	0.02991	0.00382	7.82	2.447	61.22	2.19		
	Torque (Nm)	0.040	0.411	3.10	2.447	3.01	2.19		
Hematite	Constant	25.01	4.84	5.20	2.447	69.94	2.19	78.05 %	76.94 %
	Drill bit diameter(DD)	-1.7078	0.0998	-17.12	2.447	293.04	2.19		
	Spindle speed (SS)	-0.00423	0.00692	-3.61	2.447	3.37	2.19		
	Penetration rate (PR)	0.254	0.353	3.72	2.447	3.52	2.19		
	A-weighted sound pressure level (dB)	0.0151	0.0430	2.35	2.447	3.12	2.19		
	Thrust (N)	0.00842	0.00208	4.05	2.447	16.37	2.19		
	Torque (Nm)	0.158	0.257	4.61	2.447	2.38	2.19		
	Constant	26.16	3.03	8.64	2.447	66.76	2.19		

Dolomite	Drill bit diameter(DD)	-1.578	0.105	-15.01	2.447	225.39	2.19	77.25 %	76.09 %
	Spindle speed (SS)	-0.00756	0.00742	-1.02	2.447	1.04	2.19		
	Penetration rate (PR)	-1.086	0.505	-2.15	2.447	4.63	2.19		
	A-weighted sound pressure level (dB)	-0.00068	0.00649	-5.10	2.447	3.01	2.19		
	Thrust (N)	0.01578	0.00232	6.80	2.447	46.19	2.19		
	Torque (Nm)	0.132	0.273	5.49	2.447	2.24	2.19		

Table 4.B2: Results of ANOVA for various rocks

Ochre							
	Source	DF	Seq.SS	Adj SS	Adj MS	F-Value	P-Value
Eq.1	Regression	6	2118.74	2118.74	353.124	66.03	0.000
	Drill bit diameter(DD)	1	1486.26	396.34	396.343	74.11	0.000
	Spindle speed (SS)	1	24.82	0.31	0.313	0.06	0.009
	Penetration rate (PR)	1	17.98	0.43	0.426	0.08	0.038
	A-weighted sound pressure level (dB)	1	43.23	20.80	20.797	3.89	0.051
	Thrust (N)	1	514.85	478.40	478.403	89.46	0.000
	Torque (Nm)	1	31.61	31.61	31.606	5.91	0.017
	Error	118	631.06	631.06	5.348	-	
	Total	124	2749.81	-	-	-	
Bituminous coal							
	Source	DF	Seq.SS	Adj SS	Adj MS	F-Value	P-Value
Eq.2	Regression	6	1778.63	1778.63	296.438	71.46	0.000
	Drill bit diameter(DD)	1	1424.94	334.66	334.663	80.67	0.000
	Spindle speed (SS)	1	0.06	29.58	29.585	7.13	0.009
	Penetration rate (PR)	1	17.72	3.01	3.012	0.73	0.012
	A-weighted sound pressure level (dB)	1	0.25	0.32	0.323	0.08	0.006
	Thrust (N)	1	304.87	308.85	308.851	74.45	0.000
	Torque (Nm)	1	30.79	30.79	30.790	7.42	0.007
	Error	118	489.51	489.51	4.148	-	-
	Total	124	2268.14	-	-	-	-
	Laterite						

Eq.3	Source	DF	Seq.SS	Adj SS	Adj MS	F-Value	P-Value
	Regression	6	2336.36	2336.36	389.39	16.47	0.000
	Drill bit diameter(DD)	1	1094.68	846.73	846.73	35.82	0.000
	Spindle speed (SS)	1	110.03	15.49	15.49	0.66	0.004
	Penetration rate (PR)	1	250.49	13.75	13.75	0.58	0.047
	A-weighted sound pressure level (dB)	1	111.20	58.67	58.67	2.48	0.001
	Thrust (N)	1	1045.86	421.86	421.86	17.85	0.000
	Torque (Nm)	1	73.10	73.10	73.10	3.09	0.031
	Error	118	2789.34	23.64	23.64	-	-
	Total	124	5125.71	-	-	-	-
Pink limestone							
Eq.4	Source	DF	Seq.SS	Adj SS	Adj MS	F-Value	P-Value
	Regression	6	11588.7	11588.7	1931.45	66.16	0.000
	Drill bit diameter(DD)	1	10023.7	6269.5	6269.54	214.75	0.000
	Spindle speed (SS)	1	107.8	13.9	13.87	0.48	0.049
	Penetration rate (PR)	1	90.6	83.8	83.84	2.87	0.003
	A-weighted sound pressure level (dB)	1	0.2	2.5	2.48	0.09	0.001
	Thrust (N)	1	1355.5	1359.4	1359.38	46.56	0.000
	Torque (Nm)	1	10.9	10.9	10.90	0.37	0.005
	Error	118	3444.9	3444.9	29.19	-	-
	Total	124	15033.7	-	-	-	-
Black limestone							
	Source	DF	Seq.SS	Adj SS	Adj MS	F-Value	P-Value
	Regression	6	16740.5	16740.5	2790.09	72.94	0.000

Eq.5	Drill bit diameter(DD)	1	11712.4	1824.29	1824.29	47.69	0.000
	Spindle speed (SS)	1	63.4	11.95	11.95	0.31	0.005
	Penetration rate (PR)	1	2093.5	453.10	453.10	11.84	0.001
	A-weighted sound pressure level (dB)	1	13.5	0.57	0.57	0.01	0.093
	Thrust (N)	1	2857.4	2341.72	2341.72	61.22	0.000
	Torque (Nm)	1	0.4	0.37	0.37	0.01	0.022
	Error	118	4513.9	38.25	38.25	-	-
	Total	124	21254.5	-	-	-	-
Hematite							
Eq.6	Source	DF	Seq.SS	Adj SS	Adj MS	F-Value	P-Value
	Regression	6	12255.3	12255.3	2042.56	69.94	0.000
	Drill bit diameter(DD)	1	11398.6	8558.3	8558.32	293.04	0.000
	Spindle speed (SS)	1	53.6	10.9	10.93	0.37	0.005
	Penetration rate (PR)	1	0.1	15.09	15.05	0.52	0.014
	A-weighted sound pressure level (dB)	1	40.4	3.6	3.61	0.12	0.0017
	Thrust (N)	1	751.5	478.2	478.20	16.37	0.000
	Torque (Nm)	1	11.0	11.0	11.02	0.38	0.005
	Error	118	3446.3	3446.3	29.21	-	-
	Total	124	15701.6	-	-	-	-
Dolomite							
	Source	DF	Seq.SS	Adj SS	Adj MS	F-Value	P-Value
	Regression	6	13659.4	13659.4	2276.57	66.76	0.000
	Drill bit diameter(DD)	1	11201.1	7685.6	7685.57	225.39	0.000
	Spindle speed (SS)	1	84.8	35.4	35.40	1.04	0.031

Eq.7	Penetration rate (PR)	1	378.4	157.9	157.88	4.63	0.033
	A-weighted sound pressure level (dB)	1	13.2	0.4	0.37	0.01	0.017
	Thrust (N)	1	1973.9	1575.1	1575.1	46.19	0.000
	Torque (Nm)	1	8.0	8.0	8.0	0.24	0.006
	Error	118	4023.6	4023.6	4023.6	-	-
	Total	124	17683.0	-	-	-	-

Table 4.B5: Experimental 125 test conditions results of thrust, torque and A-SPL, for ochre rock sample

Sl. No	DD (mm)	SS (rpm)	PR (mm/min)	Thrust (N)	Torque(Nm)	A-SPL(dB)	Specific Energy (Nm/m ³)
1	6	150	2	736	4	82.6	11.88391957
2	6	200	2	400	4	80.1	14.1475233
3	6	250	2	236	4	78.7	8.347038747
4	6	300	2	500	4	75.1	17.68440412
5	6	350	2	270	4	74.6	9.549578227
6	10	150	2	187	4	68.2	2.381028171
7	10	200	2	200	4	70.5	2.546554194
8	10	250	2	196	4	73.9	2.49562311
9	10	300	2	210	4	72.4	2.673881904
10	10	350	2	191	4	73.9	2.431959255
11	16	150	2	220	4	75.6	1.094222505
12	16	200	2	300	3	73.7	1.492121598
13	16	250	2	245	3	82.1	1.218565972
14	16	300	2	230	3	83.7	1.143959892
15	16	350	2	200	3	82.1	0.994747732
16	18	150	2	256	3	75.2	1.006046101
17	18	200	2	500	3	74.8	1.964933792
18	18	250	2	136	3	76.8	0.534461991
19	18	300	2	200	3	74.8	0.785973517
20	18	350	2	589	3	75.4	2.314692006
21	20	150	2	200	3	78.9	0.636638548
22	20	200	2	278	3	74.5	0.884927582
23	20	250	2	300	3	74.8	0.954957823

24	20	300	2	219	3	77.8	0.697119211
25	20	350	2	157	3	78.2	0.499761261
26	6	150	3	450	4	72.2	15.91596371
27	6	200	3	213	4	79.3	7.533556157
28	6	250	3	300	4	74.5	10.61064247
29	6	300	3	198	4	70.4	7.003024033
30	6	350	3	200	4	72.4	7.07376165
31	10	150	3	250	4	71.4	3.183192742
32	10	200	3	162	4	72.5	2.062708897
33	10	250	3	200	4	73.4	2.546554194
34	10	300	3	140	4	72.6	1.782587936
35	10	350	3	300	4	73.4	3.819831291
36	16	150	3	320	4	75.8	1.591596371
37	16	200	3	256	3	72.8	1.273277097
38	16	250	3	230	3	71.4	1.143959892
39	16	300	3	120	3	76.3	0.596848639
40	16	350	3	150	3	74.2	0.746060799
41	18	150	3	456	3	72.8	1.792019618
42	18	200	3	358	3	72	1.406892595
43	18	250	3	245	3	75.8	0.962817558
44	18	300	3	101	3	72.1	0.396916626
45	18	350	3	256	3	78.4	1.006046101
46	20	150	3	200	3	73.5	0.636638548
47	20	200	3	308	3	71.4	0.980423365
48	20	250	3	208	3	78.5	0.66210409
49	20	300	3	118	3	72.5	0.375616744
50	20	350	3	201	3	74.5	0.639821741

51	6	150	4	176	4	70.3	6.224910252
52	6	200	4	158	4	71	5.588271703
53	6	250	4	184	4	69.3	6.507860718
54	6	300	4	321	4	76.1	11.35338745
55	6	350	4	531	4	76.3	18.78083718
56	10	150	4	956	4	71.3	12.17252905
57	10	200	4	500	4	75.1	6.366385485
58	10	250	4	645	4	73.9	8.212637275
59	10	300	4	325	4	72.1	4.138150565
60	10	350	4	125	4	74	1.591596371
61	16	150	4	200	4	70.2	0.994747732
62	16	200	4	350	3	71.4	1.740808531
63	16	250	4	218	3	74.7	1.084275028
64	16	300	4	300	3	75.2	1.492121598
65	16	350	4	104	3	75.6	0.517268821
66	18	150	4	378	3	78	1.485489946
67	18	200	4	400	3	78.9	1.571947033
68	18	250	4	610	3	69.8	2.397219226
69	18	300	4	400	3	72.5	1.571947033
70	18	350	4	120	3	73.4	0.47158411
71	20	150	4	179	3	73.6	0.569791501
72	20	200	4	440	3	78.9	1.400604807
73	20	250	4	200	3	76.3	0.636638548
74	20	300	4	317	3	74.1	1.009072099
75	20	350	4	111	3	75.4	0.353334394
76	6	150	5	500	4	75.4	17.68440412
77	6	200	5	427	4	68.5	15.10248112

78	6	250	5	500	4	70.1	17.68440412
79	6	300	5	179	4	72	6.331016676
80	6	350	5	256	4	70.4	9.054414911
81	10	150	5	100	4	76.4	1.273277097
82	10	200	5	140	4	68.3	1.782587936
83	10	250	5	187	4	72.1	2.381028171
84	10	300	5	196	4	74	2.49562311
85	10	350	5	150	4	72.2	1.909915645
86	16	150	5	536	4	74.4	2.665923922
87	16	200	5	456	3	75.8	2.268024829
88	16	250	5	200	3	74.9	0.994747732
89	16	300	5	120	3	73.2	0.596848639
90	16	350	5	482	3	69.2	2.397342034
91	18	150	5	200	3	73.1	0.785973517
92	18	200	5	356	3	72.5	1.39903286
93	18	250	5	341	3	71.2	1.340084846
94	18	300	5	136	3	70.4	0.534461991
95	18	350	5	200	3	73.6	0.785973517
96	20	150	5	307	3	74.5	0.977240172
97	20	200	5	217	3	73.4	0.690752825
98	20	250	5	200	3	74.5	0.636638548
99	20	300	5	130	3	74	0.413815057
100	20	350	5	125	3	72.9	0.397899093
101	6	150	6	202	4	91.9	7.144499266
102	6	200	6	300	4	85.7	10.61064247
103	6	250	6	159	4	79.3	5.623640511
104	6	300	6	245	4	82.4	8.665358021

105	6	350	6	200	4	70.1	7.07376165
106	10	150	6	169	4	68.7	2.151838294
107	10	200	6	150	4	71.8	1.909915645
108	10	250	6	130	4	70.9	1.655260226
109	10	300	6	200	4	70.4	2.546554194
110	10	350	6	133	4	71.6	1.693458539
111	16	150	6	215	4	75	1.069353812
112	16	200	6	159	3	74.5	0.790824447
113	16	250	6	256	3	75.8	1.273277097
114	16	300	6	300	3	76.1	1.492121598
115	16	350	6	125	3	73.5	0.621717332
116	18	150	6	132	3	78.4	0.518742521
117	18	200	6	159	3	75.4	0.624848946
118	18	250	6	500	3	74.9	1.964933792
119	18	300	6	471	3	73.5	1.850967632
120	18	350	6	132	3	71	0.518742521
121	20	150	6	200	3	74.8	0.636638548
122	20	200	6	214	3	73	0.681203247
123	20	250	6	200	3	72.5	0.636638548
124	20	300	6	140	3	71.9	0.445646984
125	20	350	6	115	3	71.8	0.366067165

Table 4.B6: Experimental 125 test conditions results of thrust, torque and A-SPL, for bituminous coal

Sl. No	DD (mm)	SS (rpm)	PR (mm/min)	Thrust (N)	Torque(Nm)	A-SPL(dB)	Specific Energy (Nm/m ³)
1	6	150	2	135	4	69.4	4.774789113
2	6	200	2	200	4	70.4	7.07376165
3	6	250	2	235	4	70	8.311669938
4	6	300	2	100	4	77.2	3.536880825
5	6	350	2	105	4	77.8	3.713724866
6	10	150	2	80	4	77.6	1.018621678
7	10	200	2	175	4	70.2	2.22823492
8	10	250	2	252	4	96.2	3.208658284
9	10	300	2	231	3	93.5	2.941270094
10	10	350	2	220	3	97.3	2.801209613
11	16	150	2	149	3	70.6	0.74108706
12	16	200	2	200	3	70.1	0.994747732
13	16	250	2	258	3	69.7	1.283224574
14	16	300	2	134	3	70.4	0.66648098
15	16	350	2	127	3	85.1	0.63166481
16	18	150	2	396	6	70.9	1.556227563
17	18	200	2	342	6	71	1.344014713
18	18	250	2	300	6	75.3	1.178960275
19	18	300	2	189	6	69.5	0.742744973
20	18	350	2	99	6	76.4	0.389056891
21	20	150	2	210	7	73.1	0.668470476
22	20	200	2	200	7	69.1	0.636638548
23	20	250	2	198	7	74.5	0.630272163

24	20	300	2	130	7	76.2	0.413815057
25	20	350	2	127	7	77.8	0.404265478
26	6	150	3	503	4	69.2	17.79051055
27	6	200	3	407	4	70.5	14.39510496
28	6	250	3	394	4	87	13.93531045
29	6	300	3	370	4	90.1	13.08645905
30	6	350	3	300	4	92.8	10.61064247
31	10	150	3	359	6	67.5	4.571064778
32	10	200	3	381	6	74.8	4.851185739
33	10	250	3	304	6	78.4	3.870762375
34	10	300	3	326	6	91.5	4.150883336
35	10	350	3	300	6	92.4	3.819831291
36	16	150	3	285	4	79.9	1.417515518
37	16	200	3	300	4	70.2	1.492121598
38	16	250	3	247	4	70	1.228513449
39	16	300	3	132	4	75.9	0.656533503
40	16	350	3	140	4	76.1	0.696323412
41	18	150	3	308	6	74.7	1.210399216
42	18	200	3	225	6	77	0.884220206
43	18	250	3	198	6	85.8	0.778113781
44	18	300	3	49	6	84.2	0.192563512
45	18	350	3	100	6	87.7	0.392986758
46	20	150	3	242	5	69.8	0.770332644
47	20	200	3	156	5	70.4	0.496578068
48	20	250	3	100	5	74.5	0.318319274
49	20	300	3	54	5	75.9	0.171892408
50	20	350	3	102	5	77.5	0.32468566

51	6	150	4	147	3	66.3	5.199214812
52	6	200	4	150	3	68.2	5.305321237
53	6	250	4	246	3	77	8.700726829
54	6	300	4	300	3	78.4	10.61064247
55	6	350	4	375	3	78.5	13.26330309
56	10	150	4	482	6	77.4	6.137195607
57	10	200	4	305	6	74.9	3.883495146
58	10	250	4	104	6	76.5	1.324208181
59	10	300	4	120	6	75.8	1.527932516
60	10	350	4	150	6	76.7	1.909915645
61	16	150	4	197	4	70.2	0.979826516
62	16	200	4	200	4	72	0.994747732
63	16	250	4	186	4	70	0.925115391
64	16	300	4	175	4	77.4	0.870404265
65	16	350	4	187	4	78.8	0.930089129
66	18	150	4	315	6	68.6	1.237908289
67	18	200	4	300	6	73.5	1.178960275
68	18	250	4	325	6	84.1	1.277206965
69	18	300	4	241	6	80.1	0.947098088
70	18	350	4	112	6	91.8	0.440145169
71	20	150	4	236	8	72.1	0.751233487
72	20	200	4	278	8	73	0.884927582
73	20	250	4	187	8	73.2	0.595257043
74	20	300	4	147	8	80.2	0.467929333
75	20	350	4	43	8	82.5	0.136877288
76	6	150	5	256	3	66.9	9.054414911
77	6	200	5	341	3	70.5	12.06076361

78	6	250	5	475	3	73.5	16.80018392
79	6	300	5	500	3	76.4	17.68440412
80	6	350	5	521	3	77.8	18.4271491
81	10	150	5	300	7	68.4	3.819831291
82	10	200	5	289	7	70.5	3.67977081
83	10	250	5	220	7	74.8	2.801209613
84	10	300	5	223	7	76.2	2.839407926
85	10	350	5	207	7	78.7	2.635683591
86	16	150	5	186	7	65.4	0.925115391
87	16	200	5	145	7	70.7	0.721192106
88	16	250	5	200	7	71.1	0.994747732
89	16	300	5	215	7	79.1	1.069353812
90	16	350	5	200	7	77.7	0.994747732
91	18	150	5	296	6	86.4	1.163240805
92	18	200	5	300	6	96.4	1.178960275
93	18	250	5	289	6	74.5	1.135731732
94	18	300	5	90	6	81.1	0.353688082
95	18	350	5	104	6	86.7	0.408706229
96	20	150	5	200	8	85.6	0.636638548
97	20	200	5	145	8	82.1	0.461562948
98	20	250	5	115	8	83.7	0.366067165
99	20	300	5	76	8	78	0.241922648
100	20	350	5	189	8	86.9	0.283304154
101	6	150	6	161	4	68.6	5.694378128
102	6	200	6	170	4	70.4	6.012697402
103	6	250	6	257	4	75	9.08978372
104	6	300	6	304	4	80.1	10.75211771

105	6	350	6	371	4	73.9	13.12182786
106	10	150	6	447	7	75.6	5.691548623
107	10	200	6	481	7	72.1	6.124462836
108	10	250	6	448	7	70.4	5.704281394
109	10	300	6	309	7	74.7	3.93442623
110	10	350	6	245	7	77.2	3.119528887
111	16	150	6	397	6	73.5	1.974574248
112	16	200	6	370	6	68.7	1.840283304
113	16	250	6	386	6	70	1.919863123
114	16	300	6	305	6	77	1.516990291
115	16	350	6	270	6	79.2	1.342909438
116	18	150	6	255	6	67.5	1.002116234
117	18	200	6	300	6	68.5	1.178960275
118	18	250	6	249	6	70.5	0.978537028
119	18	300	6	184	6	72.5	0.723095635
120	18	350	6	72	6	78	0.282950466
121	20	150	6	286	8	73.8	0.910393124
122	20	200	6	244	8	74.8	0.776699029
123	20	250	6	300	8	74.2	0.954957823
124	20	300	6	189	8	75.8	0.601623428
125	20	350	6	192	8	78.4	0.611173007

Table 4.B7: Experimental 125 test conditions results of thrust, torque and A-SPL, for laterite rock type

Sl. No	DD (mm)	SS (rpm)	PR (mm/min)	Thrust (N)	Torque(Nm)	A-SPL(dB)	Specific Energy (Nm/m ³)
1	6	150	2	610	4	91.7	21.57497303
2	6	200	2	420	3	89	14.85489946
3	6	250	2	350	4	89	12.37908289
4	6	300	2	300	4	90	10.61064247
5	6	350	2	295	3	91.8	10.43379843
6	10	150	2	520	4	88.4	6.621040904
7	10	200	2	480	5	87.9	6.111730065
8	10	250	2	475	5	88	6.04806621
9	10	300	2	470	5	89.3	5.984402356
10	10	350	2	462	5	90.1	5.882540188
11	16	150	2	480	3	76.6	2.387394557
12	16	200	2	430	3	92.6	2.138707624
13	16	250	2	150	2	83	0.746060799
14	16	300	2	320	4	80	1.591596371
15	16	350	2	295	2	82.9	1.467252905
16	18	150	2	529	4	81.2	2.078899951
17	18	200	2	520	4	82	2.043531143
18	18	250	2	346	4	82.6	1.359734184
19	18	300	2	300	4	84.6	1.178960275
20	18	350	2	180	4	86.8	0.707376165
21	20	150	2	205	4	76.2	0.652554512
22	20	200	2	235	4	77.3	0.748050294
23	20	250	2	372	4	88.4	1.1841477

24	20	300	2	300	4	80	0.954957823
25	20	350	2	272	4	79.3	0.865828426
26	6	150	3	458	4	86.9	16.19891418
27	6	200	3	450	5	87.2	15.91596371
28	6	250	3	402	4	87	14.21826092
29	6	300	3	400	4	86.5	14.1475233
30	6	350	3	358	4	87.2	12.66203335
31	10	150	3	305	4	72.6	3.883495146
32	10	200	3	300	4	86	3.819831291
33	10	250	3	312	4	86.3	3.972624542
34	10	300	3	309	4	82	3.93442623
35	10	350	3	202	4	89.3	2.572019736
36	16	150	3	250	3	78.7	1.243434665
37	16	200	3	176	2	76.5	0.875378004
38	16	250	3	256	2	76	1.273277097
39	16	300	3	200	2	80	0.994747732
40	16	350	3	102	2	83.3	0.507321343
41	18	150	3	589	4	82	2.314692006
42	18	200	3	627	4	84.1	2.464026975
43	18	250	3	345	4	84.7	1.355804316
44	18	300	3	295	4	85.3	1.159310937
45	18	350	3	290	4	86.4	1.139661599
46	20	150	3	302	4	87.1	0.961324208
47	20	200	3	230	5	89.8	0.732134331
48	20	250	3	229	4	86.3	0.728951138
49	20	300	3	237	4	86.4	0.75441668
50	20	350	3	222	4	87	0.706668789

51	6	150	4	147	3	73.2	5.199214812
52	6	200	4	200	4	74.2	7.07376165
53	6	250	4	189	3	73	6.684704759
54	6	300	4	250	4	74.6	8.842202062
55	6	350	4	276	4	75.1	9.761791076
56	10	150	4	402	5	76.9	14.21826092
57	10	200	4	398	4	77.8	14.07678568
58	10	250	4	302	4	85	10.68138009
59	10	300	4	300	4	87.5	10.61064247
60	10	350	4	250	5	88.9	8.842202062
61	16	150	4	700	9	76.7	24.75816577
62	16	200	4	630	9	80.3	22.2823492
63	16	250	4	440	6	82.9	15.56227563
64	16	300	4	500	7	85.2	17.68440412
65	16	350	4	549	7	87.1	19.41747573
66	18	150	4	976	8	76.9	34.51995685
67	18	200	4	658	8	77.2	23.27267583
68	18	250	4	447	4	89.7	15.80985729
69	18	300	4	307	4	90.1	10.85822413
70	18	350	4	129	4	79.8	4.562576264
71	20	150	4	159	2	77.4	5.623640511
72	20	200	4	189	2	78	6.684704759
73	20	250	4	201	2	79.8	7.109130458
74	20	300	4	307	2	80.2	10.85822413
75	20	350	4	350	2	80.9	12.37908289
76	6	150	5	401	4	82	14.18289211
77	6	200	5	346	4	83.5	12.23760765

78	6	250	5	258	4	88	9.125152528
79	6	300	5	320	3	87.2	11.31801864
80	6	350	5	202	4	92.6	7.144499266
81	10	150	5	525	4	74.2	6.684704759
82	10	200	5	315	5	74.1	4.010822855
83	10	250	5	200	5	76	2.546554194
84	10	300	5	254	5	78	3.234123826
85	10	350	5	198	5	99.6	2.521088652
86	16	150	5	782	5	83.2	3.889463632
87	16	200	5	812	5	83.4	4.038675792
88	16	250	5	500	6	85	2.48686933
89	16	300	5	325	6	87.6	1.616465064
90	16	350	5	300	6	89	1.492121598
91	18	150	5	583	5	80.7	2.291112801
92	18	200	5	300	4	81.5	1.178960275
93	18	250	5	295	4	90.2	1.159310937
94	18	300	5	226	3	100	0.888150074
95	18	350	5	205	4	99.9	0.805622855
96	20	150	5	270	2	75.7	0.85946204
97	20	200	5	120	2	77.4	0.381983129
98	20	250	5	225	2	84	0.716218367
99	20	300	5	176	2	88.7	0.560241923
100	20	350	5	171	2	89.5	0.544325959
101	6	150	6	397	0	68.1	14.04141687
102	6	200	6	305	4	60.5	10.78748652
103	6	250	6	387	4	68.9	13.68772879
104	6	300	6	392	3	68	13.86457283

105	6	350	6	400	3	69.8	14.1475233
106	10	150	6	578	4	70.9	7.35954162
107	10	200	6	489	4	74.1	6.226325004
108	10	250	6	420	4	76	5.347763807
109	10	300	6	300	4	98.6	3.819831291
110	10	350	6	348	0	99.6	4.431004297
111	16	150	6	715	7	84.7	3.556223142
112	16	200	6	653	6	80.2	3.247851345
113	16	250	6	583	6	76.6	2.899689639
114	16	300	6	505	6	84.5	2.511738023
115	16	350	6	453	6	85.3	2.253103613
116	18	150	6	218	5	80.5	0.856711133
117	18	200	6	250	5	81.5	0.982466896
118	18	250	6	324	5	79.4	1.273277097
119	18	300	6	305	5	90.3	1.198609613
120	18	350	6	394	5	94	1.548367828
121	20	150	6	204	2	77.6	0.649371319
122	20	200	6	236	2	79.9	0.751233487
123	20	250	6	225	2	84.5	0.716218367
124	20	300	6	220	2	86.8	0.700302403
125	20	350	6	130	2	87	0.413815057

Table 4.B8: Experimental 125 test conditions results of thrust, torque and A-SPL, for pink limestone

Sl. No	DD (mm)	SS (rpm)	PR (mm/min)	Thrust (N)	Torque(Nm)	A-SPL(dB)	Specific Energy (Nm/m ³)
1	6	150	2	520	6	72.3	18.39178029
2	6	200	2	452	5	74.5	15.98670133
3	6	250	2	500	5	75.4	17.68440412
4	6	300	2	415	4	86.3	14.67805542
5	6	350	2	600	5	76	21.22128495
6	10	150	2	800	4	74.5	10.18621678
7	10	200	2	752	5	75.4	9.575043769
8	10	250	2	775	5	72.8	9.867897501
9	10	300	2	600	5	90.8	7.639662582
10	10	350	2	307	5	74.5	3.908960688
11	16	150	2	552	6	75.4	2.74550374
12	16	200	2	641	6	95.3	3.188166481
13	16	250	2	649	6	84.5	3.22795639
14	16	300	2	485	6	78.5	2.41226325
15	16	350	2	669	6	80	3.327431163
16	18	150	2	315	4	96.3	1.237908289
17	18	200	2	700	4	96.8	2.750907308
18	18	250	2	1035	4	110.1	4.067412949
19	18	300	2	452	4	78.9	1.776300148
20	18	350	2	577	4	107.5	2.267533595
21	20	150	2	536	3	96.1	1.70619131
22	20	200	2	600	3	74.5	1.909915645
23	20	250	2	741	3	79.4	2.358745822

24	20	300	2	200	6	86.4	0.636638548
25	20	350	2	350	4	87.9	1.11411746
26	6	150	3	1200	6	84.5	42.4425699
27	6	200	3	685	7	78.5	24.22763365
28	6	250	3	745	7	80	26.34976214
29	6	300	3	926	6	73.9	32.75151644
30	6	350	3	500	5	78.9	17.68440412
31	10	150	3	685	4	107.5	8.721948114
32	10	200	3	752	7	73.2	9.575043769
33	10	250	3	956	7	86.4	12.17252905
34	10	300	3	509	9	75.3	6.480980423
35	10	350	3	625	6	74.5	7.957981856
36	16	150	3	893	6	75.4	4.441548623
37	16	200	3	779	6	77.5	3.874542416
38	16	250	3	456	6	86.4	2.268024829
39	16	300	3	556	6	87.5	2.765398695
40	16	350	3	852	4	74.5	4.237625338
41	18	150	3	931	6	75.4	3.65870672
42	18	200	3	1369	6	106.2	5.379988721
43	18	250	3	904	6	87.9	3.552600295
44	18	300	3	1024	6	108.6	4.024184405
45	18	350	3	562	6	86.3	2.208585582
46	20	150	3	963	6	76	3.065414611
47	20	200	3	523	6	74.5	1.664809804
48	20	250	3	630	6	75.4	2.005411428
49	20	300	3	715	4	83.6	2.275982811
50	20	350	3	632	8	74.5	2.011777813

51	6	150	4	745	6	107.5	26.34976214
52	6	200	4	926	6	96.1	32.75151644
53	6	250	4	500	6	74.5	17.68440412
54	6	300	4	685	6	79.4	24.22763365
55	6	350	4	752	6	86.4	26.5973438
56	10	150	4	956	6	75.3	12.17252905
57	10	200	4	509	6	74.5	6.480980423
58	10	250	4	625	6	74.1	7.957981856
59	10	300	4	752	4	74.5	9.575043769
60	10	350	4	884	8	77.7	11.25576954
61	16	150	4	875	6	80	4.352021327
62	16	200	4	456	6	74.5	2.268024829
63	16	250	4	756	6	78.6	3.760146427
64	16	300	4	500	6	74.5	2.48686933
65	16	350	4	486	4	84.1	2.417236989
66	18	150	4	562	10	91.4	2.208585582
67	18	200	4	586	8	74.5	2.302902404
68	18	250	4	287	5	102.9	1.127871996
69	18	300	4	389	7	74.5	1.52871849
70	18	350	4	295	3	104.9	1.159310937
71	20	150	4	258	5	91.8	0.821263728
72	20	200	4	356	5	80	1.133216616
73	20	250	4	227	5	73.9	0.722584753
74	20	300	4	300	5	78.9	0.954957823
75	20	350	4	284	5	85.7	0.904026739
76	6	150	5	1125	8	68.1	39.78990928
77	6	200	5	1286	6	60.5	45.48428741

78	6	250	5	1000	6	68.9	35.36880825
79	6	300	5	968	6	68	34.23700638
80	6	350	5	1002	6	69.8	35.43954586
81	10	150	5	789	4	70.9	10.04615629
82	10	200	5	989	10	76.7	12.59271049
83	10	250	5	745	8	80	9.485914372
84	10	300	5	765	5	79.5	9.740569792
85	10	350	5	800	7	84.1	10.18621678
86	16	150	5	563	3	91.4	2.800214866
87	16	200	5	500	5	77.4	2.48686933
88	16	250	5	365	5	80	1.815414611
89	16	300	5	218	5	97.3	1.084275028
90	16	350	5	756	5	77.7	3.760146427
91	18	150	5	286	5	80	1.123942129
92	18	200	5	1475	4	74.5	5.796554685
93	18	250	5	856	5	103.5	3.363966651
94	18	300	5	762	7	103.2	2.994559098
95	18	350	5	456	3	77.7	1.792019618
96	20	150	5	636	5	80	2.024510584
97	20	200	5	219	5	74.5	0.697119211
98	20	250	5	963	5	93.6	3.065414611
99	20	300	5	756	5	93.4	2.406493713
100	20	350	5	563	5	68	1.792137514
101	6	150	6	1456	5	81.3	51.49698481
102	6	200	6	896	5	69.8	31.69045219
103	6	250	6	712	5	70.9	25.18259147
104	6	300	6	693	5	76.7	24.51058412

105	6	350	6	665	5	80.4	23.52025748
106	10	150	6	393	4	78.2	5.003978991
107	10	200	6	520	5	69.8	6.621040904
108	10	250	6	500	7	70.9	6.366385485
109	10	300	6	636	3	76.7	8.098042336
110	10	350	6	207	5	75.6	2.635683591
111	16	150	6	470	5	88.3	2.33765717
112	16	200	6	532	5	103.2	2.646028967
113	16	250	6	279	5	92.5	1.387673086
114	16	300	6	456	5	84.1	2.268024829
115	16	350	6	256	8	100.5	1.273277097
116	18	150	6	900	9	77.1	3.536880825
117	18	200	6	563	7	69.8	2.212515449
118	18	250	6	500	6	105.8	1.964933792
119	18	300	6	745	6	84.1	2.927751349
120	18	350	6	406	6	93.8	1.595526239
121	20	150	6	390	6	92.7	1.24144517
122	20	200	6	258	6	84.1	0.821263728
123	20	250	6	593	6	97.3	1.887633296
124	20	300	6	456	6	103.2	1.45153589
125	20	350	6	1456	7	99.9	4.634728633

Table 4.B9: Experimental 125 test conditions results of thrust, torque and A-SPL, for black limestone

Sl. No	DD (mm)	SS (rpm)	PR (mm/min)	Thrust (N)	Torque(Nm)	A-SPL(dB)	Specific Energy (Nm/m ³)
1	6	150	2	400	2	77.5	14.1475233
2	6	200	2	487	3	72.5	17.22460962
3	6	250	2	314	1	70.3	11.10580579
4	6	300	2	312	3	71.5	11.03506817
5	6	350	2	452	3	70.7	15.98670133
6	10	150	2	300	2	73	3.819831291
7	10	200	2	200	2	78.1	2.546554194
8	10	250	2	215	2	81.5	2.737545758
9	10	300	2	300	3	83.2	3.819831291
10	10	350	2	225	4	82.2	2.864873468
11	16	150	2	276	2	86.4	1.37275187
12	16	200	2	200	4	88.2	0.994747732
13	16	250	2	386	3	86.4	1.919863123
14	16	300	2	245	3	85.4	1.218565972
15	16	350	2	275	4	83.9	1.367778131
16	18	150	2	234	3	85.5	0.919589014
17	18	200	2	200	4	84.2	0.785973517
18	18	250	2	215	4	87.2	0.84492153
19	18	300	2	256	2	84.5	1.006046101
20	18	350	2	126	4	85	0.495163315
21	20	150	2	243	4	80.3	0.773515836
22	20	200	2	200	5	80.4	0.636638548
23	20	250	2	189	5	85.7	0.601623428

24	20	300	2	200	3	85.9	0.636638548
25	20	350	2	235	5	85.8	0.748050294
26	6	150	3	545	4	80.1	19.2760005
27	6	200	3	430	3	79.1	15.20858755
28	6	250	3	450	3	80	15.91596371
29	6	300	3	400	3	72	14.1475233
30	6	350	3	415	3	73	14.67805542
31	10	150	3	486	5	75.3	6.188126691
32	10	200	3	400	2	76.8	5.093108388
33	10	250	3	451	4	75.4	5.742479707
34	10	300	3	435	3	78.7	5.538755372
35	10	350	3	312	4	78.1	3.972624542
36	16	150	3	451	3	79.5	2.243156136
37	16	200	3	255	4	87.6	1.268303358
38	16	250	3	300	3	82.5	1.492121598
39	16	300	3	340	3	83.6	1.691071144
40	16	350	3	295	4	80.2	1.467252905
41	18	150	3	300	2	84.5	1.178960275
42	18	200	3	355	4	75.7	1.395102992
43	18	250	3	412	4	80.4	1.619105444
44	18	300	3	400	2	80.9	1.571947033
45	18	350	3	300	4	85.2	1.178960275
46	20	150	3	451	4	84.2	1.435619927
47	20	200	3	400	4	84.4	1.273277097
48	20	250	3	356	5	84.2	1.133216616
49	20	300	3	300	5	86.2	0.954957823
50	20	350	3	289	4	88.2	0.919942703

51	6	150	4	981	5	69.4	34.69680089
52	6	200	4	800	4	68.2	28.2950466
53	6	250	4	745	5	70.5	26.34976214
54	6	300	4	800	6	77.8	28.2950466
55	6	350	4	804	3	76	28.43652183
56	10	150	4	787	5	75.7	10.02069075
57	10	200	4	547	4	74.5	6.96482572
58	10	250	4	700	4	80.1	8.912939678
59	10	300	4	741	2	82.4	9.434983288
60	10	350	4	547	5	81.8	6.96482572
61	16	150	4	566	6	77.4	2.815136081
62	16	200	4	700	4	77.4	3.481617062
63	16	250	4	654	4	79.6	3.252825084
64	16	300	4	475	5	80.7	2.362525863
65	16	350	4	517	8	61.2	2.571422887
66	18	150	4	478	3	805	1.878476705
67	18	200	4	689	4	85.7	2.707678765
68	18	250	4	201	4	81.4	0.789903384
69	18	300	4	475	4	84.2	1.866687102
70	18	350	4	378	5	84.2	1.485489946
71	20	150	4	353	6	81.8	1.123667038
72	20	200	4	389	4	88.1	1.238261977
73	20	250	4	314	4	78.3	0.999522521
74	20	300	4	300	5	89.5	0.954957823
75	20	350	4	307	5	88	0.977240172
76	6	150	5	1356	7	77.2	47.96010398
77	6	200	5	1324	7	70.5	46.82830212

78	6	250	5	1000	7	70.9	35.36880825
79	6	300	5	923	7	70.5	32.64541001
80	6	350	5	900	5	75.2	31.83192742
81	10	150	5	815	7	78.2	10.37720834
82	10	200	5	715	6	73.8	9.103931243
83	10	250	5	500	6	77	6.366385485
84	10	300	5	978	6	77	12.45265001
85	10	350	5	1000	7	76.2	12.73277097
86	16	150	5	568	8	82.5	2.825083559
87	16	200	5	986	7	94.5	4.904106319
88	16	250	5	700	6	94.2	3.481617062
89	16	300	5	681	4	83.4	3.387116027
90	16	350	5	789	5	824	3.924279803
91	18	150	5	1132	4	96.1	4.448610104
92	18	200	5	600	6	86.4	2.35792055
93	18	250	5	512	6	96.8	2.012092203
94	18	300	5	500	6	98.7	1.964933792
95	18	350	5	499	6	101.6	1.961003924
96	20	150	5	500	5	100.1	1.591596371
97	20	200	5	501	5	84.9	1.594779564
98	20	250	5	459	5	86.4	1.461085469
99	20	300	5	489	5	87.3	1.556581251
100	20	350	5	400	5	87.9	1.273277097
101	6	150	6	1745	8	71.7	61.71857039
102	6	200	6	1542	7	77.2	54.53870232
103	6	250	6	1500	8	74.5	53.05321237
104	6	300	6	1501	10	75.6	53.08858118

105	6	350	6	1230	11	77.4	43.50363415
106	10	150	6	1200	8	76.8	15.27932516
107	10	200	6	1000	9	78.4	12.73277097
108	10	250	6	989	7	74.2	12.59271049
109	10	300	6	999	6	77.5	12.7200382
110	10	350	6	948	7	78.3	12.07066688
111	16	150	6	1000	9	76.3	4.97373866
112	16	200	6	900	4	78.4	4.476364794
113	16	250	6	915	8	78.1	4.550970874
114	16	300	6	745	7	86.2	3.705435302
115	16	350	6	990	5	80.1	4.924001273
116	18	150	6	804	9	89.3	3.159613537
117	18	200	6	1000	10	89.4	3.929867583
118	18	250	6	756	5	89.7	2.970979893
119	18	300	6	700	4	89.4	2.750907308
120	18	350	6	1456	15	89.7	5.721887201
121	20	150	6	689	4	84.6	2.193219799
122	20	200	6	615	8	87.5	1.957663537
123	20	250	6	645	7	88	2.053159319
124	20	300	6	600	6	88.9	1.909915645
125	20	350	6	580	4	88.7	1.846251791

Table 4.B10: Experimental 125 test conditions results of thrust, torque and A-SPL, for hematite

Sl. No	DD (mm)	SS (rpm)	PR (mm/min)	Thrust (N)	Torque(Nm)	A-SPL(dB)	Specific Energy (Nm/m ³)
1	6	150	2	1200	13	109.7	42.4425699
2	6	200	2	986	6	100.7	34.87364493
3	6	250	2	700	5	73.4	24.75816577
4	6	300	2	647	5	82.1	22.88361894
5	6	350	2	1000	10	76.3	35.36880825
6	10	150	2	1624	14	76.2	20.67802005
7	10	200	2	586	5	75.4	7.461403788
8	10	250	2	865	6	85.9	11.01384689
9	10	300	2	520	5	89.3	6.621040904
10	10	350	2	638	7	79.7	8.123507878
11	16	150	2	750	8	83.6	3.730303995
12	16	200	2	745	8	100	3.705435302
13	16	250	2	863	8	99.7	4.292336463
14	16	300	2	596	4	100.1	2.964348241
15	16	350	2	589	4	93.6	2.929532071
16	18	150	2	925	10	104.5	3.635127514
17	18	200	2	700	6	100.7	2.750907308
18	18	250	2	652	5	84.2	2.562273664
19	18	300	2	777	9	96.3	3.053507112
20	18	350	2	569	6	92.5	2.236094655
21	20	150	2	952	10	81.7	3.030399491
22	20	200	2	825	7	89.7	2.626134012
23	20	250	2	693	7	93.6	2.20595257

24	20	300	2	500	6	80.7	1.591596371
25	20	350	2	729	6	75.3	2.320547509
26	6	150	3	650	6	96.3	22.98972536
27	6	200	3	900	8	100.8	31.83192742
28	6	250	3	1000	10	82.3	35.36880825
29	6	300	3	456	5	79.3	16.12817656
30	6	350	3	896	7	77.5	31.69045219
31	10	150	3	1000	13	86.3	12.73277097
32	10	200	3	1140	13	79.3	14.5153589
33	10	250	3	1520	14	69.2	19.35381187
34	10	300	3	963	6	66.8	12.26165844
35	10	350	3	856	6	75.2	10.89925195
36	16	150	3	923	6	71.5	4.590760783
37	16	200	3	685	5	81.7	3.407010982
38	16	250	3	836	8	67.5	4.15804552
39	16	300	3	1000	9	85.3	4.97373866
40	16	350	3	1012	10	86.3	5.033423524
41	18	150	3	1000	10	96.3	3.929867583
42	18	200	3	2578	5	107.7	10.13119863
43	18	250	3	639	5	86.3	2.511185386
44	18	300	3	563	5	100.7	2.212515449
45	18	350	3	759	5	89.6	2.982769496
46	20	150	3	856	5	96.4	2.724812987
47	20	200	3	1000	10	90.3	3.183192742
48	20	250	3	563	5	100	1.792137514
49	20	300	3	756	6	112.2	2.406493713
50	20	350	3	963	8	101.7	3.065414611

51	6	150	4	962	6	85.3	34.02479353
52	6	200	4	562	5	86.3	19.87727024
53	6	250	4	520	5	90.3	18.39178029
54	6	300	4	100	5	75.2	3.536880825
55	6	350	4	856	5	71.5	30.27569986
56	10	150	4	756	5	81.7	9.625974853
57	10	200	4	963	6	67.5	12.26165844
58	10	250	4	1001	7	116.9	12.74550374
59	10	300	4	963	5	75.2	12.26165844
60	10	350	4	600	5	71.5	7.639662582
61	16	150	4	752	5	81.7	3.740251472
62	16	200	4	689	5	67.5	3.426905937
63	16	250	4	1025	8	100.3	5.098082126
64	16	300	4	860	6	75.2	4.277415247
65	16	350	4	700	6	71.5	3.481617062
66	18	150	4	500	4	81.7	1.964933792
67	18	200	4	630	4	67.5	2.475816577
68	18	250	4	530	4	100.1	2.082829819
69	18	300	4	500	4	100.8	1.964933792
70	18	350	4	589	4	82.3	2.314692006
71	20	150	4	507	4	79.3	1.61387872
72	20	200	4	601	6	76.3	1.913098838
73	20	250	4	528	6	103	1.680725768
74	20	300	4	496	6	77.5	1.5788636
75	20	350	4	500	6	86.3	1.591596371
76	6	150	5	1121	6	90.3	39.64843405
77	6	200	5	1000	8	75.2	35.36880825

78	6	250	5	1252	6	71.5	44.28174793
79	6	300	5	689	7	81.7	24.36910888
80	6	350	5	1025	9	67.5	36.25302845
81	10	150	5	860	6	116.9	10.95018303
82	10	200	5	700	5	71.5	8.912939678
83	10	250	5	500	5	81.7	6.366385485
84	10	300	5	657	8	87.3	8.365430527
85	10	350	5	520	6	71.5	6.621040904
86	16	150	5	630	6	71.5	3.133455356
87	16	200	5	523	4	81.7	2.601265319
88	16	250	5	623	4	87.3	3.098639185
89	16	300	5	1178	10	103.7	5.859064141
90	16	350	5	860	4	71.5	4.277415247
91	18	150	5	700	4	81.7	2.750907308
92	18	200	5	500	4	87.3	1.964933792
93	18	250	5	630	5	71.5	2.475816577
94	18	300	5	400	6	81.7	1.571947033
95	18	350	5	860	7	87.3	3.379686121
96	20	150	5	600	5	71.5	1.909915645
97	20	200	5	520	5	81.7	1.655260226
98	20	250	5	630	5	87.3	2.005411428
99	20	300	5	700	5	104.3	2.22823492
100	20	350	5	500	5	81.7	1.591596371
101	6	150	6	963	9	71.5	34.06016234
102	6	200	6	756	6	81.7	26.73881904
103	6	250	6	643	5	93.1	22.7421437
104	6	300	6	865	5	71.5	30.59401913

105	6	350	6	1000	11	81.7	35.36880825
106	10	150	6	1240	6	87.3	15.788636
107	10	200	6	789	6	71.5	10.04615629
108	10	250	6	1200	12	81.7	15.27932516
109	10	300	6	1500	10	87.3	19.09915645
110	10	350	6	600	10	89.2	7.639662582
111	16	150	6	635	4	81.7	3.158324049
112	16	200	6	765	4	87.3	3.804910075
113	16	250	6	562	4	91.5	2.795241127
114	16	300	6	863	5	96.7	4.292336463
115	16	350	6	632	6	107.2	3.143402833
116	18	150	6	500	6	81.7	1.964933792
117	18	200	6	657	6	87.3	2.581923002
118	18	250	6	520	4	71.5	2.043531143
119	18	300	6	630	4	81.7	2.475816577
120	18	350	6	846	10	102.3	3.324667975
121	20	150	6	500	4	71.5	1.591596371
122	20	200	6	657	4	81.7	2.091357632
123	20	250	6	630	6	87.3	2.005411428
124	20	300	6	751	6	71.5	2.390577749
125	20	350	6	656	6	106.8	2.088174439

Table 4.B11: Experimental 125 test conditions results of thrust, torque and A-SPL, for dolomite

Sl. No	DD (mm)	SS (rpm)	PR (mm/min)	Thrust (N)	Torque(Nm)	A-SPL(dB)	Specific Energy (Nm/m ³)
1	6	150	2	397	9	87.2	14.04141687
2	6	200	2	721	4	85.1	25.50091075
3	6	250	2	612	7	82.7	21.64571065
4	6	300	2	600	7	86.7	21.22128495
5	6	350	2	220	6	83.4	7.781137815
6	10	150	2	358	5	78.8	4.558332007
7	10	200	2	500	6	85.1	6.366385485
8	10	250	2	256	7	86	3.259589368
9	10	300	2	217	2	81.2	2.7630113
10	10	350	2	147	2	82.6	1.871717332
11	16	150	2	156	4	78.9	0.775903231
12	16	200	2	200	5	72.1	0.994747732
13	16	250	2	562	5	83.1	2.795241127
14	16	300	2	241	4	85	1.198671017
15	16	350	2	108	4	86	0.537163775
16	18	150	2	876	4	94.4	3.442564003
17	18	200	2	214	6	88.4	0.840991663
18	18	250	2	189	5	89.2	0.742744973
19	18	300	2	174	5	92	0.683796959
20	18	350	2	200	4	95.6	0.785973517
21	20	150	2	167	4	92.5	0.531593188
22	20	200	2	201	5	97.2	0.639821741
23	20	250	2	189	4	96.3	0.601623428

24	20	300	2	175	5	94.1	0.55705873
25	20	350	2	325	5	96.5	1.034537641
26	6	150	3	986	3	82.7	34.87364493
27	6	200	3	1000	2	86.9	35.36880825
28	6	250	3	956	2	85.7	33.81258069
29	6	300	3	812	4	75	28.7194723
30	6	350	3	560	5	72.7	19.80653262
31	10	150	3	486	5	81.8	6.188126691
32	10	200	3	500	4	86.4	6.366385485
33	10	250	3	900	4	80	11.45949387
34	10	300	3	541	4	80.2	6.888429094
35	10	350	3	397	6	81.9	5.054910075
36	16	150	3	415	5	88	2.064101544
37	16	200	3	600	5	79.1	2.984243196
38	16	250	3	845	4	87.4	4.202809168
39	16	300	3	665	5	95.6	3.307536209
40	16	350	3	475	4	98.7	2.362525863
41	18	150	3	582	5	100	2.287182933
42	18	200	3	330	5	95.5	1.296856302
43	18	250	3	641	3	99.4	2.519045121
44	18	300	3	290	7	96.6	1.139661599
45	18	350	3	452	5	96.7	1.776300148
46	20	150	3	374	7	89.7	1.190514086
47	20	200	3	250	4	94.9	0.795798186
48	20	250	3	500	8	93.4	1.591596371
49	20	300	3	386	6	95.7	1.228712399
50	20	350	3	297	6	96	0.945408244

51	6	150	4	1000	9	89.2	35.36880825
52	6	200	4	1201	12	86.2	42.47793871
53	6	250	4	1576	10	83.2	55.7412418
54	6	300	4	956	5	87.2	33.81258069
55	6	350	4	678	9	75.3	23.98005199
56	10	150	4	758	8	82.1	9.651440395
57	10	200	4	601	8	87.4	7.652395353
58	10	250	4	754	7	93.1	9.600509311
59	10	300	4	756	7	98.4	9.625974853
60	10	350	4	825	5	97.5	10.50453605
61	16	150	4	690	7	97	3.431879675
62	16	200	4	685	5	86	3.407010982
63	16	250	4	600	6	84.7	2.984243196
64	16	300	4	745	6	82.4	3.705435302
65	16	350	4	766	5	82.6	3.809883813
66	18	150	4	515	4	95.3	2.023881805
67	18	200	4	584	5	100	2.295042669
68	18	250	4	712	5	102.1	2.798065719
69	18	300	4	623	3	101.1	2.448307504
70	18	350	4	700	7	100.8	2.750907308
71	20	150	4	622	5	95.6	1.979945886
72	20	200	4	500	7	92.3	1.591596371
73	20	250	4	658	4	98.1	2.094540824
74	20	300	4	501	8	85.6	1.594779564
75	20	350	4	496	6	101	1.5788636
76	6	150	5	1200	13	86.3	42.4425699
77	6	200	5	1145	12	80	40.49728544

78	6	250	5	1150	9	79.4	40.67412949
79	6	300	5	900	10	75.4	31.83192742
80	6	350	5	578	10	86.3	20.44317117
81	10	150	5	325	5	80.4	4.138150565
82	10	200	5	1200	10	77.1	15.27932516
83	10	250	5	745	6	85.3	9.485914372
84	10	300	5	600	10	90.3	7.639662582
85	10	350	5	640	8	84.2	8.14897342
86	16	150	5	499	9	96.3	2.481895591
87	16	200	5	779	9	84.1	3.874542416
88	16	250	5	589	5	1002	2.929532071
89	16	300	5	703	5	93.5	3.496538278
90	16	350	5	1000	11	100.8	4.97373866
91	18	150	5	900	8	96.5	3.536880825
92	18	200	5	1185	12	99.7	4.656893086
93	18	250	5	751	6	82.1	2.951330555
94	18	300	5	345	5	96.4	1.355804316
95	18	350	5	896	8	100.8	3.521161354
96	20	150	5	658	8	96.5	2.094540824
97	20	200	5	700	7	97.5	2.22823492
98	20	250	5	641	6	98.7	2.040426548
99	20	300	5	895	9	86.2	2.848957504
100	20	350	5	798	6	83.3	2.540187808
101	6	150	6	1124	12	74	39.75454047
102	6	200	6	800	9	85	28.2950466
103	6	250	6	778	8	75	27.51693282
104	6	300	6	625	6	85	22.10550516

105	6	350	6	900	8	96	31.83192742
106	10	150	6	508	7	75	6.468247652
107	10	200	6	745	7	100	9.485914372
108	10	250	6	523	5	95.6	6.659239217
109	10	300	6	965	9	100.1	12.28712399
110	10	350	6	1126	13	81.5	14.33710011
111	16	150	6	692	5	93.5	3.441827153
112	16	200	6	785	6	100	3.904384848
113	16	250	6	693	7	112	3.446800891
114	16	300	6	1000	9	96.7	4.97373866
115	16	350	6	896	8	89.5	4.456469839
116	18	150	6	1298	14	100.4	5.100968123
117	18	200	6	1201	13	96.3	4.719770967
118	18	250	6	639	6	92.4	2.511185386
119	18	300	6	758	7	100.7	2.978839628
120	18	350	6	548	8	98.4	2.153567436
121	20	150	6	1124	13	92.5	3.577908642
122	20	200	6	745	6	93.5	2.371478593
123	20	250	6	852	7	86.4	2.712080216
124	20	300	6	968	9	94.2	3.081330575
125	20	350	6	2150	13	100	6.843864396

PUBLICATIONS

International Journals

1. Kumar, Ch.V., Vardhan, H., Murthy, Ch.S.N. and Karmakar, N.C. (2019). “Estimating Rock Properties using Sound Signal Dominant Frequencies during Diamond core Drilling Operations.” *Journal of Rock Mechanics and Geotechnical Engineering (SCI. Expanded - Elsevier)*, 11 (4), 850 - 859.
2. Kumar, Ch.V., Vardhan, H. and Murthy, Ch.S.N. (2019). “Quantification of Rock Properties using Frequency Analysis during Diamond Core Drilling Operations.” *Journal of The Institution of Engineers (India): Series D (Scopus-Springer)*, 100 (1), 67 - 81.
3. Kumar, Ch.V., Vardhan, H. and Murthy, Ch.S.N. (2019). “Multiple Regression Model for Prediction of Rock Properties using Acoustic Frequency during Core Drilling Operations.” *Geomechanics and Geoengineering: An International Journal (Scopus-Taylor&Francis)*, 15(4), 297 - 312.
4. Kumar, Ch.V., Vardhan, H. and Murthy, Ch.S.N. (2019). “Artificial Neural Network for Prediction of Rock Properties using Acoustic Frequencies Recorded during Rock Drilling Operations.” *Modeling Earth Systems and Environment* <https://doi.org/10.1007/s40808-021-01103-w>, (*Springer -scopus*).
5. Kumar, Ch.V., Murthy, Ch.S.N. and Vardhan, H. (2019). “Rock Properties versus Specific Energy during Diamond Drilling Operations.” *Geotechnical and Geological Engineering, (Springer Under-Review)*.

International Conferences

1. Kumar, Ch.V., Vardhan, H. and Murthy, Ch.S.N. (2016). “Laboratory Investigations on Diamond Core Drilling Operations”. ENCO 2019 International Conference and Exhibition on Energy & Environment : Challenges & Opportunities (CSIR-CIMFR). 20th to 22nd February - 2019, Vigyan Bhawan, New Delhi, India.

2. Kumar, Ch.V., Murthy, Ch.S.N. and Vardhan, H. (2020). “Prediction of Specific Energy Using Dominant Frequency of Acoustics Produced During Diamond Core Drilling Operations” Second International Conference on Emerging Research in Civil, Aeronautical and Mechanical Engineering ERCAM, 20th to 22nd February - 2019, Bangalore, Scopus, AIP Conference Proceedings 2204, 040003 (2020); <https://doi.org/10.1063/1.5141576>

National Conferences

1. Kumar, Ch.V., Murthy, Ch.S.N. and Vardhan, H. (2016). “Noise Assessment in Mines – A Critical Review.” Concurrent Advances in Mechanical Engineering Journal, 2 (1), 6-11. National Conference FAME 2K16, 8th to 9th August - 2019. Thalassery, Kerala.
2. Kumar, Ch.V., Vardhan, H. and Murthy, Ch.S.N. (2016). “Influence of Thrust and Noise levels on Operational Parameters in Diamond core Drilling Operation”. National Symposium on Mining Safety 360 Degree under Tamilnadu Mines Safety Association. Pondicherry, 13th to 14th July - 2018.

Abstract of published papers are incorporated

CURRICULUM VITAE

Mr. Ch.Vijaya Kumar
 S/o Chakradhara Rao
 Door No. 4-74, Pedapalem Post,
 Duggirala (M), Tenali Taluka
 Guntur District, A.P -522305
 Mobile: +91 9642120299
Email: vijayakumarch.nitk@gmail.com



Date of birth : 16-04-1986

Qualification :

Ph.D	Thesis submitted	National Institute of Technology Karnataka	NITK Surathkal	7.38 (CGPA)	Prediction of Rock Properties and Specific Energy using Sound Levels Produced during Diamond Drilling
M.Tech	2011-2013	Jawaharlal Nehru Technological University Hyderabad (JNTUH)	TKRCE, Hyderabad	68.38%	CAD/CAM
B.Tech	2005-2009	Jawaharlal Nehru Technological University Hyderabad (JNTUH)	MITS Kodad	60.64%	Mechanical Engineering

Ph.D. Thesis Title: Prediction of Rock Properties and Specific Energy using Sound Levels Produced during Diamond Drilling

Area of Research Interest: Vibration and acoustics, Drilling, Design and Manufacturing process, Robotics.

Research Score :

	Citations	h-index	RG-Score
Scopus	10	02	-
Google Scholar	23	03	-
Research Gate	26	03	5.13

Scopus: <https://www.scopus.com/authid/detail.uri?authorId=57208280276>

Google Scholar: <https://scholar.google.co.in/citations?user=rev8MksAAAAJ&hl=en>

Research gate: https://www.researchgate.net/profile/Chvijaya_Kumar

ORCID: <https://orcid.org/0000-0001-6926-7852>

Web of Science Researcher (Publons) ID: AAF-3340-2019

Journal Reviewer :

1. Geotechnical and Geological Engineering; An International Journal (**Springer International Publishing-Scopus**)
2. Environmental Earth Sciences (**Springer-Verlag GmbH Germany, part of Springer Nature, SCI - Science Citation Index**)

Experience :

Period	Designation	College	No. of years/months
16.07.2010 - 23.04.2011	Assistant Professor	Madhira Educational Society Group of Institutions, Hyderabad	10 Months
30.08.2011 - 11.10.2013	Assistant Professor	Sphoorthy Engineering College, Hyderabad	2 yrs 2 Months
22.04.2014 -18.01.2016	Assistant Professor	Brilliant Group of Technical Institutions, Hyderabad	1 year 9 Months
Dec 2015- till date	Research Scholar/ Teaching Assistant	National Institute of Technology Karnataka (NITK), Surathkal	3 yrs 10 Months
Total			08 Yrs 11months

Journal (International)	05 No's
Conference (National)	02 No's
Conference (International)	02 No's

Subject Handled:

1. Engineering Drawing
2. Machine Tools
3. Machine Drawing
4. Thermodynamics
5. Refrigeration and Air conditioning

Under Graduate Projects Guided

UG Project Guide: 1 No's

PG Project Guide: Nil

Awards:

- Award selected for “BEST RESEARCHER OF THE YEAR 2019” by International Research Leadership Awards 2019 (RULA AWARDS & IJRULA, MALAYSIA) for excellence in “Estimating rock properties using sound signal dominant frequencies during diamond core drilling operations.”

International Journals:

1. Kumar, Ch.V., Vardhan, H, Murthy, Ch.S.N. and Karmakar, N.C. (2019) “Estimating Rock Properties using Sound Signal Dominant Frequencies during Diamond core Drilling Operations.” *Journal of Rock Mechanics and Geotechnical Engineering*, **SCI Expanded (Elsevier)** I.F: **2.256**, <https://doi.org/10.1016/j.jrmge.2019.01.001>.
2. Kumar, Ch.V., Vardhan, H. and Murthy, Ch.S.N. (2019) “Quantification of Rock Properties using Frequency Analysis during Diamond Core Drilling Operations.” *Journal of The Institution of Engineers (India): Series D*, 100 (1), 67-81. Scopus (**Springer**) I.F: **0.465**, <https://doi.org/10.1007/s40033-019-00174-5>.
3. Kumar, Ch.V., Vardhan, H. and Murthy, Ch.S.N. (2019) “Multiple regression model for prediction of rock properties using acoustic frequency during core drilling operations.” *Geomechanics and Geoengineering: An International Journal*. Scopus (**Taylor & Francis**) I.F: **0.67**, <https://doi.org/10.1080/17486025.2019.1641631>.
4. Kumar, Ch.V., Abhilash, J., Anjaiah, M., Mohan, A. (2014) “FE Analysis on Vehicle Bumper Using Different Materials and Speeds” *International Journal of Mechanical Engineering*, Vol. 4(2), pp. 99-110.
5. Kumar, Ch.V., Kumar, D. (2014) “Performance Analysis of Regenerative Feed Heating in A Steam Power Plant” *IOSR Journal of Mechanical and Civil Engineering (IOSR-JMCE)*, Vol. 11(2), pp. 01-08. DOI: 10.9790/1684-11250108.
6. Kumar, Ch.V., Vardhan, H. and Murthy, Ch.S.N. (2019). “Artificial Neural Network for Prediction of Rock Properties using Acoustic Frequencies Recorded during Rock Drilling Operations.” *Modeling Earth Systems and Environment* <https://doi.org/10.1007/s40808-021-01103-w>, (**Springer -scopus**).
7. Kumar, Ch.V., Murthy, Ch.S.N. and Vardhan, H. (2019). “Rock Properties versus Specific Energy during Diamond Drilling Operations.” *Geotechnical and Geological Engineering*, (**Springer Under-Review**).

International Conferences:

1. Kumar, Ch.V., Vardhan, H. and Murthy, Ch.S.N. (2016) “Laboratory Investigations on Diamond Core Drilling Operations”. ENCO 2019 International Conference and Exhibition on Energy & Environment : Challenges & Opportunities (CSIR-CIMFR). 20th to 22nd February - 2019, Vigyan Bhawan, New Delhi, India.
2. Kumar, Ch.V., Murthy, Ch.S.N. and Vardhan, H. (2016) “Prediction of Specific Energy Using Dominant Frequency of Acoustics Produced During Diamond Core Drilling Operations” Second International Conference on Emerging Research in Civil, Aeronautical and Mechanical Engineering ERCAM, 25th to 26th July - 2019 Scopus AIP Conference Proceedings 2204, 040003 (2020); <https://doi.org/10.1063/1.5141576>

National Conferences:

1. Kumar, Ch.V., Murthy, Ch.S.N. and Vardhan, H. (2016) “Noise Assessment in Mines – A Critical Review.” Concurrent Advances in Mechanical Engineering Journal, 2 (1), 6-11. National Conference FAME 2K16, 8th to 9th August - 2019. Thalassery, Kerala.
2. Kumar, Ch.V., Vardhan, H. and Murthy, Ch.S.N. (2016) “Influence of Thrust and Noise levels on Operational Parameters in Diamond core Drilling Operation”. National Symposium on Mining Safety 360 Degree under tamilnadu mines safety association. Pondicherry 13th to 14th July – 2018.

Faculty Development Programme:

1. Participated in one days training course on “Effective Methods of Teaching” Organized by the Institute of Public Enterprise (IPE), Osmania University, Hyderabad on 28th September, 2013 at Sphoorthy Engineering College.
2. Participated in one days training course on “Intellectual Property Rights and Center for Intellectual Property Rights Research and Advocacy” Organized by National Law School of India University (TEQIP-II), held at National Institute of Technology Karnataka, Surathkal on 1st September 2016.
3. Participated in four days short term course (GIAN) on “Computer Application and Data Analysis in Mining and Other Core Industries” Organized by Ministry of Human Resources Development (MHRD), Govt. of India, held at Department of Mining Engineering, National Institute of Technology Karnataka, Surathkal on 12th to 16th March, 2018.

Workshops attended:

1. Attended two day workshop on “Recent Trends in Environment, Health and Safety Management in Mining and other Core Industries” sponsored by TEQIP-II, organized by the Department Mining Engineering, National Institute of Technology Karnataka, Surathkal (NITK) during 27th to 28th January 2017.
2. Attended two day workshop on “Minerals Beneficiation” sponsored by TEQIP-II, organized by the Department of Metallurgical and Materials Engineering, National Institute of Technology Karnataka, Surathkal (NITK) during 20th to 21st February 2017.
3. Attended three day workshop on “Recent Advances in Reliability Engineering and Maintenance Management” sponsored by TEQIP-III, organized by the Department Mining Engineering, National Institute of Technology Karnataka, Surathkal (NITK) during 1st to 3rd November 2018.
4. Attended three day workshop on “Concepts of Operations Analysis and Geo-mechanics for Improved Production and Safety” organized by the Department Mining Engineering, National Institute of Technology Karnataka, Surathkal (NITK) during 11th to 13th February 2019.
5. Attended one day workshop on “Art of Writing Thesis” organized by Rehoboth Academic Services, held at Rosario College of Management Studies, Mangalore on 3rd August 2019.

Organized workshops:

1. Worked as coordinator for one day workshop on “Recent Advances in Reliability Engineering and Maintenance Management” sponsored by TEQIP-III, organized by the Department Mining Engineering, National Institute of Technology Karnataka, Surathkal (NITK) during 1st to 3rd November 2018.
2. Worked as coordinator for two day workshop on “Recent Trends in Environment, Health and Safety Management in Mining and other Core Industries” sponsored by TEQIP-II, organized by the Department Mining Engineering, National Institute of Technology Karnataka, Surathkal (NITK) during 27th to 28th January 2017.